– Stable and Unstable –

Binary Opposition in Pnictogens

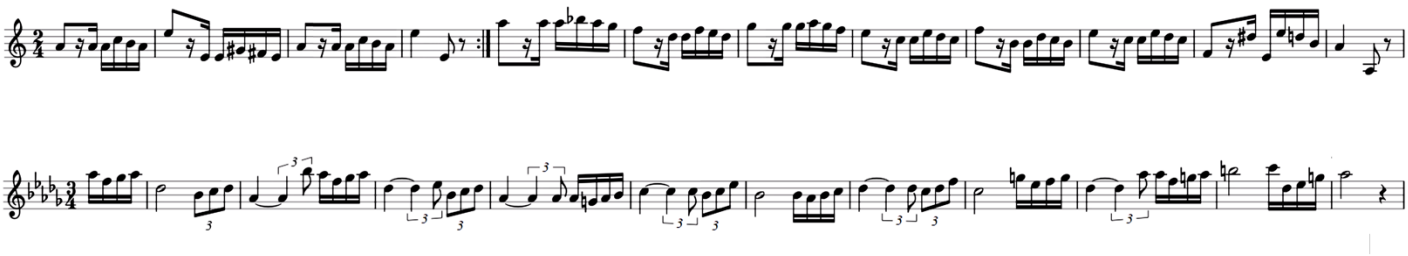

Wissenschaftliche Arbeit zur Erlangung des Doktorgrades der Naturwissenschaftlichen Fachbereiche im Fachgebiet Organische Chemie der Justus-Liebig-Universität Gießen

Vorgelegt von
Weiyu Qian

Gießen
2025

Eidesstattliche Erklärung

Hiermit versichere ich, die vorgelegte Dissertation selbstständig und ohne unerlaubte fremde Hilfe und nur mit den Hilfen angefertigt zu haben, die ich in der Dissertation angegeben habe. Alle Textstellen, die wörtlich oder sinngemäß aus veröffentlichten Schriften entnommen sind, und alle Angaben, die auf mündlichen Auskünften beruhen, sind als solche kenntlich gemacht.

Bei den von mir durchgeführten und in der Dissertation erwähnten Untersuchungen habe ich die Grundsätze guter wissenschaftlicher Praxis, wie sie in der „Satzung der Justus-Liebig-Universität zur Sicherung guter wissenschaftlicher Praxis“ niedergelegt sind, eingehalten.

Ort. Datum	Unterschrift

Dekan: Prof. Holger Zorn

Erstgutachter: Prof. Peter R. Schreiner

Zweitgutachter: Prof. Hermann A. Wegner

“Le seul moyen d'affronter un monde sans liberté est de devenir si absolument libre qu'on fasse de sa propre existence un acte de révolte.”

“The only way to deal with an unfree world is to become so absolutely free that your very existence is an act of rebellion.”

—— L'Homme révolté, Albert Camus (1913–1960)

Zusammenfassung

Die Dualität von Stabilität und Instabilität in der Chemie bestimmen grundlegendend das Wesen der Reaktivität. Diese Dualität ist geprägt durch die Verbindung von kinetischer und thermodynamischer Prinzipien als auch durch quantenmechanisches Tunneln. Instabile Spezies neigen dazu, in einen stabilen Zustand überzugehen, um Energie zu minimieren und das Gleichgewicht zu maximieren. Im Gegensatz dazu muss eine stabile Spezies durch äußere Einflüsse oder chemische Manipulationen in einen instabilen Zustand versetzt werden, um ihre Reaktivität zu erhöhen oder Energie zu speichern. Diese dynamische Beziehung verdeutlicht die intrinsische Wechselwirkung zwischen Stabilität und Instabilität; sie sind keine absoluten Zustände. Sie existieren in einem ständigen Spannungsfeld, welches je nach Kontext und Bedingungen ineinander umgekehrt werden kann.

Aus philosophischer Perspektive lassen sich Stabilität und Instabilität als zwei komplementäre Aspekte derselben fundamentalen Dichotomie betrachten – analog zu den apollinischen und dionysischen Prinzipien in Friedrich Nietzsches Die Geburt der Tragödie aus dem Geiste der Musik. Dabei definiert und verstärkt jede dieser beiden Gegensätze die Bedeutung der anderen: Stabilität verleiht der Instabilität ihre Faszination des Flüchtigen und motiviert die wissenschaftliche Herausforderung, vergängliche Spezies zu erfassen, die sich konventionellen Normen entziehen. Gleichzeitig erhält Stabilität ihren intrinsischen Wert durch die Instabilität, da die Bestrebung, das Ephemere zu stabilisieren, entscheidende Impulse für Innovationen in der Chemie liefert. Diese Dualität spiegelt eine tiefere natürliche Ordnung wider, in der Gegensätze nicht nur koexistieren, sondern auch den wissenschaftlichen Fortschritt vorantreiben, Grenzen hinterfragen und kreative Entwicklungen inspirieren.

Im Rahmen dieser Dissertation sollen instabile „Oligomere“ – höhere neutrale Stickstoffallotrope – aus stabilen Dinitrogeneinheiten konstruiert werden. Darüber hinaus werden Methoden zur Erzeugung und Untersuchung instabiler schwererer Analoga von Dinitrogen erforscht sowie neuartige Eigenschaften hochreaktiver, elektronenarmer Spezies untersucht, die gegen die Oktettregel in Hauptgruppenelementen verstoßen. Diese wissenschaftliche Arbeit ist sowohl eine philosophische als auch eine experimentelle Reise – mit dem Ziel, das Flüchtige greifbar zu machen, das Instabile zu bewahren und das schwer Fassbare zu realisieren.

In der ersten Arbeit habe ich das interstellare Kandidatenmolekül Phosphormononitrid (PN), eine unter Standardbedingungen metastabile Spezies, durch Hochvakuum-Flash-Pyrolyse von (o-Phenyldioxyl)phosphinoazid in kryogenen Matrizen erzeugt. Zudem wurde erstmals ein o-Benzochinon-PN-Komplex identifiziert, der sich unter Bestrahlung mit Licht einer Wellenlänge von 523 nm zu (*o*-Phenyldioxyl)-λ^5-Phosphinonitril rekombiniert. Dies stellt den ersten Nachweis der Reaktivität von PN mit einer organischen Verbindung dar.

In der zweiten Arbeit habe ich die in situ Charakterisierung von Triplet-Phenylarsiniden mittels Matrix-Isolations-IR- und UV/Vis-Spektroskopie beschrieben. Durch Dotierung der Matrix mit molekularem Sauerstoff wurde das kinetische Intermediat *anti*-Dioxyphenylarsin nachgewiesen, eine bislang unbekannte Spezies mit völlig anderer Reaktivität als die korrespondierenden Phenylnitrene und Phenylphosphinidene. Unter Bestrahlung mit 465 nm wandelt sich *anti*-Dioxyphenylarsin in die neuartige Verbindung Dioxophenylarsin um.

In der dritten Arbeit habe ich die Synthese und spektroskopische Charakterisierung von Vinylarsiniden, einem höheren Kongener von Vinylnitrenen. Triplet-Vinylarsiniden wurde durch IR- und UV/Vis-Spektroskopie charakterisiert und zeigt eine bemerkenswert vielseitige unimolekulare Photochemie. Durch selektive Photoanregung kann es sich in Vinylidenarsin, 2H-Arsirene oder einen Arsiniden-(H–As)-Acetylen-Komplex umlagern. Zudem wurde die Stabilität von Vinylphosphiniden mittels Multireferenz-Berechnungen untersucht.

In der vierten Arbeit habe ich das erste Beispiel eines skalierbar synthetisierbaren neutralen Stickstoffallotrops, C_{2h}-N_6, die in der Gasphase bei Raumtemperatur erzeugt und anschließend entweder in Argon-Matrizen bei 10 K oder als Film bei flüssiger Stickstofftemperatur (77 K) charakterisiert wurde. Die Verbindung weist eine unerwartet hohe Stabilität auf. Energetische Leistungsberechnungen auf CCSD(T)/cc-pVTZ-Niveau anhand der Kamlet-Jacobs-Gleichung prognostizieren eine hervorragende Detonationsleistung, die mehrere bekannte Explosivstoffe wie TNT (2,4,6-Trinitrotoluol) und RDX (1,3,5-Trinitro-1,3,5-triazinan) übertrifft.

Abstract

The stability and instability is one of the most fundamental dualities in chemistry, which governs the essence of reactivity with a linkage of energy through kinetic and thermodynamic principles, as well as quantum-mechanical tunneling. The "unstable" species, driven by a natural inclination, strives to transform into a "stable" state, minimizing energy and pushing the reaction equilibrium. Conversely, a "stable" species must be "compelled" into an unstable state—whether by external forces or chemical manipulation—to unlock its reactivity or achieve energy storage. This dynamic relationship underscores the intrinsic interdependence of stability and instability; they are not absolutes but rather exist in a state of constant tension, capable of mutual inversion depending on context and conditions.

From a philosophical perspective, stability and instability can be viewed as two sides of the same coin (like Apollonian and Dionysian, from *Die Geburt der Tragödie aus dem Geiste der Musik*, Friedrich Nietzsche), where each defines and elevates the significance of the other. Stability gives instability its allure of transient, prompting the quest to capture fleeting species that defy conventional norms. Meanwhile, instability imbues stability with its intrinsic value, as the effort to stabilize the ephemeral drives innovation in chemistry. This duality reflects a broader natural order, where opposites not only coexist but also fuel progress, challenge boundaries, and inspire creativity.

In this thesis, I'm going to constitute unstable "oligomer" (higher neutral nitrogen allotropes) with the units of stable dinitrogen, explore methods to generate and study the chemistry of unstable heavier analogs of stable dinitrogen, and investigate novel properties of highly reactive, electron-deficient species that violate the octet rule in main group elements. This endeavor embodies a philosophical and scientific journey—transforming the transient into the tangible, the unstable into the cherished, and the elusive into the achievable.

In the first publication, the interstellar candidate phosphorus mononitride PN, a metastable species under ambient conditions, was generated through high-vacuum flash pyrolysis of (*o*-phenyldioxyl)phosphinoazide in cryogenic matrices. Moreover, an elusive *o*-benzoquinone-PN complex formed and its recombination to (*o*-phenyldioxyl)-λ^5-phosphinonitrile was observed upon irradiation with the light λ = 523 nm, which demonstrates for the first time the reactivity of PN towards an organic molecule.

In the second publication, we report the *in situ* characterization of triplet phenylarsinidene by matrix-isolation infrared and UV/Vis spectroscopy. Doping the matrices containing phenylarsinidene with molecular oxygen leads to the formation of hitherto unknown kinetic intermediate *anti*-dioxyphenylarsine, which demonstrates a completely different reactivity with corresponding phenylnitrene and phenylphosphinidene. The *anti*-dioxyphenylarsine undergoes isomerization to novel dioxophenylarsine upon 465 nm irradiation.

In the third publication, we report the synthesis and spectroscopic characterization of vinylarsinidene, a higher congener of vinylnitrene. Triplet vinylarsinidene was characterized by IR and UV/Vis spectroscopy and displays remarkably rich unimolecular photochemistry. Upon selective photoirradiation, it rearranges to vinylidenearsine, 2*H*-arsirene, or an arsinidene (H–As) acetylene complex. Furthermore, the stability of vinylphosphinidene was projected with multireference computations.

In the fourth publication, the first example of scalably synthesizable neutral nitrogen allotrope, C_{2h}-N_6 was prepared in the gas-phase at ambient temperature, followed by characterized in argon matrices at 10 K or neatly as a film at liquid nitrogen temperature (77 K), demonstrating unexpectedly high stability. Energetic performance computations at the CCSD(T)/cc-pVTZ level with Kamlet-Jacob equation predict an excellent detonation performance over several well-known explosives, for example, TNT (2,4,6-trinitrotoluene) and RDX (1,3,5-trinitro-1,3,5-triazinane).

Dedicated to my parents

Table of Contents

1. Introduction

A pnictogen is an element in Group 15 of the periodic table (formerly Group V or Group VA), which includes nitrogen, phosphorus, arsenic, antimony, and bismuth (Scheme 1). All pnictogens are solids at room temperature, with the exception of nitrogen, which is a gas. The defining characteristic of this group is that each element has five valence electrons—two in the *s* sub-shell and three unpaired electrons in the *p* sub-shell. Within the group, nitrogen and phosphorus are classified as non-metals, arsenic and antimony are metalloids, and bismuth is a metal.

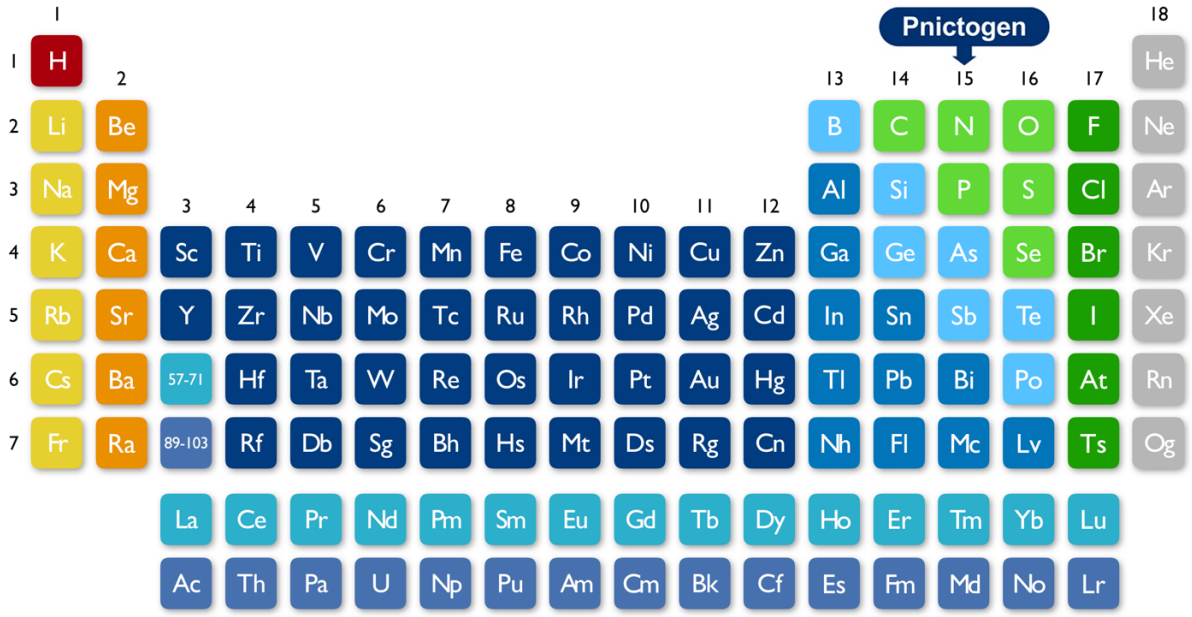

Scheme 1. The periodic table shows where the pnictogens are.

Nitrogen (N) is a colorless, odorless gas at room temperature and makes up about 78% of earth's atmosphere. It plays a crucial role in biological processes, forming the basis of amino acids and nucleic acids.[1-5] No stable allotrope of nitrogen other than N_2 has been discovered under ambient circumstance to date. In contrast, phosphorus (P) is a solid at room temperature and exists in various allotropes (e.g., white phosphorus P_4, red phosphorus, and black phosphorus).[6-15] Phosphorus is also essential for life, playing a crucial role in energy transfer (e.g., adenosine triphosphate, ATP) and forming key structural components of DNA and cell membranes.[7, 16-18] Arsenic (As) is known for its toxic properties and can exist in multiple oxidation states similar to phosphorus. However, it has found modern applications in semiconductors and certain alloys,[19-26] as well as in medical and agricultural applications.[27-30] Antimony (Sb) is also used in alloys and has flame-retardant properties.[31-32] It was also been widely used in cosmetics in ancient times, though was abandoned after its toxicity was realized.[33-34] Both arsenic and antimony have intermediate properties between metals and non-metals, which is characteristic of metalloids.

Bismuth (Bi) is a dense, brittle metal with low toxicity compared to other heavy metals, which makes it valuable in pharmaceuticals, cosmetics, and environmentally friendly applications.[35-40] It is also used in low-melting alloys and has unique electronic properties, such as low electrical conductivity.[41-44] This project mainly focused on nitrogen, phosphorus, and arsenic.

1.1 Dipnictogens

As the simplest molecules that pnictogens can form, dipnictogens are of great interest in synthetic chemistry, interstellar chemistry, and prebiotic chemistry. The lightest dipnictogen, dinitrogen (N_2), is the predominant component of earth's atmosphere, constituting about 78% of the air. Dinitrogen's triple bond gives it remarkable thermodynamic and kinetic stability, making it relatively inert under standard conditions. To render N_2 viable as a primary nitrogen source, both biological systems and the chemical industry have developed complicated catalytic processes aimed primarily at converting N_2 to ammonia (NH_3).[45-47] In addition to the industrial Haber-Bosch process (Scheme 2),[48] alternative strategies that realize the transformation from N_2 to NH_3 under mild conditions are a long-lasting goal in chemistry. In the past decades, several transition-metal species have been found to weaken chemical bonds in N_2. The prevalence of transition metals in dinitrogen activation is attributed to the fact that the unoccupied and occupied *d*-orbitals could be both energetically and symmetrically accessible to accept electron density from and back donate to N_2. Nevertheless, the development of low-valent, low-coordinate main-group elements which mimic the electronic properties of transition metal provides more opportunities to unearth the N_2 activation by main group elements, for example, low-valent calcium,[49] low-valent boron, and low-valent carbon complexes (Scheme 3).[50]

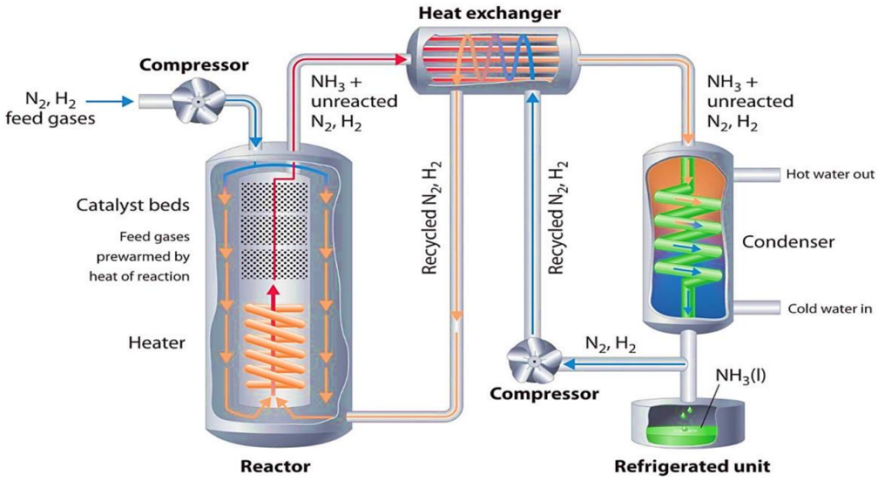

Scheme 2. Haber-Bosch process.[51]

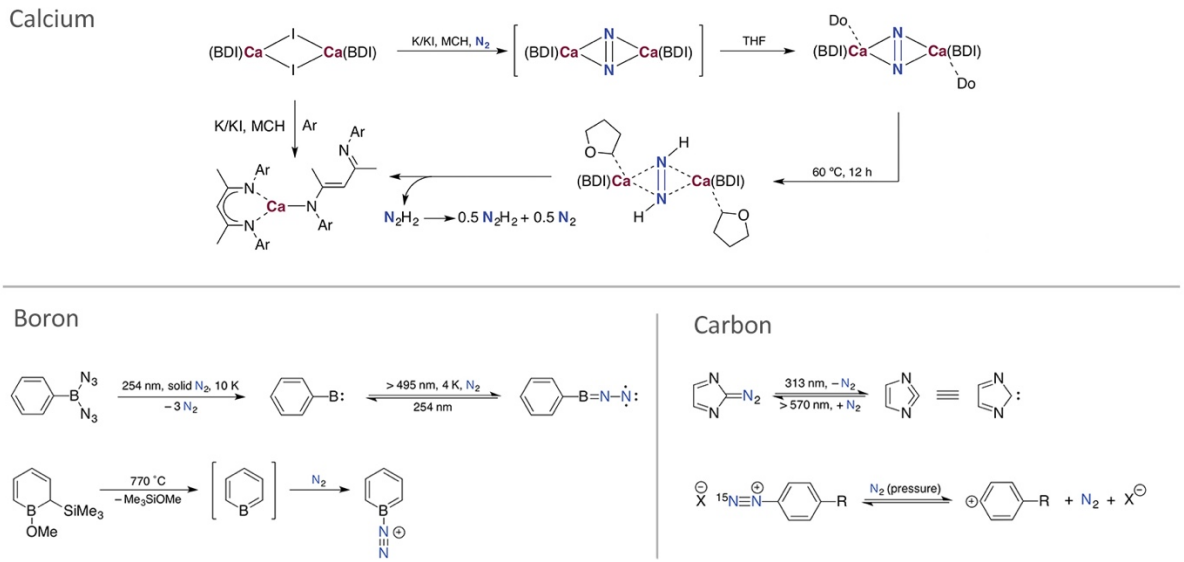

Scheme 3. Examples of activation of N_2.

As a stable form of nitrogen element is N_2 with a strong triple bond, the stable form of phosphorus is the tetrahedral P_4, known as white phosphorus, of which the dissociation to two P_2 molecules can be achieved upon heating (> 1100 K).[52] However, heavier dipnictogens, such as phosphorus mononitride (PN), diphosphorus (P_2), and arsenic mononitride (AsN), exist only transiently under normal conditions due to their highly reactive nature (Scheme 4). They play significant roles in synthetic chemistry, interstellar chemistry, and prebiotic chemistry. PN is particularly notable in astrochemistry, as it has been detected in interstellar clouds, where it may contribute to prebiotic molecular pathways.[53-61] AsN, while less common, has applications in materials science due to its electronic properties.[62] The study of these molecules provides valuable insights into bonding, electron distribution in multiple bonds, and the reactivity of pnictogen compounds, offering implications across various fields, from astrochemistry to the origins of life.

Due to their high reactivity, several strategies were invented to stabilize and store heavier dipnictogens for use (Scheme 5). For example, Bertrand et al. synthesized the iminophosphenium tetrachloroaluminate bearing a PN moiety in 1988.[63] Schulz et al. launched the *in situ* trapping of a PN tetramer via the elimination of trimethylsilyl chloride from $(Me_3Si)_2NPCl_2$ using dimethyl butadiene.[64] Similarly, Cummins et al. reported an *in situ* trapping of P_2 from white phosphorus with dimethyl butadiene.[65] Photoisomerization in the single crystal could be detected for $[Mo](PN)^-$ to $[Mo](NP)^-$ when exposed to white light.[66] Recently, Cummins and coworkers reported the first-time PN releasing using the representative anthracene precursor. The releasing was subsequently confirmed with the exchange of $[(dppe)Fe(Cp^*)(N_2)][BArF_{24}]$ to $[(dppe)Fe(Cp^*)(NP)][BArF_{24}]$ in solution.[67] For even heavier dipinictogen, Cummins et al.

presented the storable and controllable release of P_2 from (η^2-Mes*NPP)Nb(N[Np]Ar)$_3$ (Mes = 2,4,6-*t*-$Bu_3C_6H_2$) with a niobium-P_2 ligand bond.[68] Such a strategy could also be extended to AsP.[69] In addition, Schulz et al. reported a synthesis of reactive four-membered arsenic nitrogen biradicaloid (**C**) and outlined its subsequent reaction with CS_2, S_8, and Se.[70] It was also reported that PN and PP could form stable formal adducts with N-heterocyclic carbene (NHC).[71-73] The first isolation and structural characterization of an *f*-element dinitrogen complex was reported in 1988. Later in 2021, synthesis of a side-on bound diphosphorus complex of uranium(IV) was accomplished using a 7λ^3-(dimethylamino)phosphadibenzonorbornadiene-mediated P-atom transfer approach, containing the activated diphosphorus ligand to its dianionic $(P_2)^{2-}$ form.[74] It also can exist as a triply bonded moiety in the corresponding platinum-centered complex.[75]

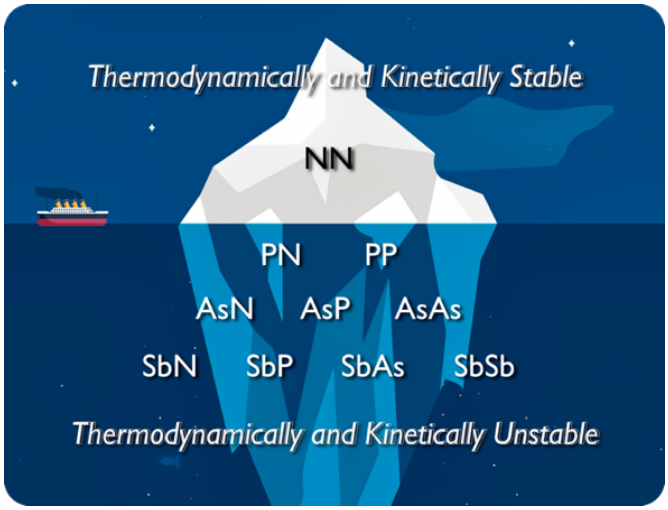

Scheme 4. Dipnictogenes in two groups.

In addition to the monomer, oligomers of heavy dipnictogens also attracted attention due to their unique bonding properties. For example, the spontaneous trimerization of PN has firstly been discovered in a cryogenic matrix upon annealing to 30 K, which gives cyclotriphosphazene (P_3N_3, **13**), an inorganic aromatic analogue of benzene (Scheme 6).[76] The aromatic nature of P_3N_3 is supported by nucleus independent chemical shift (NICS) computations.[77] The negative NICS(1) values of –3.9 ppm for P_3N_3 and –10.2 ppm for C_6H_6 indicate that, in contrast to the borazine $B_3N_3H_3$, which is not regarded as an aromatic molecule, P_3N_3 is aromatic but much less so than benzene. Besides, a homodesmotic evaluation also indicates that P_3N_3 captures only about one-third of the aromatic stabilization of benzene, cyclotriphosphazene has been computed as the most favorable structure among the many isomers that can be envisaged.[78] It later could be generated from the decomposition of hexaazidephosphazene P_3N_{21} or by selectively breaking six chlorine-phosphorus bonds of precursor $P_3N_3Cl_6$ on surface with STM tip.[79] Some other isomers, for example, the iso-valent analog of Dewar benzene, 1,2,4-triaza-3,5,6-triphosphabicyclo[2.2.0]hexa-2,5-diene (**14**), and the iso-valent counterpart of prismane,

prismatic P_3N_3 (1,2,3-triaza-4,5,6-triphosphatetracyclo[2.2.0.0^{2,6}.0^{3,5}]hexane, **15**), were also detected by the tunable soft photoionization reflectron time-of-flight mass spectrometry.[80-81]

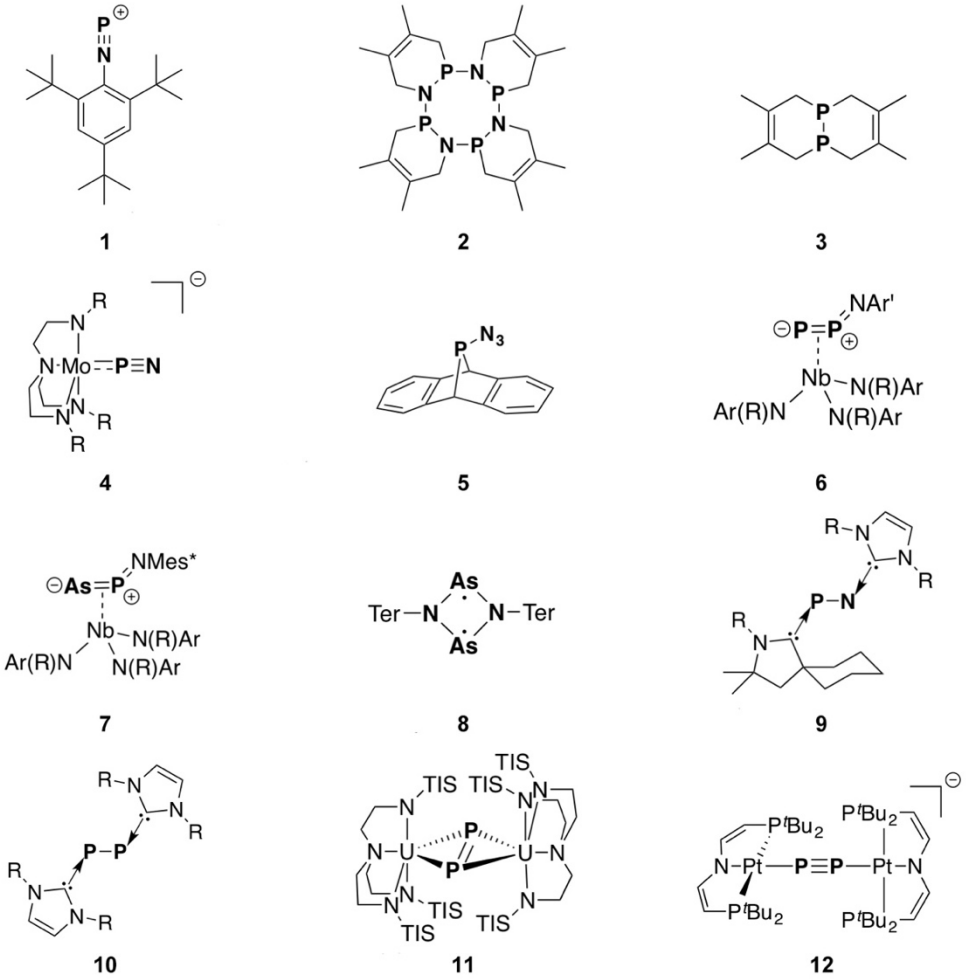

Scheme 5. Compounds and complexes containing dipnictogen moieties.

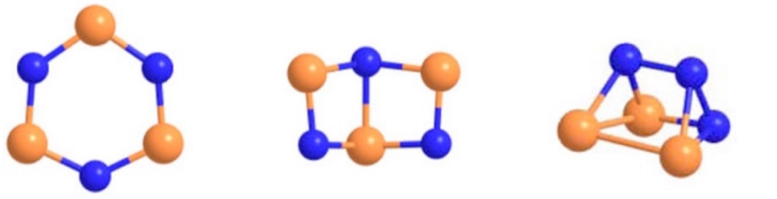

Scheme 6. Detected isomers of cyclotriphosphazene (**13**). The structures were computed at the B3LYP/cc-pVTZ level of theory. Relative energies in kcal mol^{-1} (black), point groups (grey), and ground states (blue) are also shown.[80]

Besides, 2D pnictogen materials have also revealed significant importance due to their outstanding performance in batteries, transitions, and photovoltaic materials.[82-86] Specifically, these materials resolve challenges related to the absence of a band-gap and pronounced chemical inertness, which have traditionally impeded the advancement of highly efficient electronic microdevices.[62, 85, 87-89] Arsenic mononitride (AsN), a heavier congener of PN, can form a distinctive polymer that qualifies as a novel semiconductor material. This compound possesses exceptional electronic and optical properties, both experimentally and theoretically validated, showcasing its promising applications in field-effect transistors (FETs).[84, 90] In a recent study by Ceppatelli et al., achieved the direct synthesis of crystalline singly-bonded AsN from elemental As and N_2 under 20 GPa (Scheme 7b).[62] The findings suggest that AsN monolayers, akin to other two-dimensional pnictogens, exhibit distinctive features, including elevated hole mobility, unique anisotropic characteristics, and ambipolar transport behavior dominated by holes. As a result, these properties position AsN as a promising candidate for the development of next-generation semiconductor materials. Gambin et al. synthesizing nanocrystalline b-AsP on-wafer via molecular beam deposition and subsequent postgrowth hermetic annealing (Scheme 7c).[91] Cross-section TEM images reveal a nanocrystalline film morphology with orthorhombic b-AsP grains on the order of ∼5 nm, which enables the development of next-generation black AsP devices for optoelectronic, digital, and radio frequency (RF) applications.

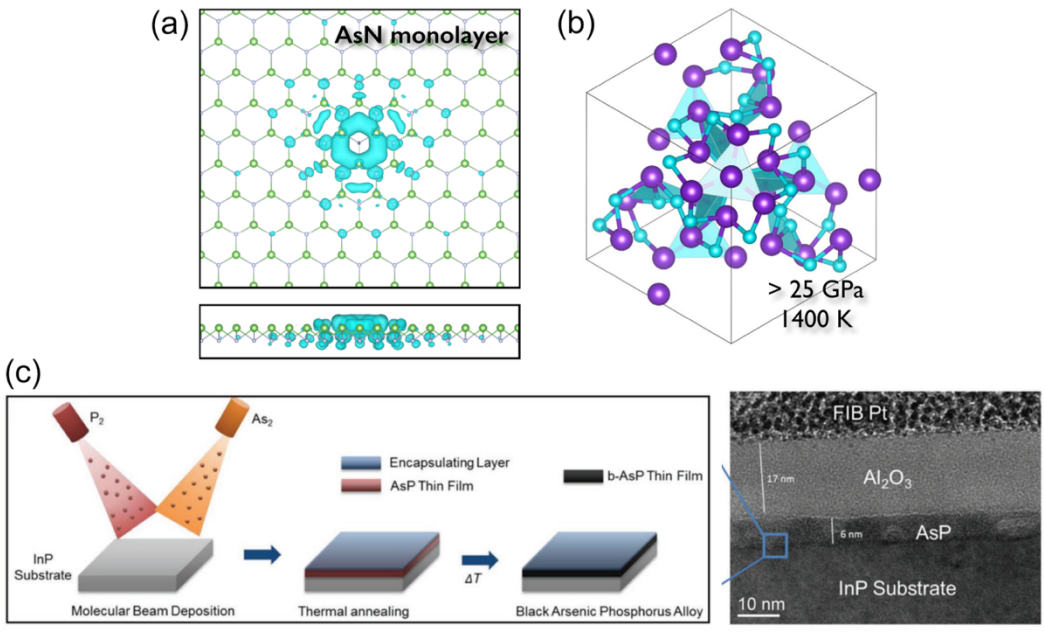

Scheme 7. Examples of heavy dipnictogen polymer. (a) AsN monolayer.[92] (b) Crystalline of AsN under 1400 K, > 25 GPa.[62] (c) Black AsP alloy.[91]

1.2 Pnictogen-Centered Diradicals

A nitrene is the nitrogen analogue of a carbene and the lightest pnictinidene. The nitrogen atom in nitrene is uncharged and monovalent with only six electrons in its valence level: two covalent bonded and four non-bonded electrons. In principle, it may have three different electronic configurations, that is closed-shell singlet, open-shell triplet, and open-shell singlet electronic states (Scheme 8). It is considered an electrophile due to the unsatisfied octet, which is the key reactive intermediate involved in many chemical reactions, for example, C–H insertion, cycloaddition, ring-expansion, and ring-contraction.[93-100] Recently, Li et al. posited that the photosensitized Pauson-Khand-type reaction utilizing diradical reactivity of a triplet nitrene could be relayed to the carbon π-bonds in pendant olefins, thereby inducing a formal [2+2+1] cycloaddition reaction upon late intersystem crossing.[101] The successful realization of this strategy would couple nonconjugated dienes with a triplet nitrene to produce bicyclic pyrrolidines, which—depending on the tether between the olefin units—would constitute a modular synthesis of three-dimensional bioisosteres of six-membered ring *N*-heterocycles with a broad range of applications in medicinal chemistry (Scheme 9).[102]

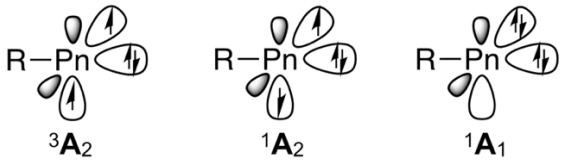

Scheme 8. Electronic configurations of pnictinidenes. Pn indicates a pnictogen atom.

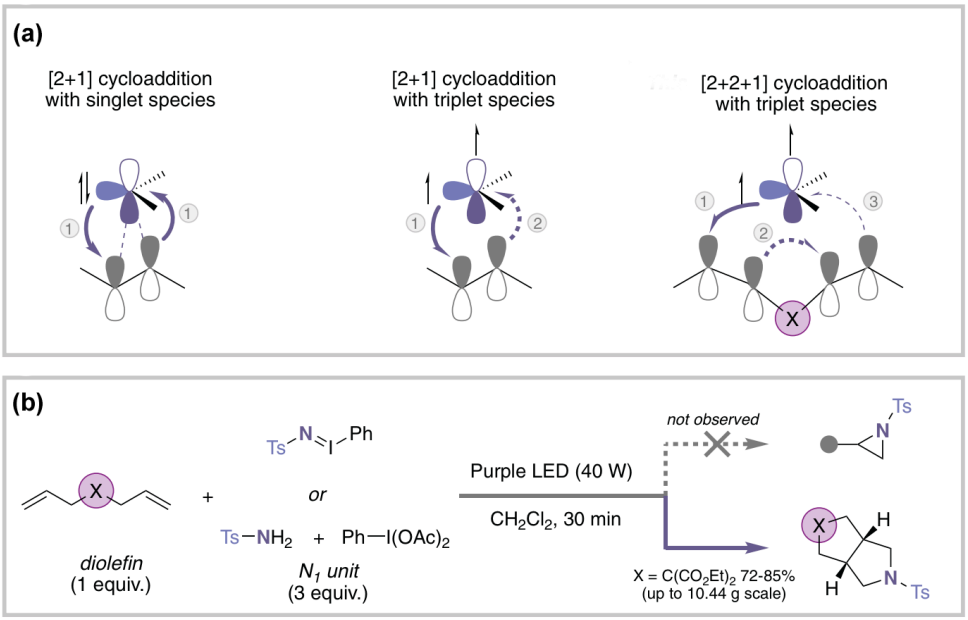

Scheme 9. (a) Reactivity paradigm of singlet and triplet reagents in cycloadditionand relay strategy. (b) [2+2+1] cycloaddition through relay of triplet reactivity. Reaction conditions: Diolefin (1 equiv.), TsNIPh (3 equiv), CH_2Cl_2 (0.1 M concentration of diolefin), 40 W purple LED light, 30 min reaction time. n indicates sequence of reaction steps.[101]

There are several methods to generate nitrenes, each tailored to the specific needs of the reaction and the desired stability of the nitrene intermediate:

1. Thermal or photolytic decomposition of azides: The most widely used method for generating nitrenes involves the decomposition of organic azides ($R–N_3$), where the azide group dissociates under heat or light to release nitrogen gas (N_2) and produces the nitrene. This method is versatile and works well for generating aryl nitrenes, especially when photolysis is used, as it allows for selective excitation and minimizes decomposition of other functional groups.[103-106]
2. Decomposition of isocyanates or imidoyl halides: Nitrenes can also be generated by decomposing of isocyanates (R–N=C=O) or imidoyl halides (R–N=CR'X). These methods are useful when a controlled thermal decomposition process is preferred over photolysis. Isocyanates tend to produce nitrenes with minimal side reactions, making this approach suitable for cases where clean generation of nitrene intermediates is essential.[107-108]
3. Oxidation of amines or amine precursors: Certain oxidation reactions can produce nitrenes by directly oxidizing amine precursors. For instance, oxidation of hydroxylamines or hydrazines can lead to nitrene formation under suitable conditions. This approach is less common due to its dependency on precise control of reaction conditions and is often used in specialized cases.[109-110]
4. Transition metal catalysis: In some cases, transition-metal catalysts can facilitate nitrene generation through nitrogen transfer reactions. For example, metal-nitrene complexes can be generated by reacting metal catalysts with nitrene precursors like azides or iminoiodinanes. These metal-nitrene species are generally more stable and can be selectively transferred to substrates, providing a controlled route for C–N and N–N bond formation in catalysis.[111-114]

Due to their high reactivity, free nitrenes are typically short-lived and tend to undergo rapid rearrangements, insertions, or dimerizations. However, the use of transition metals or stabilizing groups can help control their reactivity and increase their lifespan, allowing for a broader range of applications. Bertrand first reported a singlet phosphinonitrene stabilized by the electron donoating effect (16, Scheme 10).[115] Recently, groups of Beckmann and Tan independently synthesized the stable nitrenes with a triplet ground state, and obtained their structures with X-ray diffraction, which is regarded as a milestone in this field.[116-117]

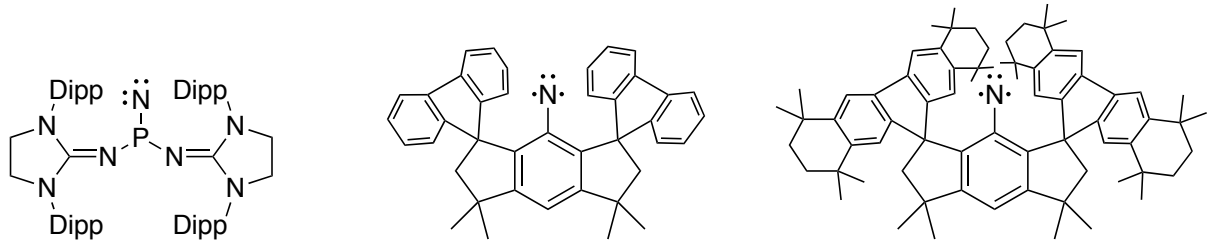

16, $^1\mathbf{A}_1$ **17**, $^3\mathbf{A}_2$ **18**, $^3\mathbf{A}_2$

Scheme 10. The bottle-able nitrenes.

A wide variety of nitrenes has been reported, for example, arylnitrenes, acylnitrenes, alkylnitrenes, sulfinylnitrenes. The attempted photochemical or thermal preparation of parent vinylnitrene from vinyl azide, however, has never succeeded. Because the rate for intersystem crossing is considered to be lower than the rate for intramolecular isomerization, the intermediacy singlet nitrene would undergo rapid isomerization (Scheme 11), although the triplet is the electronic ground state (ΔE_{ST} = 14 kcal mol^{-1}).[118-122] Hence, it is highly unlikely to access the triplet state through conventional nitrene preparation methods.[123-125] However, the structural rigidity of vinylnitrenes attached to cyclic structural moieties (e.g., naphthalene-1,4-dione, 1H-inden-1-one) can make them accessible at cryogenic temperatures, favoring the formation of their triplet states.[126] Vinylphosphinidene is the unreported higher congener of 19. It has been proposed that vinylphosphinidene is produced as a fleeting intermediate in the pyrolysis of vinylphosphirane, which is subsequently converted to phosphapropyne.[127-129]

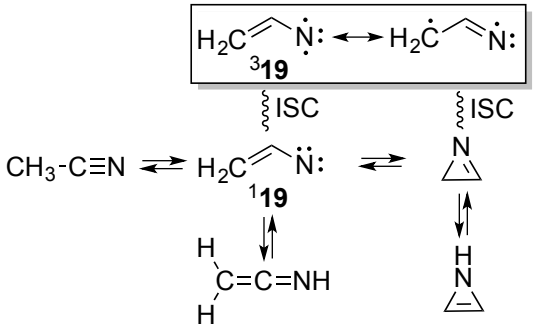

Scheme 11. The unimolecular reactivity of vinylnitrene (**19**).

Phosphinidenes (R–P), the phosphorus analogs of nitrenes, are highly reactive species and versatile intermediates with significant applications across synthetic chemistry, materials science, and catalysis.[130-135] This versatility allows them to participate in numerous bond-forming reactions, including cycloaddition, insertion, and coupling reactions. In addition, transition-metal-stabilized phosphinidenes can activate small molecules such as CO and H_2, showcasing their potential in catalytic transformations and energy-related applications.[136] In recent years, phosphinidenes have also garnered attention in the development of advanced materials,

including phosphorus-containing polymers[137] and phosphorus-based ligands for catalysis,[138] due to their ability to introduce phosphorus into organic frameworks.

In contrast to the straightforward generation nitrenes, the preparation of phosphinidenes is more challenging.[134-135, 139-142] Certain transition-metal complexes have been developed to generate phosphinidenes in a controlled manner.[143-146] Stabilizing phosphinidenes is also challenging, as they readily undergo oxidation, dimerization, or polymerization, especially under ambient conditions. To mitigate this, researchers employ bulky substituents or coordination with transition metals to stabilize the R–P species and prevent premature decomposition. The use of transition-metal coordination, in particular, allows phosphinidenes to exhibit enhanced stability and controlled reactivity, enabling their storage and handling over extended periods. The first example of stable singlet phosphinidene was reported by Bertrand et al. by a similar strategy as used for preparing a stable nitrene.[142] A phosphinophosphinidene was readily generated from the photolysis of the corresponding phosphaketene. The reactivity towards a variety of compounds indicates its role as an electrophile (Scheme 12). Later, Tan et al. attempted to synthesize a stable phosphinidene with a triplet ground state but only obtained the phosphanorcaradiene. Surprisingly, it manifests the same reactivity as a triplet phosphinidene, for example, bond insertion or acts as an electrophile (Scheme 13). Analogously, astable stibinidene[147] and a bismuthinidene[148] were also synthesized with a similar strategy.

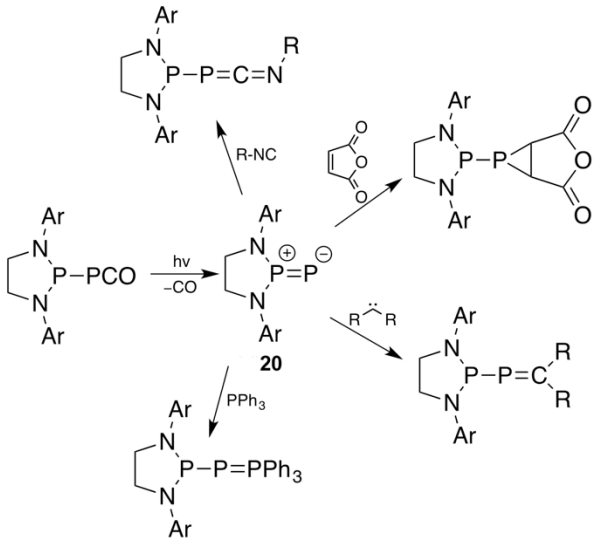

Scheme 12. The reactivity of singlet phosphinidenes (**20**). Ar = ?

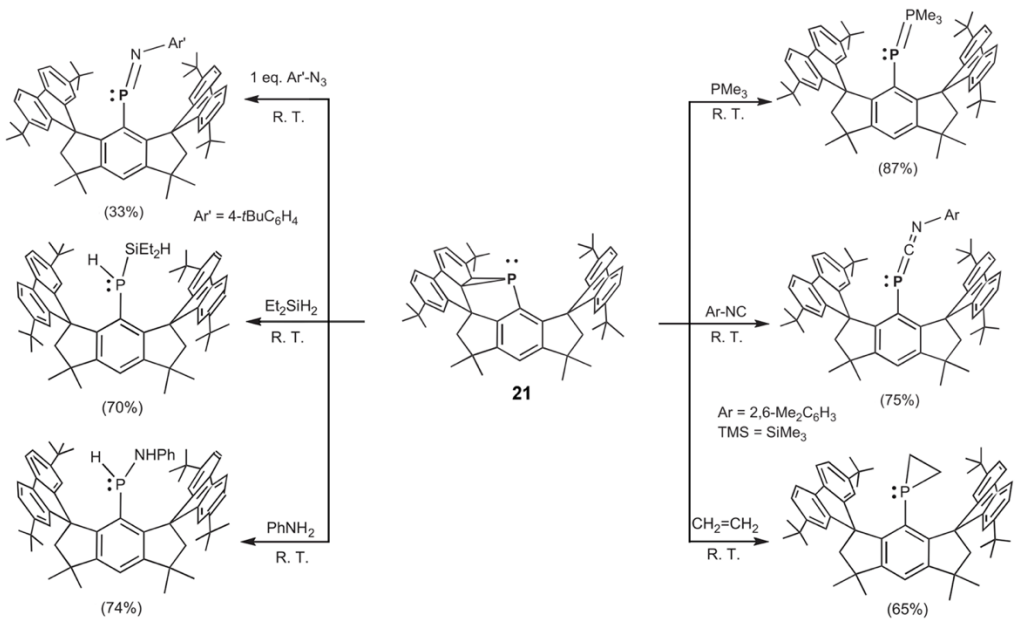

Scheme 13. The reactivity of phosphanorcaradiene (**21**) serving as phosphinidene.

Arsinidenes (R–As), the arsenic analogs of the nitrenes, share some similarities with phosphinidenes but present distinct synthetic challenges and properties due to the heavier arsenic atom. Arsinidenes are less stable and more reactive, with As=X bonds being weaker and more prone to decomposition or rearrangement. As a result, generating and stabilizing arsinidenes is considerably more difficult. Nevertheless, recent advances in synthetic techniques have allowed researchers to generate arsinidene species, often stabilized via coordination with transition metals or bulky ligands.[149-157] These arsinidene complexes, while rare, have demonstrated potential in catalysis and could provide valuable insights into the behavior of heavier pnictogen compounds.

In summary, while phosphinidenes are already well-studied intermediates with applications in catalysis and materials science, arsinidenes remain largely unexplored due to their toxicity, challenging reactivity and stability. Advances in arsinidene chemistry, however, continue to push the boundaries of heavy main-group chemistry and open possibilities for developing new materials and catalytic systems.

1.3 Nitrogen-Rich High-Energy-Density-Materials

Energetic materials are substances capable of storing substantial amounts of chemical energy and releasing it rapidly under specific external stimuli. The development of these materials traces back to the accidental discovery of black powder in China around 220 BC. It was used to make firecrackers for a quite long time afterwards. In Europe, this critical innovation remained largely unexplored until the 13th and 14th centuries, when Roger Bacon (1249) and Berthold Schwarz

(1320) began investigating its properties. Black powder was introduced into military applications towards the end of the 13th century, marking a significant shift in warfare. However, it was not until 1425 that the production methods were significantly refined by the process known as corning. This improvement enhanced the powder's consistency and performance, enabling its use as a propellant in both small arms and, later, large-caliber artillery. Black powder remains in use today, with the U.S. military consuming over 100,000 pounds annually.[158]

Later, some other single-component explosives such as nitroglycerine (NG), mercury fulminate ($Hg(CNO)_2$, MF), nitrocellulose (NC), and picric acid (PA) were developed. In 1863, Joseph Wilbrand first synthesized the famous explosive trinitrotoluene (TNT),[159] which was first used as a dye and later put into military use in 1902 and is still used today. With the advent of high-energy explosives such as RDX (1,3,5-trinitro-1,3,5-triazinane), HMX (1,3,5,7-tetranitro-1,3,5,7-tetrazocane), and CL-20 (or HNIW, hexanitrohexaazaisowurtzitane), weapons and equipment have been continuously upgraded and their combat capabilities have been continuously improved. As the commanding heights of current conventional damage technology, the development and application of ultra-high-energy energetic materials (new high-energy materials with energy levels at least one order of magnitude higher than conventional explosives) can improve the combat effectiveness of weapons and will fundamentally change the combat style and form of war. Therefore, the development of a new generation of ultra-high-energy energetic materials has received great attention from countries around the world.

Given the great demand for high-energy-density materials (HEDMs), in addition to the continuous exploration of metallic hydrogen and metastable nuclear isomers, full-nitrogen compounds or polynitrogens — molecular species that consist entirely of nitrogen atoms are also one of the frontiers and research hot topics in the field of energetic materials because they contain a large amount of energy stored in their bonds and only release harmless nitrogen upon decomposition.[160-161]

Calculations show that the total energy released by polynitrogens can reach 3-8 times the TNT equivalent, the theoretical propulsion specific impulse can be over 350 s, and most importantly, it has the advantages of clean detonation products. However, usually the more nitrogen atoms in the molecular structure, the more unstable the compound, resulting in the great challenge for the synthesis of energetic compounds fully composed of nitrogen. From a thermodynamic point of view, these compounds are likely to decompose into N_2 molecules. In order to achieve the preparation of compounds fully composed of nitrogen, researchers have been striving to seek novel synthesis methods and stabilization technologies to continuously challenge the higher limits of the nitrogen content of a molecule.

Tetrazole is often used as a key unit for the preparation of nitrogen-rich HEDMs due to its high nitrogen content.[162-165] Cheng et al. used 1,5-diaminotetrazole as the raw material and prepared

an energetic salt (Scheme 14) with eleven nitrogen atoms directly connected by an –NH–N^+–NH– bridge through a diazotization coupling reaction, and the structure was confirmed through X-ray single crystal diffraction.[166] This is the longest nitrogen chain in a nitrogen-rich compound reported so far, which provides a new entry point for the synthesis of novel structures, longer nitrogen chains and even compounds fully composed of nitrogen. However, the presence of chloride ions in the molecule greatly reduces its nitrogen content (74%). Subsequently, Ye et al. used 5-aminotetrazole and synthesized a nitrogen-rich compound with four tetrazoles bridged by azo through a two-steps procedure of ring closure and oxidation (Scheme 15).[167] It further reacted with hydrazine hydrate to prepare a novel nitrogen-rich hydrazine salt with a nitrogen content of 84% and a decomposition temperature of up to 202°C. It has the advantages of a simple synthesis route and easy large-scale preparation. Klapötke et al. prepared a new type of nitrogen-rich compound (C_2N_{14}) through diazotization and intramolecular ring closure reaction, with a nitrogen content of up to 89%.[168] However, this compound is extremely sensitive to external stimuli and can explode under extremely slight shock or friction with the shock and friction sensitivity lower than the experimentally determine limits of 0.25 J in impact and 1 N, respectively. This sensitivity is thought to be due to the enormous inequality in the charge distribution and extremely high heat of formation (1495 kJ mol^{-1}). In addition, tetraazidomethane (CN_{12}, **24**) was prepared by Banert et al., which pushed the nitrogen content to a new level (93%).[169] It could be readily synthesized from $NCCCl_3$ or $(N_3)_3C^+$ $SbCl_6^-$ by treating with the azide-transfer agent and its reactivity towards variety substrates was also investigated (Scheme 16). The ^{15}N-isotope labeling could be achieved by treating with the reagent $(Me_2N)_2C{=}NH_2^+$ $^{15}N_3^-$. The ionic dissociation was evidenced by the transformation into the triazidocarbenium salt 3b by addition of $SbCl_5$. In addtion, it could be used as a synthon of NCN as shown in the reaction with PPh_3 and $Ph_2PCH_2CH_2PPh_2$. A click reaction product could be detected when reacting with a cyclic alkene or an alkyne. Compound **24** can also hydrolyze to carbonyl diazide $OC(N_3)_2$.

However, the presence of carbon atoms in the molecule greatly limits the further increase of nitrogen content. Researchers continue to explore the preparation method with nitrogen-rich materials, among which ions fully composed of nitrogen are very likely to be prepared first. In terms of polynitrogen cation, Christe et al. first synthesized V-shaped chain-like N_5^+ in 1998, which is recognized as a breakthrough in the separation of nitrogen-rich energetic materials.[170] However, $AsF_6^-N_5^+$ has extremely poor stability and requires harsh reaction conditions. It needs to be prepared at ultra-low temperatures and with anhydrous HF, which makes quantitative production difficult, hindering the development of polynitrogen cation based energetic ionic compounds, and the presence of counteranions reduces the nitrogen content to only 27%. Later, by replacing the arsenic center with antimony, another new salt $SbF_6^-N_5^+$ was prepared from $SbF_6^-N_2F^+$ and HN_3 in anhydrous HF solution. The white solid is surprisingly stable, decomposing only at 70 °C, and is relatively insensitive to impact.[171]

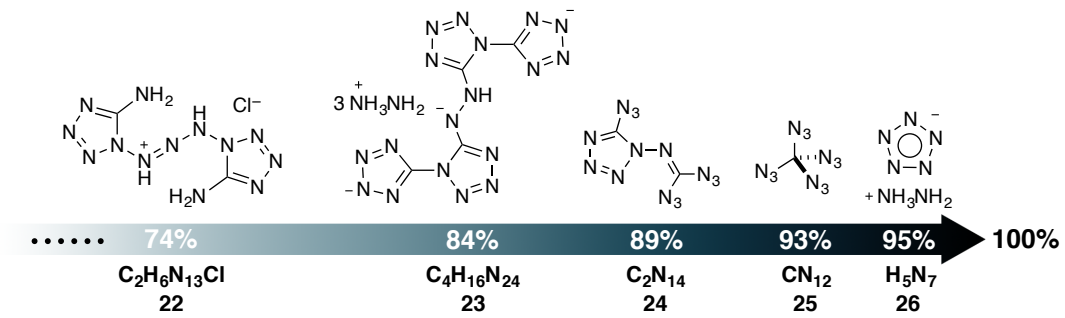

Scheme 14. Representative materials with high nitrogen content.

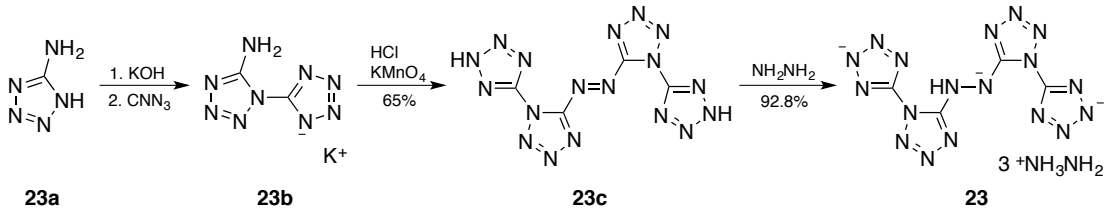

Scheme 15. The preparation of compound **23**.

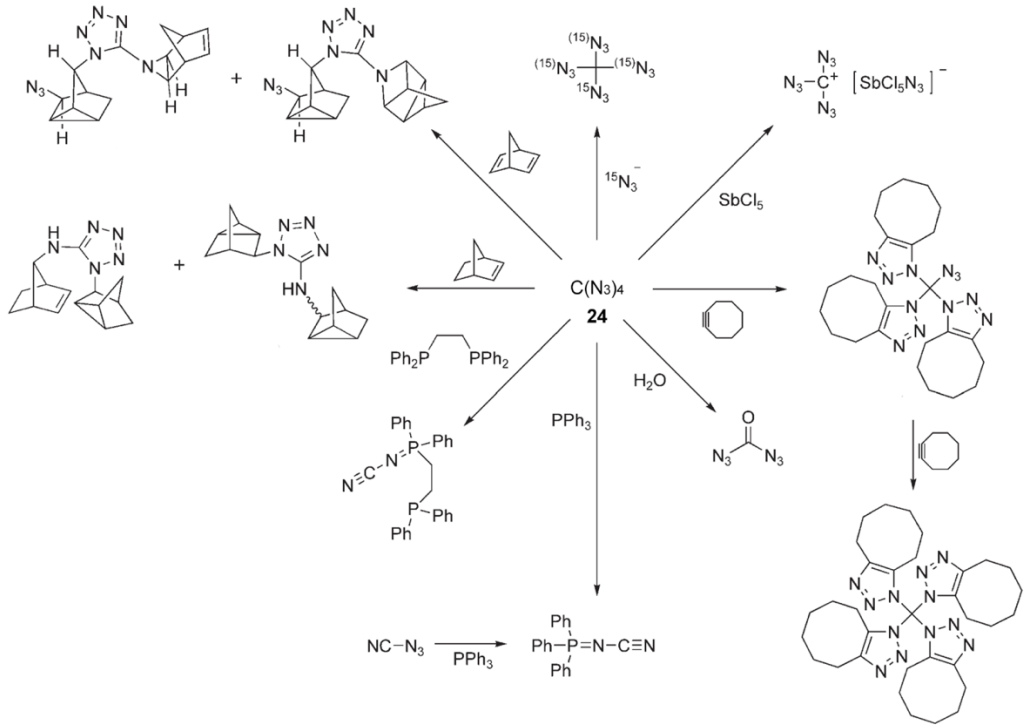

Scheme 16. Reactions of tetraazidomethane (**24**).

One of the most promising approaches until now to stabilize and study these reactive nitrogen allotropes is through the use of a diamond anvil cell (DAC, Scheme 17), which can apply extreme pressures, often exceeding several million atmospheres, and high temperatures to break and reform the strong triple bond in molecular nitrogen (N_2) as well as to create environments where polynitrogens and nitrogen ions can form and persist.

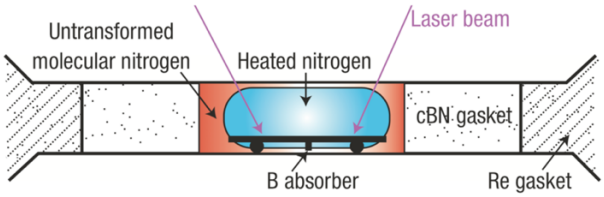

Scheme 17. Laser-heated diamond anvil cell (DAC).

The study of materials composed fully of nitrogen using a diamond anvil cell (DAC) has led to the discovery of several unique nitrogen allotropes and structures with potential applications in high-energy-density materials. Here are a few notable examples:

1. Polymeric nitrogen (cg-N, Scheme 18a): one of the most studied forms of polynitrogen is cubic gauche nitrogen (cg-N), a nitrogen allotrope discovered under extreme conditions in a DAC. In cg-N, nitrogen atoms are linked in a three-dimensional network structure, similar to the carbon atoms in diamond, making it a high-density material with a high energy release potential. Upon decompression, cg-N can release substantial energy due to the transformation back to molecular nitrogen (N_2), making it a potential candidate for high-energy applications such as propellants and explosives.[172]
2. Nitrogen-rich phases (linear N_8, Scheme 18b): DAC experiments have also enabled the formation of nitrogen clusters and ring structures, such as N_8. These ring systems, analogous to carbon rings, involve nitrogen atoms bonded in cyclic configurations. N_8, for example, consists of eight nitrogen atoms arranged in a linear structure and is a potential candidate for high-energy storage, given that breaking the ring releases energy. Such linear structures, while difficult to stabilize, provide insights into the bonding versatility of nitrogen and could inspire new synthetic methods for energy materials.[173-175]
3. Layered nitrogen phases (lp-N, Scheme 18c; hlp-N, Scheme 18d; and bp-N, Scheme 18e): researchers have also observed nitrogen phases under DAC conditions that adopt layered structures similar to graphite, with nitrogen atoms arranged in two-dimensional sheets. These layered nitrogen allotropes are of interest due to their potential for creating two-dimensional materials analogous to graphene, but with nitrogen. In addition, the nitrogen analogue of black-phosphorus phase (bp-N) was also synthesized.[176-177] Like black phosphorus, bp-N is an electrical conductor. The existence of bp-N structure matches the behavior of heavier pnictogens, and reaffirms the trend that elements at high pressure adopt the same structures as heavier congeners at lower pressures. Such materials could have unique electronic and mechanical properties and may be useful in semiconductor applications if stable at lower pressures.[176, 178-179]
4. High-pressure phase of molecular nitrogen (ε-N_2, Scheme 18f): at pressures above 110 GPa, molecular nitrogen can be transformed into a high-density phase known as ε-N_2,

where N_2 molecules are arranged in a highly ordered structure. While this phase does not feature the extended bonding found in cg-N or α-N, it demonstrates how DAC can alter the molecular arrangement and properties of nitrogen. ε-N_2 has attracted interest as it could offer a denser form of nitrogen storage and potentially be useful in applications where high-pressure energy release is required.[180-181]

Each of these allotropes and nitrogen-containing ions illustrates the versatility and potential of nitrogen under extreme conditions. DAC experiments not only enable the exploration of these unique forms of nitrogen but also contribute to our understanding of high-energy materials, offering future possibilities for applications in propulsion, explosives, and novel electronic materials.

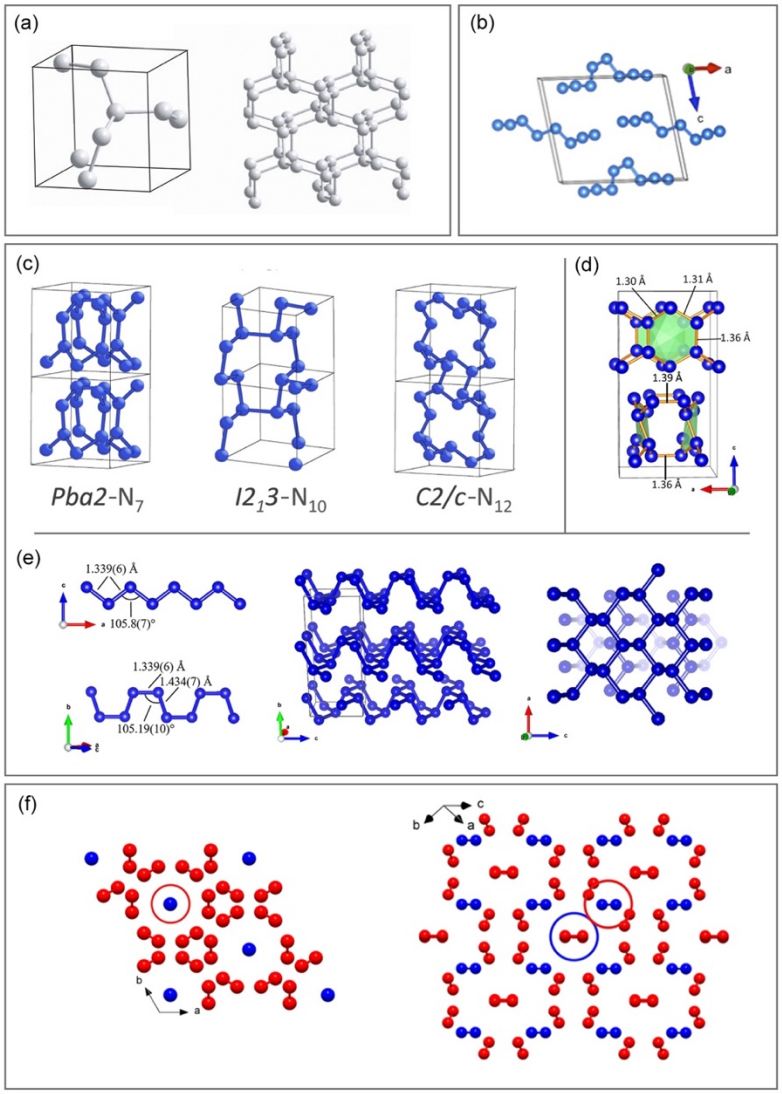

Scheme 18. Sturctures of polynitrogens in DAC. (a) cg-N structure.[172] (b) Crystal structures of N_8 molecule.[173] (c) Crystal structures of the proposed phases showing the layered *Pba2* structure

made of seven-membered N-N (N_7) rings in comparison with the $I2_13$ and $C2/c$ structures made of even-numbered N_{10} and N_{12} rings in 3D networks, respectively.[178] (d) Drawing of the $P4_2bc$ crystal structure at 235 GPa, with the five distinct N-N bond lengths marked. For clarity, the inner surface of the N_6 hexagons is filled with a light green plane. The layered nature of the $P4_2bc$ structure is clearly seen.[179] (e) Crystal structure of bp-N. Left: the zigzag and armchair arrangements forming the bp-N layers. Middle: the crystal structure of bp-N, where the zigzag and armchair chains are visible. Right: two superimposed layers of the bp-N structure, highlighting the puckered honeycomb arrangement of fused N_6 hexagons.[176] (f) The structure of ε-N_2 viewed along the c direction (the blue and red spheres represent the N1 and N2 atoms, respectively); (f) the structure of ε-N_2 in the orientation simplifying a comparison with the structure of ζ-N_2.[180]

1.4 Outlook

Pnictogen chemistry remains a rich and largely unexplored field, particularly for low-valent and low-coordinate species. As mentioned in previous sections, the reactivity of heavy pnictinidenes—such as arsinidene (R-As)—remain largely unknown due to their intrinsic instability, toxicity and synthetic challenges. Further studies on the reaction towards small molecules (e.g., CO, NO) and organic substrates (e.g., ethylene, methanol) could offer critical insights into their difference with carbenes and nitrenes. Moreover, the study of heavy dipnictogen species (e.g., AsN, AsP) had been hindered by their transient nature and the lacking of selective generation methods. Investigation in this work now offers facile approach for selectively preparing these elusive species. Future research may focus on the capture of free heavy dipnictogens in solution, the mechanism of oligomerization and optimizing precursors to improve yields. Lastly, the preparation of neutral nitrogen allotropes beyond the stable N_2. Preliminary experimental and theoretical studies suggest the existence of higher allotropes, though their preparation remain challenging. Further investigations are required to determine whether a trend or regularity exist in their structures or stabilities.

In summary, these unexplored or underexplored areas of pnictogen chemistry present potential opportunities for future research. By combining new synthetic strategies, spectroscopic techniques, and theoretical prediction, it would not only deepen the understanding of the bonding and reactivity but also pave the way for and applications of pnictogen-bearing compounds in the field of catalysis, small molecule activation, materials science or high-energy-density materials.

References

[1] L. Y. Stein, M. G. Klotz, The nitrogen cycle, *Curr. Biol.* **2016**, *26*, R94-R98.
[2] H. R. Schulten, M. Schnitzer, The chemistry of soil organic nitrogen: a review, *Biol. Fertil. Soils* **1997**, *26*, 1-15.

[3] P. Hlavica, Functional interaction of nitrogenous organic bases with cytochrome P450: A critical assessment and update of substrate features and predicted key active-site elements steering the access, binding, and orientation of amines, *Biochim. Biophys. Acta, Proteins Proteomics* **2006**, *1764*, 645-670.

[4] P. H. Mhatre, C. Karthik, K. Kadirvelu, K. L. Divya, E. P. Venkatasalam, S. Srinivasan, G. Ramkumar, C. Saranya, R. Shanmuganathan, Plant growth promoting rhizobacteria (PGPR): A potential alternative tool for nematodes bio-control, *Biocatal. Agric. Biotechnol.* **2019**, *17*, 119-128.

[5] A. Blanco, G. Blanco, in *Medical Biochemistry* (Eds.: A. Blanco, G. Blanco), Academic Press, **2017**, pp. 413-423.

[6] Y. Kim, Y. Park, A. Choi, N.-S. Choi, J. Kim, J. Lee, J. H. Ryu, S. M. Oh, K. T. Lee, An Amorphous Red Phosphorus/Carbon Composite as a Promising Anode Material for Sodium Ion Batteries, *Adv. Mater.* **2013**, *25*, 3045-3049.

[7] M. B. Geeson, C. C. Cummins, Phosphoric acid as a precursor to chemicals traditionally synthesized from white phosphorus, *Science* **2018**, *359*, 1383-1385.

[8] P. Mal, B. Breiner, K. Rissanen, J. R. Nitschke, White Phosphorus Is Air-Stable Within a Self-Assembled Tetrahedral Capsule, *Science* **2009**, *324*, 1697-1699.

[9] B. M. Cossairt, N. A. Piro, C. C. Cummins, Early-Transition-Metal-Mediated Activation and Transformation of White Phosphorus, *Chem. Rev.* **2010**, *110*, 4164-4177.

[10] W. L. Roth, T. W. DeWitt, A. J. Smith, Polymorphism of Red Phosphorus, *J. Am. Chem. Soc.* **1947**, *69*, 2881-2885.

[11] R. W. Keyes, The Electrical Properties of Black Phosphorus, *Phys. Rev.* **1953**, *92*, 580-584.

[12] Y. Zhang, C. Ma, J. Xie, H. Ågren, H. Zhang, Black Phosphorus/Polymers: Status and Challenges, *Adv. Mater.* **2021**, *33*, 2100113.

[13] X. Ling, H. Wang, S. Huang, F. Xia, M. S. Dresselhaus, The renaissance of black phosphorus, *Proc. Natl. Acad. Sci. U.S.A.* **2015**, *112*, 4523-4530.

[14] L. Li, Y. Yu, G. J. Ye, Q. Ge, X. Ou, H. Wu, D. Feng, X. H. Chen, Y. Zhang, Black phosphorus field-effect transistors, *Nat. Nanotechnol.* **2014**, *9*, 372-377.

[15] Y. Sui, J. Zhou, X. Wang, L. Wu, S. Zhong, Y. Li, Recent advances in black-phosphorus-based materials for electrochemical energy storage, *Mater. Today* **2021**, *42*, 117-136.

[16] M. A. Pasek, Thermodynamics of Prebiotic Phosphorylation, *Chem. Rev.* **2020**, *120*, 4690-4706.

[17] J. Diaz, E. Ingall, C. Benitez-Nelson, D. Paterson, M. D. de Jonge, I. McNulty, J. A. Brandes, Marine Polyphosphate: A Key Player in Geologic Phosphorus Sequestration, *Science* **2008**, *320*, 652-655.

[18] A. M. Turner, A. Bergantini, M. J. Abplanalp, C. Zhu, S. Góbi, B.-J. Sun, K.-H. Chao, A. H. H. Chang, C. Meinert, R. I. Kaiser, An interstellar synthesis of phosphorus oxoacids, *Nat. Commun.* **2018**, *9*, 3851.

[19] M. S. Ram, K.-M. Persson, A. Irish, A. Jönsson, R. Timm, L.-E. Wernersson, High-density logic-in-memory devices using vertical indium arsenide nanowires on silicon, *Nat. Electron.* **2021**, *4*, 914-920.

[20] M. S. Lundstrom, M. A. Alam, Moore's law: The journey ahead, *Science* **2022**, *378*, 722-723.

[21] W. Metaferia, K. L. Schulte, J. Simon, S. Johnston, A. J. Ptak, Gallium arsenide solar cells grown at rates exceeding 300 μm h−1 by hydride vapor phase epitaxy, *Nat. Commun.* **2019**, *10*, 3361.

[22] M. Wuttig, N. Yamada, Phase-change materials for rewriteable data storage, *Nat. Mater.* **2007**, *6*, 824-832.

[23] W. Zhang, R. Mazzarello, M. Wuttig, E. Ma, Designing crystallization in phase-change materials for universal memory and neuro-inspired computing, *Nat. Rev. Mater.* **2019**, *4*, 150-168.

[24] R. Calarco, F. Arciprete, Keep it simple and switch to pure tellurium, *Science* **2021**, *374*, 1321-1322.

[25] J. Shen, S. Jia, N. Shi, Q. Ge, T. Gotoh, S. Lv, Q. Liu, R. Dronskowski, S. R. Elliott, Z. Song, M. Zhu, Elemental electrical switch enabling phase segregation–free operation, *Science* **2021**, *374*, 1390-1394.

[26] F. A. Rahman, D. L. Allan, C. J. Rosen, M. J. Sadowsky, Arsenic Availability from Chromated Copper Arsenate (CCA)–Treated Wood, *J. Environ. Qual.* **2004**, *33*, 173-180.

[27] P. Büscher, G. Cecchi, V. Jamonneau, G. Priotto, Human African trypanosomiasis, *Lancet* **2017**, *390*, 2397-2409.

[28] S. Gibaud, G. Jaouen, in *Medicinal Organometallic Chemistry* (Eds.: G. Jaouen, N. Metzler-Nolte), Springer Berlin Heidelberg, Berlin, Heidelberg, **2010**, pp. 1-20.

[29] E. Nachman Keeve, P. Graham Jay, B. Price Lance, K. Silbergeld Ellen, Arsenic: A Roadblock to Potential Animal Waste Management Solutions, *Environ. Health Perspect.* **2005**, *113*, 1123-1124.

[30] S. C. Grund, K. Hanusch, H. U. Wolf, in *Ullmann's Encyclopedia of Industrial Chemistry*, **2008**.

[31] S. C. Grund, K. Hanusch, H. J. Breunig, H. U. Wolf, in *Ullmann's Encyclopedia of Industrial Chemistry*, **2006**.

[32] J. W. Hastie, Mass spectrometric studies of flame inhibition: Analysis of antimony trihalides in flames, *Combust. Flame* **1973**, *21*, 49-54.

[33] J. G. Downing, COSMETICS — PAST AND PRESENT, *J. Am. Med. Assoc.* **1934**, *102*, 2088-2091.

[34] A. Al-Kaff, A. Al-Rajhi, K. Tabbara, A. El-Yazigi, Kohl-The Traditional Eyeliner: Use and Analysis, *Ann. Saudi Med.* **1993**, *13*, 26-30.

[35] E. Svensson Grape, V. Rooth, M. Nero, T. Willhammar, A. K. Inge, Structure of the active pharmaceutical ingredient bismuth subsalicylate, *Nat. Commun.* **2022**, *13*, 1984.

[36] T. E. Sox, C. A. Olson, Binding and killing of bacteria by bismuth subsalicylate, *Antimicrob. Agents Chemother.* **1989**, *33*, 2075-2082.

[37] R. J. G. Parnell, Bismuth in the Treatment of Syphilis, *Proc. R. Soc. Med.* **1924**, *17*, 19-26.

[38] K. D. Hopper, S. H. King, M. E. Lobell, T. R. TenHave, J. S. Weaver, The breast: in-plane x-ray protection during diagnostic thoracic CT--shielding with bismuth radioprotective garments, *Radiology* **1997**, *205*, 853-858.

[39] A. La Fontaine, V. J. Keast, Compositional distributions in classical and lead-free brasses, *Mater. Charact.* **2006**, *57*, 424-429.

[40] F. J. Maile, G. Pfaff, P. Reynders, Effect pigments—past, present and future, *Prog. Org. Coat.* **2005**, *54*, 150-163.
[41] N. Thompson, The electrical resistance of bismuth alloys, *Proc. R. Soc. Lond. A Math. Phys. Sci.* **1997**, *155*, 111-123.
[42] M. Yan, M. Šob, D. E. Luzzi, V. Vitek, G. J. Ackland, M. Methfessel, C. O. Rodriguez, Interatomic forces and atomic structure of grain boundaries in copper-bismuth alloys, *Phys. Rev. B* **1993**, *47*, 5571-5582.
[43] J. M. Reynolds, C. T. Lane, Superconducting Bismuth Alloys, *Phys. Rev.* **1950**, *79*, 405-406.
[44] Z. Yu, P. R. Cantwell, Q. Gao, D. Yin, Y. Zhang, N. Zhou, G. S. Rohrer, M. Widom, J. Luo, M. P. Harmer, Segregation-induced ordered superstructures at general grain boundaries in a nickel-bismuth alloy, *Science* **2017**, *358*, 97-101.
[45] M. J. Chalkley, M. W. Drover, J. C. Peters, Catalytic N_2-to-NH_3 (or -N_2H_4) Conversion by Well-Defined Molecular Coordination Complexes, *Chem. Rev.* **2020**, *120*, 5582-5636.
[46] C. M. Johansen, E. A. Boyd, J. C. Peters, Catalytic transfer hydrogenation of N_2 to NH_3 via a photoredox catalysis strategy, *Sci. Adv.* **2022**, *8*, eade3510.
[47] J. M. Thomas, Handbook Of Heterogeneous Catalysis. 2., completely revised and enlarged Edition. Vol. 1–8. Edited by G. Ertl, H. Knözinger, F. Schüth, and J. Weitkamp, *Angew. Chem. Int. Ed.* **2009**, *48*, 3390-3391.
[48] F. Haber, G. van Oordt, Über die Bildung von Ammoniak den Elementen, *Zeitschrift für anorganische Chemie* **1905**, *44*, 341-378.
[49] B. Rösch, T. X. Gentner, J. Langer, C. Färber, J. Eyselein, L. Zhao, C. Ding, G. Frenking, S. Harder, Dinitrogen complexation and reduction at low-valent calcium, *Science* **2021**, *371*, 1125-1128.
[50] T.-T. Liu, D.-D. Zhai, B.-T. Guan, Z.-J. Shi, Nitrogen fixation and transformation with main group elements, *Chem. Soc. Rev.* **2022**, *51*, 3846-3861.
[51] A. Ikpe, E. Wilson, E. Usungurua, *Dynamics of Ammonia Synthesis from Industrial Reactors: a Gaze towards Production Diversity*, **2024**.
[52] O. J. Scherer, Small Neutral P Molecules, *Angew. Chem. Int. Ed.* **2000**, *39*, 1029-1030.
[53] L. Weber, A Different View of Coordination Chemistry: Bis(carbene) Adducts of (P≡N) and (P≡N)+, *Angew. Chem. Int. Ed.* **2010**, *49*, 5829-5830.
[54] L. M. Ziurys, D. R. Schmidt, J. J. Bernal, New Circumstellar Sources of PO and PN: The Increasing Role of Phosphorus Chemistry in Oxygen-rich Stars, *Astrophys. J.* **2018**, *856*, 169.
[55] B. Lefloch, C. Vastel, S. Viti, I. Jimenez-Serra, C. Codella, L. Podio, C. Ceccarelli, E. Mendoza, J. R. D. Lepine, R. Bachiller, Phosphorus-bearing molecules in solar-type star-forming regions: first PO detection, *Mon. Not. R. Astron. Soc.* **2016**, *462*, 3937-3944.
[56] L. M. Ziurys, Detection of Interstellar PN: The First Phosphorus-bearing Species Observed in Molecular Clouds, *Astrophys. J.* **1987**, *321*, L81.
[57] T. Yamaguchi, S. Takano, N. Sakai, T. Sakai, S.-Y. Liu, Y.-N. Su, N. Hirano, S. Takakuwa, Y. Aikawa, H. Nomura, S. Yamamoto, Detection of Phosphorus Nitride in the Lynds 1157 B1 Shocked Region, *Publ. Astron. Soc. Japan* **2011**, *63*, L37-L41.
[58] R. B. Viana, P. S. S. Pereira, L. G. M. Macedo, A. S. Pimentel, A quantum chemical study on the formation of phosphorus mononitride, *Chem. Phys.* **2009**, *363*, 49-58.
[59] B. E. Turner, J. Bally, Detection of Interstellar PN: The First Identified Phosphorus Compound in the Interstellar Medium, *Astrophys. J.* **1987**, *321*, L75.
[60] J. Curry, L. Herzberg, G. Herzberg, Spectroscopic Evidence for the Molecule PN, *J. Chem. Phys.* **1933**, *1*, 749-749.
[61] K. A. Gingerich, Gaseous phosphorus compounds. III. Mass spectrometric study of the reaction between diatomic nitrogen and phosphorus vapor and dissociation energy of phosphorus mononitride and diatomic phosphorus, *J. Phys. Chem.* **1969**, *73*, 2734-2741.
[62] M. Ceppatelli, D. Scelta, M. Serrano-Ruiz, K. Dziubek, M. Morana, V. Svitlyk, G. Garbarino, T. Poręba, M. Mezouar, M. Peruzzini, R. Bini, Single-Bonded Cubic AsN from High-Pressure and High-Temperature Chemical Reactivity of Arsenic and Nitrogen, *Angew. Chem. Int. Ed.* **2022**, *61*, e202114191.
[63] E. Niecke, M. Nieger, F. Reichert, Arylmino(halogeno)phosphanes XP=$NC_6H_2tBu_3$ (X = Cl, Br, I) and the Iminophosphenium Tetrachloroaluminate $[P{\equiv}NC_6H_2tBu_3]^{\oplus}[AlCl_4]^{\ominus}$: the First Stable Compound with a PN Triple Bond, *Angew. Chem., Int. Ed. Engl.* **1988**, *27*, 1715-1716.
[64] C. Hering, A. Schulz, A. Villinger, Diatomic PN – trapped in a cyclo-tetraphosphazene, *Chem. Sci.* **2014**, *5*, 1064-1073.
[65] D. Tofan, C. C. Cummins, Photochemical Incorporation of Diphosphorus Units into Organic Molecules, *Angew. Chem. Int. Ed.* **2010**, *49*, 7516-7518.
[66] D. Tofan, A. Velian, Interstellar Chemistry in a Glovebox: Elusive Diatomic P≡N, Exposed, *ACS Cent. Sci.* **2020**, *6*, 1485-1487.
[67] A. K. Eckhardt, M.-L. Y. Riu, M. Ye, P. Müller, G. Bistoni, C. C. Cummins, Taming phosphorus mononitride, *Nat. Chem.* **2022**, *14*, 928-934.
[68] N. A. Piro, J. S. Figueroa, J. T. McKellar, C. C. Cummins, Triple-Bond Reactivity of Diphosphorus Molecules, *Science* **2006**, *313*, 1276-1279.
[69] H. A. Spinney, N. A. Piro, C. C. Cummins, Triple-Bond Reactivity of an AsP Complex Intermediate: Synthesis Stemming from Molecular Arsenic, As_4, *J. Am. Chem. Soc.* **2009**, *131*, 16233-16243.
[70] S. Demeshko, C. Godemann, R. Kuzora, A. Schulz, A. Villinger, An Arsenic–Nitrogen Biradicaloid: Synthesis, Properties, and Reactivity, *Angew. Chem. Int. Ed.* **2013**, *52*, 2105-2108.
[71] R. Kinjo, B. Donnadieu, G. Bertrand, Isolation of a Carbene-Stabilized Phosphorus Mononitride and Its Radical Cation (PN+.), *Angew. Chem. Int. Ed.* **2010**, *49*, 5930-5933.

[72] O. Back, G. Kuchenbeiser, B. Donnadieu, G. Bertrand, Nonmetal-Mediated Fragmentation of P_4: Isolation of P_1 and P_2 Bis(carbene) Adducts, *Angew. Chem. Int. Ed.* **2009**, *48*, 5530-5533.

[73] Y. Wang, Y. Xie, P. Wei, R. B. King, H. F. Schaefer, III, P. v. R. Schleyer, G. H. Robinson, Carbene-Stabilized Diphosphorus, *J. Am. Chem. Soc.* **2008**, *130*, 14970-14971.

[74] J. Du, D. Hunger, J. A. Seed, J. D. Cryer, D. M. King, A. J. Wooles, J. van Slageren, S. T. Liddle, Dipnictogen f-Element Chemistry: A Diphosphorus Uranium Complex, *J. Am. Chem. Soc.* **2021**, *143*, 5343-5348.

[75] J. Sun, H. Verplancke, J. I. Schweizer, M. Diefenbach, C. Würtele, M. Otte, I. Tkach, C. Herwig, C. Limberg, S. Demeshko, M. C. Holthausen, S. Schneider, Stabilizing P≡P: P_2^{2-}, $P_2^{\bullet-}$, and P_2^0 as bridging ligands, *Chem* **2021**, *7*, 1952-1962.

[76] R. M. Atkins, P. L. Timms, The matrix infrared spectrum of PN and SiS, *Spectrochim. Acta, Part A* **1977**, *33*, 853-857.

[77] P. v. R. Schleyer, C. Maerker, A. Dransfeld, H. Jiao, N. J. R. van Eikema Hommes, Nucleus-Independent Chemical Shifts: A Simple and Efficient Aromaticity Probe, *J. Am. Chem. Soc.* **1996**, *118*, 6317-6318.

[78] A. A. Starikova, N. M. Boldyreva, R. M. Minyaev, A. I. Boldyrev, V. I. Minkin, Computational Assessment of an Elusive Aromatic N_3P_3 Molecule, *ACS Omega* **2018**, *3*, 286-291.

[79] Q. Zhong, A. Mardyukov, E. Solel, D. Ebeling, A. Schirmeisen, P. R. Schreiner, On-Surface Synthesis and Real-Space Visualization of Aromatic P3N3, *Angew. Chem. Int. Ed.* **2023**, *62*, e202310121.

[80] C. Zhu, A. K. Eckhardt, A. Bergantini, S. K. Singh, P. R. Schreiner, R. I. Kaiser, The elusive cyclotriphosphazene molecule and its Dewar benzene–type valence isomer (P3N3), *Sci. Adv.* **2020**, *6*, eaba6934.

[81] C. Zhu, A. K. Eckhardt, S. Chandra, A. M. Turner, P. R. Schreiner, R. I. Kaiser, Identification of a prismatic P_3N_3 molecule formed from electron irradiated phosphine-nitrogen ices, *Nat. Commun.* **2021**, *12*, 5467.

[82] Y. Zhang, T. Ouyang, C. He, J. Li, C. Tang, Extremely promising monolayer materials with robust ferroelectricity and extraordinary piezoelectricity: δ-AsN, δ-SbN, and δ-BiN, *Nanoscale* **2023**, *15*, 6363-6370.

[83] Y. Chen, C. Chen, R. Kealhofer, H. Liu, Z. Yuan, L. Jiang, J. Suh, J. Park, C. Ko, H. S. Choe, J. Avila, M. Zhong, Z. Wei, J. Li, S. Li, H. Gao, Y. Liu, J. Analytis, Q. Xia, M. C. Asensio, J. Wu, Black Arsenic: A Layered Semiconductor with Extreme In-Plane Anisotropy, *Adv. Mater.* **2018**, *30*, 1800754.

[84] M. A. Tapia, R. Gusmão, N. Serrano, Z. Sofer, C. Ariño, J. M. Díaz-Cruz, M. Esteban, Phosphorene and other layered pnictogens as a new source of 2D materials for electrochemical sensors, *TrAC, Trends Anal. Chem.* **2021**, *139*, 116249.

[85] Q. H. Wang, K. Kalantar-Zadeh, A. Kis, J. N. Coleman, M. S. Strano, Electronics and optoelectronics of two-dimensional transition metal dichalcogenides, *Nat. Nanotechnol.* **2012**, *7*, 699-712.

[86] S. Zhang, M. Xie, F. Li, Z. Yan, Y. Li, E. Kan, W. Liu, Z. Chen, H. Zeng, Semiconducting Group 15 Monolayers: A Broad Range of Band Gaps and High Carrier Mobilities, *Angew. Chem. Int. Ed.* **2016**, *55*, 1666-1669.

[87] R. Gusmão, Z. Sofer, D. Bouša, M. Pumera, Pnictogen (As, Sb, Bi) Nanosheets for Electrochemical Applications Are Produced by Shear Exfoliation Using Kitchen Blenders, *Angew. Chem. Int. Ed.* **2017**, *56*, 14417-14422.

[88] J. Sturala, Z. Sofer, M. Pumera, Chemistry of Layered Pnictogens: Phosphorus, Arsenic, Antimony, and Bismuth, *Angew. Chem. Int. Ed.* **2019**, *58*, 7551-7557.

[89] P. Liu, Y.-z. Nie, Q.-l. Xia, G.-h. Guo, Structural and electronic properties of arsenic nitrogen monolayer, *Phys. Lett. A* **2017**, *381*, 1102-1106.

[90] W. E. Jones, Rotational analysis of the 1Π-X1Σ+ system of AsN, *J. Mol. Spectrosc.* **1970**, *34*, 320-326.

[91] E. P. Young, J. Park, T. Bai, C. Choi, R. H. DeBlock, M. Lange, S. Poust, J. Tice, C. Cheung, B. S. Dunn, M. S. Goorsky, V. Ozoliņš, D. C. Streit, V. Gambin, Wafer-Scale Black Arsenic–Phosphorus Thin-Film Synthesis Validated with Density Functional Perturbation Theory Predictions, *ACS Appl. Nano Mat.* **2018**, *1*, 4737-4745.

[92] S. Guo, Y. Zhang, Y. Ge, S. Zhang, H. Zeng, H. Zhang, 2D V-V Binary Materials: Status and Challenges, *Adv. Mater.* **2019**, *31*, 1902352.

[93] Y. Guo, C. Pei, R. M. Koenigs, A combined experimental and theoretical study on the reactivity of nitrenes and nitrene radical anions, *Nat. Commun.* **2022**, *13*, 86.

[94] Y.-C. Wang, X.-J. Lai, K. Huang, S. Yadav, G. Qiu, L. Zhang, H. Zhou, Unravelling nitrene chemistry from acyclic precursors: recent advances and challenges, *Org. Chem. Front.* **2021**, *8*, 1677-1693.

[95] P. F. Kuijpers, J. I. van der Vlugt, S. Schneider, B. de Bruin, Nitrene Radical Intermediates in Catalytic Synthesis, *Chem. Eur. J.* **2017**, *23*, 13819-13829.

[96] H.-Y. Thu, W.-Y. Yu, C.-M. Che, Intermolecular Amidation of Unactivated sp^2 and sp^3 C–H Bonds via Palladium-Catalyzed Cascade C–H Activation/Nitrene Insertion, *J. Am. Chem. Soc.* **2006**, *128*, 9048-9049.

[97] I. D. G. Watson, L. Yu, A. K. Yudin, Advances in Nitrogen Transfer Reactions Involving Aziridines, *Acc. Chem. Res.* **2006**, *39*, 194-206.

[98] P. Brandt, M. J. Södergren, P. G. Andersson, P.-O. Norrby, Mechanistic Studies of Copper-Catalyzed Alkene Aziridination, *J. Am. Chem. Soc.* **2000**, *122*, 8013-8020.

[99] D. A. Evans, M. T. Bilodeau, M. M. Faul, Development of the Copper-Catalyzed Olefin Aziridination Reaction, *J. Am. Chem. Soc.* **1994**, *116*, 2742-2753.

[100] G. Dequirez, V. Pons, P. Dauban, Nitrene Chemistry in Organic Synthesis: Still in Its Infancy?, *Angew. Chem. Int. Ed.* **2012**, *51*, 7384-7395.

[101] F. Li, W. F. Zhu, C. Empel, O. Datsenko, A. Kumar, Y. Xu, J. H. M. Ehrler, I. Atodiresei, S. Knapp, P. K. Mykhailiuk, E. Proschak, R. M. Koenigs, Photosensitization enables Pauson-Khand–type reactions with nitrenes, *Science* **2024**, *383*, 498-503.

[102] F. Lovering, J. Bikker, C. Humblet, Escape from Flatland: Increasing Saturation as an Approach to Improving Clinical Success, *J. Med. Chem.* **2009**, *52*, 6752-6756.

[103] D. Dam, N. R. Lagerweij, K. M. Janmaat, K. Kok, E. Bouwman, J. D. C. Codée, Organic Dye-Sensitized Nitrene Generation: Intermolecular Aziridination of Unactivated Alkenes, *J. Org. Chem.* **2024**, *89*, 3251-3258.

[104] H. Sun, B. Zhu, Z. Wu, X. Zeng, H. Beckers, W. S. Jenks, Thermally Persistent Carbonyl Nitrene: FC(O)N, *J. Org. Chem.* **2015**, *80*, 2006-2009.

[105] Y. Qin, B. Lu, G. Rauhut, M. Hagedorn, K. Banert, C. Song, X. Chu, L. Wang, X. Zeng, The Simplest, Isolable, Alkynyl Isocyanate HC≡CNCO: Synthesis and Characterization, *Angew. Chem. Int. Ed.* **2019**, *58*, 17277-17281.

[106] N. Gritsan, M. Platz, *Photochemistry of Azides: The Azide/Nitrene Interface*, **2009**.

[107] D. M. Sawant, G. Joshi, A. J. Ansari, Nitrene-transfer from azides to isocyanides: Unveiling its versatility as a promising building block for the synthesis of bioactive heterocycles, *iScience* **2024**, *27*, 109311.

[108] S. Cenini, G. La Monica, Organic azides and isocyanates as sources of nitrene species in organometallic chemistry, *Inorg. Chim. Acta* **1976**, *18*, 279-293.

[109] S. Gao, A. Das, E. Alfonzo, K. M. Sicinski, D. Rieger, F. H. Arnold, Enzymatic Nitrogen Incorporation Using Hydroxylamine, *J. Am. Chem. Soc.* **2023**, *145*, 20196-20201.

[110] Y. Gao, H. Li, Y. Zhao, X.-Q. Hu, Nitrene transfer reaction with hydroxylamine derivatives, *Chem. Commun.* **2023**, *59*, 1889-1906.

[111] F. Dielmann, D. M. Andrada, G. Frenking, G. Bertrand, Isolation of Bridging and Terminal Coinage Metal–Nitrene Complexes, *J. Am. Chem. Soc.* **2014**, *136*, 3800-3802.

[112] Y. M. Badiei, A. Dinescu, X. Dai, R. M. Palomino, F. W. Heinemann, T. R. Cundari, T. H. Warren, Copper–Nitrene Complexes in Catalytic C-H Amination, *Angew. Chem. Int. Ed.* **2008**, *47*, 9961-9964.

[113] K. M. Carsch, I. M. DiMucci, D. A. Iovan, A. Li, S.-L. Zheng, C. J. Titus, S. J. Lee, K. D. Irwin, D. Nordlund, K. M. Lancaster, T. A. Betley, Synthesis of a copper-supported triplet nitrene complex pertinent to copper-catalyzed amination, *Science* **2019**, *365*, 1138-1143.

[114] F. Thomas, M. Oster, F. Schön, K. C. Göbgen, B. Amarouch, D. Steden, A. Hoffmann, S. Herres-Pawlis, A new generation of terminal copper nitrenes and their application in aromatic C–H amination reactions, *Dalton Trans.* **2021**, *50*, 6444-6462.

[115] F. Dielmann, O. Back, M. Henry-Ellinger, P. Jerabek, G. Frenking, G. Bertrand, A Crystalline Singlet Phosphinonitrene: A Nitrogen Atom–Transfer Agent, *Science* **2012**, *337*, 1526-1528.

[116] M. Janssen, T. Frederichs, M. Olaru, E. Lork, E. Hupf, J. Beckmann, Synthesis of a stable crystalline nitrene, *Science* **2024**, *385*, 318-321.

[117] D. Wang, W. Chen, H. Chen, Y. Chen, S. Ye, G. Tan, Isolation and characterization of a triplet nitrene, *Nat. Chem.* **2025**, *17*, 38-43.

[118] G. Maier, C. Schmidt, H. P. Reisenauer, E. Endlein, D. Becker, J. Eckwert, B. H. Andes Jr, L. J. Schaad, Blausäure-N-methylid: Darstellung, spektroskopische Eigenschaften und seine Beziehung zu anderen C_2H_3N-Isomeren, *Chem. Ber.* **1993**, *126*, 2337-2352.

[119] D. J. R. Duarte, M. S. Miranda, J. C. G. Esteves da Silva, Computational Study on the Vinyl Azide Decomposition, *J. Phys. Chem. A* **2014**, *118*, 5038-5045.

[120] Å. Sjöholm Timén, E. Risberg, P. Somfai, Improved procedure for cyclization of vinyl azides into 3-substituted-2H-azirines, *Tetrahedron Lett.* **2003**, *44*, 5339-5341.

[121] G. L'Abbe, G. Mathys, Mechanism of the thermal decomposition of vinyl azides, *J. Org. Chem.* **1974**, *39*, 1778-1780.

[122] C. Wentrup, C. M. Nunes, I. Reva, Comment on "Computational Study on the Vinyl Azide Decomposition", *J. Phys. Chem. A* **2014**, *118*, 5122-5123.

[123] G. Smolinsky, E. Wasserman, W. A. Yager, The E.P.R. of Ground State Triplet Nitrenes, *J. Am. Chem. Soc.* **1962**, *84*, 3220-3221.

[124] J. Mieres-Pérez, E. Mendez-Vega, K. Velappan, W. Sander, Reaction of Triplet Phenylnitrene with Molecular Oxygen, *J. Org. Chem.* **2015**, *80*, 11926-11931.

[125] J. Mieres-Perez, P. Costa, E. Mendez-Vega, R. Crespo-Otero, W. Sander, Switching the Spin State of Pentafluorophenylnitrene: Isolation of a Singlet Arylnitrene Complex, *J. Am. Chem. Soc.* **2018**, *140*, 17271-17277.

[126] S. K. Sarkar, A. Sawai, K. Kanahara, C. Wentrup, M. Abe, A. D. Gudmundsdottir, Direct Detection of a Triplet Vinylnitrene, 1,4-Naphthoquinone-2-ylnitrene, in Solution and Cryogenic Matrices, *J. Am. Chem. Soc.* **2015**, *137*, 4207-4214.

[127] D. J. Berger, P. P. Gaspar, P. LeFloch, F. Mathey, R. S. Grev, Computational View of the Mechanism of Vinylphosphirane Pyrolysis and a New Route to Phosphaalkynes, *Organometallics* **1996**, *15*, 4904-4915.

[128] D. J. Berger, P. P. Gaspar, R. S. Grev, F. Mathey, Molecular orbital study of the vinylphosphinidene to phosphapropyne rearrangement, *Organometallics* **1994**, *13*, 640-646.

[129] S. Haber, P. Le Floch, F. Mathey, Synthesis of phosphapropyne by flash thermolysis of 1-vinylphosphirane or divinylphosphine, *J. Chem. Soc., Chem. Commun.* **1992**, 1799-1800.

[130] B. Wittwer, F. Heim, K. Wurst, S. Hohloch, A bridging bis-phosphanido-phosphinidene complex of lanthanum supported by a sterically encumbering PN ligand, *Chem. Commun.* **2024**, *60*, 7299-7302.

[131] J. K. Pagano, B. J. Ackley, R. Waterman, Evidence for Iron-Catalyzed α-Phosphinidene Elimination with Phenylphosphine, *Chem. Eur. J.* **2018**, *24*, 2554-2557.

[132] T. Krachko, M. Bispinghoff, A. M. Tondreau, D. Stein, M. Baker, A. W. Ehlers, J. C. Slootweg, H. Grützmacher, Facile Phenylphosphinidene Transfer Reactions from Carbene–Phosphinidene Zinc Complexes, *Angew. Chem. Int. Ed.* **2017**, *56*, 7948-7951.

[133] K. Hansen, T. Szilvási, B. Blom, S. Inoue, J. Epping, M. Driess, A Fragile Zwitterionic Phosphasilene as a Transfer Agent of the Elusive Parent Phosphinidene (:PH), *J. Am. Chem. Soc.* **2013**, *135*, 11795-11798.

[134] W. J. Transue, A. Velian, M. Nava, C. García-Iriepa, M. Temprado, C. C. Cummins, Mechanism and Scope of Phosphinidene Transfer from Dibenzo-7-phosphanorbornadiene Compounds, *J. Am. Chem. Soc.* **2017**, *139*, 10822-10831.

[135] K. Lammertsma, in *New Aspects in Phosphorus Chemistry III* (Ed.: J.-P. Majoral), Springer Berlin Heidelberg, Berlin, Heidelberg, **2003**, pp. 95-119.

[136] A. Mardyukov, D. Niedek, Photochemical reactions of triplet phenylphosphinidene with carbon monoxide and nitric oxide, *Chem. Commun.* **2018**, *54*, 13694-13697.

[137] V. A. Wright, B. O. Patrick, C. Schneider, D. P. Gates, Phosphorus Copies of PPV: π-Conjugated Polymers and Molecules Composed of Alternating Phenylene and Phosphaalkene Moieties, *J. Am. Chem. Soc.* **2006**, *128*, 8836-8844.

[138] P. Sreejyothi, K. Bhattacharyya, S. Kumar, P. Kumar Hota, A. Datta, S. K. Mandal, An NHC-Stabilised Phosphinidene for Catalytic Formylation: A DFT-Guided Approach, *Chem. Eur. J.* **2021**, *27*, 11656-11662.

[139] A. Marinetti, F. Mathey, J. Fischer, A. Mitschler, Generation and trapping of terminal phosphinidene complexes. Synthesis and x-ray crystal structure of stable phosphirene complexes, *J. Am. Chem. Soc.* **1982**, *104*, 4484-4485.

[140] A. Marinetti, F. Mathey, J. Fischer, A. Mitschler, Stabilization of 7-phosphanorbornadienes by complexation; X-ray crystal structure of 2,3-bis(methoxycarbonyl)-5,6-dimethyl-7-phenyl-7-phosphanorbornadiene(pentacarbonyl)-chromium, *J. Chem. Soc., Chem. Commun.* **1982**, 667-668.

[141] F. Mathey, The Development of a Carbene-like Chemistry with Terminal Phosphinidene Complexes, *Angew. Chem., Int. Ed. Engl.* **1987**, *26*, 275-286.

[142] L. Liu, David A. Ruiz, D. Munz, G. Bertrand, A Singlet Phosphinidene Stable at Room Temperature, *Chem* **2016**, *1*, 147-153.

[143] M. M. Hansmann, G. Bertrand, Transition-Metal-like Behavior of Main Group Elements: Ligand Exchange at a Phosphinidene, *J. Am. Chem. Soc.* **2016**, *138*, 15885-15888.

[144] G. Trinquier, G. Bertrand, Binding phosphinidenes to transition-metal fragments, *Inorg. Chem.* **1985**, *24*, 3842-3856.

[145] M. Peters, A. Doddi, T. Bannenberg, M. Freytag, P. G. Jones, M. Tamm, N-Heterocyclic Carbene-Phosphinidene and Carbene-Phosphinidenide Transition Metal Complexes, *Inorg. Chem.* **2017**, *56*, 10785-10793.

[146] A. Schmer, P. Junker, A. Espinosa Ferao, R. Streubel, M/X Phosphinidenoid Metal Complex Chemistry, *Acc. Chem. Res.* **2021**, *54*, 1754-1765.

[147] M. Wu, H. Li, W. Chen, D. Wang, Y. He, L. Xu, S. Ye, G. Tan, A triplet stibinidene, *Chem* **2023**, *9*, 2573-2584.

[148] Y. Pang, N. Nöthling, M. Leutzsch, L. Kang, E. Bill, M. van Gastel, E. Reijerse, R. Goddard, L. Wagner, D. SantaLucia, S. DeBeer, F. Neese, J. Cornella, Synthesis and isolation of a triplet bismuthinidene with a quenched magnetic response, *Science* **2023**, *380*, 1043-1048.

[149] M. K. Sharma, B. Neumann, H.-G. Stammler, D. M. Andrada, R. S. Ghadwal, Electrophilic terminal arsinidene-iron(0) complexes with a two-coordinated arsenic atom, *Chem. Commun.* **2019**, *55*, 14669-14672.

[150] M. Fischer, F. Reiß, C. Hering-Junghans, Titanocene pnictinidene complexes, *Chem. Commun.* **2021**, *57*, 5626-5629.

[151] J. B. Bonanno, P. T. Wolczanski, E. B. Lobkovsky, Arsinidene, Phosphinidene, and Imide Formation via 1,2-H_2-Elimination from $(silox)_3HTaEHPh$ (E = N, P, As): Structures of $(silox)_3Ta{:}EPh$ (E = P, As), *J. Am. Chem. Soc.* **1994**, *116*, 11159-11160.

[152] E. P. Wildman, G. Balázs, A. J. Wooles, M. Scheer, S. T. Liddle, Triamidoamine thorium-arsenic complexes with parent arsenide, arsinidiide and arsenido structural motifs, *Nat. Commun.* **2017**, *8*, 14769.

[153] T. Pugh, A. Kerridge, R. A. Layfield, Yttrium Complexes of Arsine, Arsenide, and Arsinidene Ligands, *Angew. Chem. Int. Ed.* **2015**, *54*, 4255-4258.

[154] A. J. Arduengo, J. C. Calabrese, A. H. Cowley, H. V. R. Dias, J. R. Goerlich, W. J. Marshall, B. Riegel, Carbene–Pnictinidene Adducts, *Inorg. Chem.* **1997**, *36*, 2151-2158.

[155] A. Doddi, M. Weinhart, A. Hinz, D. Bockfeld, J. M. Goicoechea, M. Scheer, M. Tamm, N-Heterocyclic carbene-stabilised arsinidene (AsH), *Chem. Commun.* **2017**, *53*, 6069-6072.

[156] C. Präsang, M. Stoelzel, S. Inoue, A. Meltzer, M. Driess, Metal-Free Activation of EH_3 (E=P, As) by an Ylide-like Silylene and Formation of a Donor-Stabilized Arsasilene with a HSi=AsH Subunit, *Angew. Chem. Int. Ed.* **2010**, *49*, 10002-10005.

[157] L. Andrews, H.-G. Cho, Matrix Infrared Spectra and Quantum Chemical Calculations of Ti, Zr, and Hf Dihydride Phosphinidene and Arsinidene Molecules, *Inorg. Chem.* **2016**, *55*, 8786-8793.

[158] T. M. Klapötke, *Chemistry of High-Energy Materials*, De Gruyter, **2022**.

[159] J. Wilbrand, Notiz über Trinitrotoluol, *Justus Liebigs Ann. Chem.* **1863**, *128*, 178-179.

[160] J. Yount, D. G. Piercey, Electrochemical Synthesis of High-Nitrogen Materials and Energetic Materials, *Chem. Rev.* **2022**, *122*, 8809-8840.

[161] O. T. O'Sullivan, M. J. Zdilla, Properties and Promise of Catenated Nitrogen Systems As High-Energy-Density Materials, *Chem. Rev.* **2020**, *120*, 5682-5744.

[162] A. A. Larin, L. L. Fershtat, High-energy hydroxytetrazoles: Design, synthesis and performance, *Energ. Mater. Front.* **2021**, *2*, 3-13.

[163] J. Singh, R. J. Staples, J. n. M. Shreeve, Increasing the limits of energy and safety in tetrazoles: dioximes as unusual precursors to very thermostable and insensitive energetic materials, *J. Mater. Chem. A* **2023**, *11*, 12896-12901.

[164] M. Jafari, K. Ghani, M. H. Keshavarz, F. Derikvandy, Assessing the Detonation Performance of New Tetrazole Base High Energy Density materials, *Propellants Explos. Pyrotech.* **2018**, *43*, 1236-1244.

[165] M. Nasrollahzadeh, Z. Nezafat, N. S. S. Bidgoli, N. Shafiei, Use of tetrazoles in catalysis and energetic applications: Recent developments, *Mol. Catal.* **2021**, *513*, 111788.

[166] Y. Tang, H. Yang, B. Wu, X. Ju, C. Lu, G. Cheng, Synthesis and Characterization of a Stable, Catenated N_{11} Energetic Salt, *Angew. Chem. Int. Ed.* **2013**, *52*, 4875-4877.

[167] Z. Dong, Z. Ye, Synthesis and properties of salts derived from $C_4N_{18}^{2-}$, $C_4N_{18}H^{3-}$ and $C_4N_{18}H^{3-}$ anions, *J. Mater. Chem. A* **2020**, *8*, 25035-25039.

[168] T. M. Klapötke, F. A. Martin, J. Stierstorfer, C_2N_{14}: An Energetic and Highly Sensitive Binary Azidotetrazole, *Angew. Chem. Int. Ed.* **2011**, *50*, 4227-4229.

[169] K. Banert, Y.-H. Joo, T. Rüffer, B. Walfort, H. Lang, The Exciting Chemistry of Tetraazidomethane, *Angew. Chem. Int. Ed.* **2007**, *46*, 1168-1171.

[170] K. O. Christe, W. W. Wilson, J. A. Sheehy, J. A. Boatz, N_5^+: A Novel Homoleptic Polynitrogen Ion as a High Energy Density Material, *Angew. Chem. Int. Ed.* **1999**, *38*, 2004-2009.

[171] A. Vij, W. W. Wilson, V. Vij, F. S. Tham, J. A. Sheehy, K. O. Christe, Polynitrogen Chemistry. Synthesis, Characterization, and Crystal Structure of Surprisingly Stable Fluoroantimonate Salts of N_5^+, *J. Am. Chem. Soc.* **2001**, *123*, 6308-6313.

[172] M. I. Eremets, A. G. Gavriliuk, I. A. Trojan, D. A. Dzivenko, R. Boehler, Single-bonded cubic form of nitrogen, *Nat. Mater.* **2004**, *3*, 558-563.

[173] S. Duwal, Y.-J. Ryu, M. Kim, C.-S. Yoo, S. Bang, K. Kim, N. H. Hur, Transformation of hydrazinium azide to molecular N_8 at 40 GPa, *J. Chem. Phys.* **2018**, *148*, 134310.

[174] B. Hirshberg, R. B. Gerber, A. I. Krylov, Calculations predict a stable molecular crystal of N_8, *Nat. Chem.* **2014**, *6*, 52-56.

[175] A. Aslandukov, A. Aslandukova, D. Laniel, S. Khandarkhaeva, Y. Yin, F. I. Akbar, S. Chariton, V. Prakapenka, E. L. Bright, C. Giacobbe, J. Wright, D. Comboni, M. Hanfland, N. Dubrovinskaia, L. Dubrovinsky, Stabilization of N_6 and N_8 anionic units and 2D polynitrogen layers in high-pressure scandium polynitrides, *Nat. Commun.* **2024**, *15*, 2244.

[176] D. Laniel, B. Winkler, T. Fedotenko, A. Pakhomova, S. Chariton, V. Milman, V. Prakapenka, L. Dubrovinsky, N. Dubrovinskaia, High-Pressure Polymeric Nitrogen Allotrope with the Black Phosphorus Structure, *Phys. Rev. Lett.* **2020**, *124*, 216001.

[177] C. Ji, A. A. Adeleke, L. Yang, B. Wan, H. Gou, Y. Yao, B. Li, Y. Meng, J. S. Smith, V. B. Prakapenka, W. Liu, G. Shen, W. L. Mao, H.-k. Mao, Nitrogen in black phosphorus structure, *Sci. Adv.* **2020**, *6*, eaba9206.

[178] D. Tomasino, M. Kim, J. Smith, C.-S. Yoo, Pressure-Induced Symmetry-Lowering Transition in Dense Nitrogen to Layered Polymeric Nitrogen (LP-N) with Colossal Raman Intensity, *Phys. Rev. Lett.* **2014**, *113*, 205502.

[179] D. Laniel, G. Geneste, G. Weck, M. Mezouar, P. Loubeyre, Hexagonal Layered Polymeric Nitrogen Phase Synthesized near 250 GPa, *Phys. Rev. Lett.* **2019**, *122*, 066001.

[180] D. Laniel, F. Trybel, A. Aslandukov, J. Spender, U. Ranieri, T. Fedotenko, K. Glazyrin, E. L. Bright, S. Chariton, V. B. Prakapenka, I. A. Abrikosov, L. Dubrovinsky, N. Dubrovinskaia, Structure determination of ζ-N_2 from single-crystal X-ray diffraction and theoretical suggestion for the formation of amorphous nitrogen, *Nat. Commun.* **2023**, *14*, 6207.

[181] M. I. Eremets, A. G. Gavriliuk, N. R. Serebryanaya, I. A. Trojan, D. A. Dzivenko, R. Boehler, H. K. Mao, R. J. Hemley, Structural transformation of molecular nitrogen to a single-bonded atomic state at high pressures, *J. Chem. Phys.* **2004**, *121*, 11296-11300.

2. Publications

2.1 Selective Preparation of Phosphorus Mononitride (P≡N) from Phosphinoazide and Reversible Oxidation to Phosphinonitrene

Abstract: The interstellar candidate phosphorus mononitride PN, a metastable species, was generated through high-vacuum flash pyrolysis of (*o*-phenyldioxyl)phosphinoazide in cryogenic matrices. Although the PN stretching band was not directly detected because of its low infrared intensity and possible overlaps with other strong bands, *o*-benzoquinone, carbon monoxide, and cyclopentadienone as additional fragmentation products were clearly identified. Moreover, an elusive *o*-benzoquinone-PN complex formed when (*o*-phenyldioxyl)phosphinoazide was exposed to UV irradiation at λ = 254 nm. Its recombination to (*o*-phenyldioxyl)-λ^5-phosphinonitrile was observed upon irradiation with the light λ = 523 nm, which demonstrates for the first time the reactivity of PN towards an organic molecule. Free energy profile computations at the B3LYP/def2-TZVP density functional theory level reveal a concerted mechanism. To provide further evidence, UV/Vis spectra of the precursor and the irradiation products were recorded and agree well with time-dependent DFT computations.

Original Source: Weiyu Qian, Raffael C. Wende, Peter R. Schreiner, Artur Mardyukov, *Angew. Chem. Int. Ed.* **2023**, *62*, e202300761. (DOI: 10.1002/anie.202300761); *Angew. Chem.* **2023**, *135*, e202300761. (DOI: 10.1002/ange.202300761)

Highlight: a) Noted as **Hot Paper**, b) Back cover of this issue, c) Wikipedia, https://en.wikipedia.org/wiki/Phosphorus_mononitride.

GDCh Research Articles Angewandte International Edition Chemie www.angewandte.org

Check for updates

How to cite: *Angew. Chem. Int. Ed.* **2023**, *62*, e202300761
doi.org/10.1002/anie.202300761

Gas-Phase Chemistry Hot Paper

Selective Preparation of Phosphorus Mononitride (P≡N) from Phosphinoazide and Reversible Oxidation to Phosphinonitrene

*Weiyu Qian, Raffael C. Wende, Peter R. Schreiner, and Artur Mardyukov**

Abstract: The interstellar candidate phosphorus mononitride PN, a metastable species, was generated through high-vacuum flash pyrolysis of (*o*-phenyldioxyl)phosphinoazide in cryogenic matrices. Although the PN stretching band was not directly detected because of its low infrared intensity and possible overlaps with other strong bands, *o*-benzoquinone, carbon monoxide, and cyclopentadienone as additional fragmentation products were clearly identified. Moreover, an elusive *o*-benzoquinone-PN complex formed when (*o*-phenyldioxyl)phosphinoazide was exposed to UV irradiation at $\lambda = 254$ nm. Its recombination to (*o*-phenyldioxyl)-λ^5-phosphinonitrile was observed upon irradiation with the light at $\lambda = 523$ nm, which demonstrates for the first time the reactivity of PN towards an organic molecule. Energy profile computations at the B3LYP/def2-TZVP density functional theory level reveal a concerted mechanism. To provide further evidence, UV/Vis spectra of the precursor and the irradiation products were recorded and agree well with time-dependent DFT computations.

Introduction

Phosphorus mononitride PN, the simplest molecule containing phosphorus and nitrogen that both are essential elements of life, is the phosphorus-bearing interstellar species that is not only the first to be detected but also the one with the highest number of detections in star-forming regions.[1–6] It was first generated in the laboratory by microwave discharging of a $P_4/N_2/Ar$ mixture; an alternative precursor is P_3N_5.[7] Gas-phase thermolysis of dimethyl phosphoramidate (DMPR) revealed that PN is the most prevalent species in its decomposition.[8] Because of its thermodynamically unstable nature, the spontaneous trimerization into cyclotriphosphazene (P_3N_3) was observed even in Kr-matrix at 30 K,[7] which makes studies of the reactivity of "free" PN scarce. Despite numerous experimental and theoretical reports on the interaction of PN with metal atoms (e.g., Cu, Ag, Au, Co, Ni, and Pd),[9,10] its reactivity with organic compounds remains unknown. In contrast to N_2 and P_2, PN does not form a stable coordination complex with vanadium.[11–13] Molecular systems that can serve as "clean PN" precursors are scarce.

Pioneering work by Niecke and co-workers described the first synthesis of a stable compound with a PN triple bond (**A**) (Scheme 1).[14] Bertrand and co-workers reported the synthesis of a stable formal carbene adduct of phosphorus mononitride NHC=N–P=CAAC (**B**; NHC = $(NHC(Dipp))_2C$, Dip = 2,6-(diisopropyl)phenyl, CAAC = cyclic alkyl amino carbene).[15] They also described the one-electron oxidation of PN to the isolable PN radical cation.[15] Velian and Cummins reported an elegant approach to generate PN in solution using anthracene ($An = C_{14}H_{10}$) based precursor (**C**) by extrusion of two molecules of $C_{14}H_{10}$ for the release of PN in solution.[16] However, they only observed anthracene and insoluble material. In 2014, Schulz et al. reported the synthesis of reactive P=N-bearing species by elimination of two molecules of TMS-Cl from $(TMS)_2NPCl_2$.[17] Product analysis of the trapping experiments with dimethylbutadiene (dmb) indicates that $Me_3SiN{=}PCl$ formed as a highly reactive intermediate, which eventually oligomerized to cyclo-tetraphosphazene ($[PN(dmb)]_4$. The first bimetallic complex featuring a P=N bridge, [Fe]-N=P-[Mo], within which the iron could be disengaged by *tert*-butyl isocyanide to form the terminal PN coordination complex $[Mo](PN)^-$ (**D**).[10] The photoinduced isomerization from kinetically stable $[Mo](PN)^-$ to N-bond isomer $[Mo](NP)^-$ was also detected.[10] Very recently, Cummins and co-workers leaped forward when they reported the release of PN via thermolysis of highly explosive $AnPN_3$ (**E**) and trapping PN with [(dppe)Fe(Cp*)(NP))][$BArF_{24}$], which revealed the reactivity of PN towards transition metal complexes in solution.[18] To our knowledge, this remains the only example of a direct capture of PN.

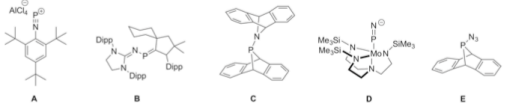

Scheme 1. Previously reported molecules featuring PN moieties.

[*] W. Qian, Dr. R. C. Wende, Prof. Dr. P. R. Schreiner, Dr. A. Mardyukov
Institute of Organic Chemistry, Justus Liebig University
Heinrich-Buff-Ring 17, 35392 Giessen (Germany)
E-mail: artur.mardyukov@org.chemie.uni-giessen.de

Moreover, in 2009, Cummins and co-workers presented another interesting molecule that possesses a hidden AsP moiety in AsPNMes* ligand complexed with tungsten pentacarbonyl $W(CO)_5$, which was shown to be susceptible to the loss of the $(AsP)W(CO)_5$ unit upon thermolysis. Even though it is bound by $W(CO)_5$, the AsP motif retains its triple bond reactivity with organic dienes.[19]

The thermally and photochemically induced elimination of nitrogen (N_2) from suitable azide precursors has proven to be a reliable method for the synthesis of reactive species.[20–22] It was demonstrated recently that phosphonic azides can be readily triggered thermally and photochemically to release N_2 and leave behind highly reactive species.[23] Bertrand and colleagues reported the synthesis of bis(imidazolidin-2-iminato)phosphinonitrene (**I**) from the corresponding azide upon irradiation at 254 nm, which is stable for days at room temperature[24] and adopts a singlet electronic ground state due to the interaction of the phosphorus lone pair with a vacant orbital of the nitrene.[25] Singlet phosphinophosphinide (**II**) was isolated in an analogous fashion.[26] The existence of singlet nitrenes, such as sulfinylnitrene (**III**) and thiophosphorylnitrene (**IV**), was confirmed by matrix isolation spectroscopy (Scheme 2).[27,28] In contrast to **I**, donor atom stabilized borylnitrene, 2-nitreno-1,3,2-benzodioxaborole (**V**) displays a triplet electronic ground state, which was confirmed by matrix isolation IR, UV/Vis, and EPR spectroscopy and by monitoring its reactivity with dinitrogen, molecular oxygen, carbon monoxide, and carbon dioxide.[29,30] In general, aryl and alkyl substituted nitrenes have triplet electronic ground states, making them highly transient species, and their detection usually requires time-resolved spectroscopy or cryogenic temperatures (**VI**).[31]

It should be stressed that there is no report on the structure and reactivity of PN with organic molecules so far. Experimentally monitoring such species is challenging because the intermediates are often elusive. Here, we report the generation of a weakly bound complex of PN with *o*-benzoquinone (**3**) by UV irradiation of (*o*-phenyldioxyl)phosphinoazide (**1**) in argon matrices, which is stabilized by O···P interactions in **3**-PN. This complex is highly photolabile and converts to (*o*-phenyldioxyl)-λ^5-phosphinonitrene (**2**) upon irradiation with light at $\lambda =$ 523 nm. Photoreversion can be further achieved upon UV light ($\lambda = 254$ nm) irradiation (Scheme 3A). In contrast to the observations in the photolysis experiments, pyrolysis of **1** at 650 °C leads to the formation of 1,4,3,2-benzodioxaphosphorine (**4**) as the major product. Pyrolysis of **1** at 850 °C yields PN, cyclopentadienone (**5**), and carbon monoxide (Scheme 3B). To the best of our knowledge, this is the first

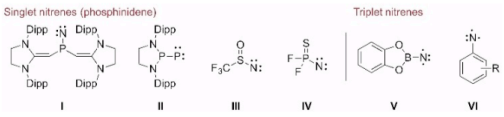

Scheme 2. Experimentally known singlet and triplet nitrenes.

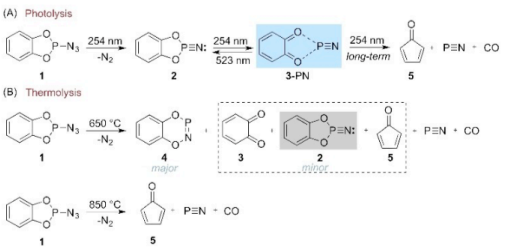

Scheme 3. Photochemical and thermal generation of **2** and **3** from **1** and subsequent reactivity.

spectroscopic example of a PN bearing organic complex that displays reversible covalent bond formation.

Results and Discussion

Our initial idea was to generate **2** by photolysis or/and pyrolysis of the corresponding azide precursor **1** followed by immediate matrix isolation at 10 K in solid argon, which would then allow us to investigate the reactions of **2** with small molecules. To generate **2**, azide **1** was isolated at 10 K in an argon matrix, which shows excellent agreement between the experimental and computed IR spectrum. Photolysis of **1** with light at $\lambda = 254$ nm for several minutes resulted in the complete bleaching of the IR bands of **1** and a set of new IR absorptions was detected (Figure 1). Short-wavelength irradiation resulted in the continuous growth of the signals of **2** (Figure S1). However, the photolysis experi-

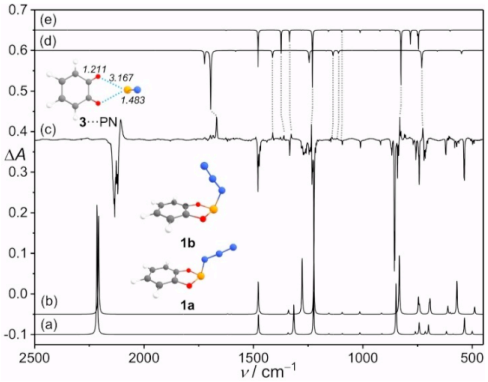

Figure 1. a) Scaled computed infrared (IR) spectrum of **1a** (factor 0.98). b) Scaled computed IR spectrum of **1b** (factor 0.98). c) IR difference spectrum shows the changes upon 6 min 254 nm. d) Scaled computed IR spectrum of **3**-PN (factor 0.98). e) Scaled computed IR spectrum of **2** (factor 0.98). The computed molecular structures for **1a**, **1b**, and 3-PN and bond lengths (in italics, Å) for **3**-PN are also depicted. All computations were done at the B3LYP/def2-TZVP level of theory.

ment revealed another set of rather intense new signals at 1669 (with satellites), 1412, 1276, and 726 cm^{-1}, which show identical growth behavior upon photolysis. The strong band at 1669 cm^{-1} suggests the presence of a carbonyl group within the conjugated system. Hence, by scrutinizing the structure of the precursor, **3** is the most likely candidate.[32] For example, the C=O stretching vibration of 1,4-benzoquinone (*p*-benzoquinone) was reported at 1671 cm^{-1} in argon matrices.[33] The ambiguous identification of **3** is also supported by comparison of the experimentally observed spectrum with the computed spectrum of **3** at the B3LYP/def2-TZVP level of theory (Table S1). Logically, the remaining fragment must be phosphorus nitride PN and it is likely that this new compound is a complex between **3** and PN (**3**-PN) (Table S1). Comparing the frequencies of **3** moiety in the complex with the results of pyrolysis experiments, some small shifts can be observed. Our extensive efforts to identify free PN in an argon matrix have been unsuccessful, due to the low intensity and the apparent overlap with some other bands of **2** and **3**.

To gain more information on the photochemical reactivity of **3**-PN, the mixture was photolyzed at 10 K with light of different wavelengths. Thus, irradiation with $\lambda = 523$ nm resulted in the disappearance of IR bands of **3**-PN and the parallel formation of strong IR absorptions at 1480, 1360, 1327, 1234, 831, 805, and 744 cm^{-1} (Figure 2 and Figure S2). The photolysis product of **3**-PN at this wavelength was identified as **2** (Table S2). With the help of the computations, additional IR bands of medium and weak intensity at 1472, 1011, 1360, 924, and 759 cm^{-1} were assigned to **2** (Table S2). This photoisomerization is reversible and **3**-PN can be regenerated upon irradiation at $\lambda = 254$ nm. The reversible photochemistry (Scheme 3) demonstrates that **2** and **3**-PN exist in equilibrium. This photoinduced reversible process is also observed in the photolysis experiment of (*o*-phenyldioxyl)phosphinoisocyanate (Figure S3). Upon subsequent 523 nm irradiation, regenerated **2** reacts with CO in situ and finally gives (*o*-phenyldioxyl)phosphinoisocyanate.

The formation of **2** and **3**-PN from **1** was also monitored by UV/Vis spectroscopy. In line with the IR experiments, the transitions at 197, 206, 272, and 278 nm of **1** vanish upon irradiation ($\lambda = 254$ nm), and simultaneously the formation of transitions at 268 nm (moderate) and 378 nm (weak, broad) (Figure 3, dashed line) appear. All bands of **3**-PN correlate well with the values of the electronic excitations at 229, 248 nm (f = 0.052 and 0.053), and 352, 378, and 408 nm (f = 0.012, 0.04, and 0.034) computed at TD–B3LYP/def2-TZVP. The broad band at 378 nm corresponds a $\pi \rightarrow \pi^*$ transition. Subsequent irradiation of the sample with $\lambda =$ 523 nm led to the disappearance of UV/Vis bands of **3**-PN and the concomitant appearance of the UV/Vis bands of **2** (Figure S4).

In order to prepare **2** and **3**, we also carried out vacuum flash pyrolysis (VFP) of **1** at 650, 700, and 850 °C (Figure S5). Sander and co-workers reported that triplet phenyl nitrene can be generated in good yields by thermolysis of phenylazide and that it can be subsequently isolated in inert gas matrices.[34] Pyrolysis of **1** at 450 °C results in almost no decomposition of **1**, and only a small amount of **2** and **3** were identified. At 650 °C, the pyrolysis products show new IR bands that were not present in the photochemical route. The infrared spectrum of VFP products of **1** shows several new strong absorptions at 1500, 1240, 1220, 800, and 750 cm^{-1} that we assigned to structure **4**. For example, the strong IR bands at 1500 and 1240 cm^{-1} are attributed to the C=C stretching and CH out-of-plane bending modes of **4** (Table S3). The experimental and computed IR spectra are in good agreement, thereby supporting the assignment of the postulated structure **4**. Note that a small amount of **2** and **3** was observed in the experimental IR spectrum. When the temperature is raised to 850 °C, **5** and CO can be found as main products in the spectrum (Figure S5). This kind of

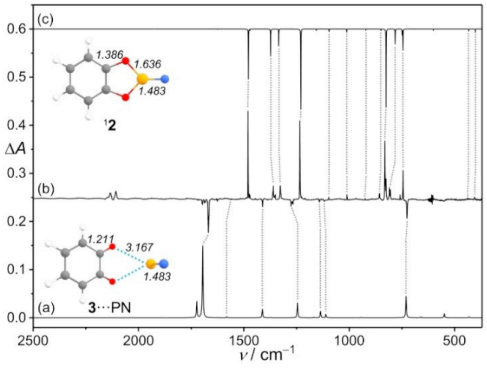

Figure 2. a) Scaled computed IR spectrum for **3**-PN (factor 0.98). b) IR difference spectrum shows the changes upon subsequently 8 min 523 nm irradiation after 254 nm UV irradiation. c) Scaled computed IR spectrum for **2** (factor 0.98). The computed molecular structures and bond lengths (in italics, Å) for **2** and **3**-PN are also depicted. All computations were done at the B3LYP/def2-TZVP level of theory.

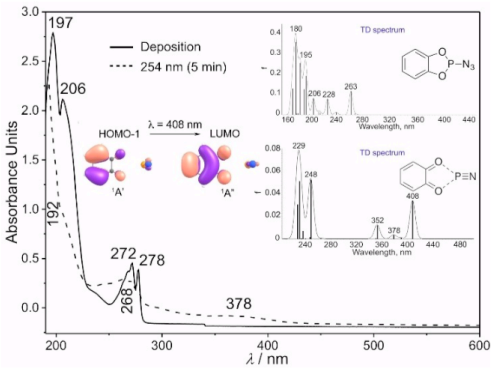

Figure 3. Solid line: UV/Vis spectrum of **1** isolated in argon at 10 K. Dashed line: UV/Vis spectrum of **3**-PN at 10 K: the photochemistry of **1** after irradiation at $\lambda = 254$ nm in argon at 10 K. Inset: Computed [TD-B3LYP/def2-TZVP] electronic transitions for **1** and **3**-PN.

decomposition was also found in the pyrolysis of *o*-phenylene sulfite with loss of sulfonic monoxide as monitored by mass spectrometry, which further lends credibility to our identification.[35]

When the pyrolysis experiment was carried out at 850 °C, only a small amount of **4** formed. Instead, the intense absorption bands at 1735, 1333, 952, 843, and 651 cm^{-1} provide evidence for the formation of cyclopentadienone (**5**) as the major product. The absorption bands of **6** are in agreement with the previously reported IR values of **5** in neon matrix.[36] Pyrolysis of **1** at 850 °C produces a large amount of carbon monoxide (CO), apparent by the strong absorption band at 2139 cm^{-1}, which most probably derives from the gas-phase decarbonylation of **3**; the latter forms by stepwise elimination of N_2 and PN from **1**. Pyrolysis of **1** at 850 °C is strongly dominated by entropy that preferentially leads to **5** and CO (Figure S5).

To gain insight into the mechanism of these reactions, we computed the relevant parts of the potential energy hypersurface surrounding **1** at B3LYP/def2-TZVP (Figure 4). According to these computations, **1** can exist in *anti* and *syn* conformations (**1a** and **1b**) with orientations of azide group relative to the opposing phenyl group; **1a** is 1.4 kcal mol^{-1} more stable than **1b**, and the rotational barrier connecting the two species amounts to 2.5 kcal mol^{-1} (including zero-point vibrational energy correction, ZPVE). Obviously, the formation of **2** and PN from **1** is a multistep process. The reaction path implies the cleavage of N_2 from **1b** to produce nitrene **2** via **TS2**. The barrier for this process is 31.3 kcal mol^{-1}. The subsequent loss of PN leads to the formation of the **3**-PN complex with a stabilization energy of 2.6 kcal mol^{-1}. The transition structure (**TS3**) for the concerted loss of PN from **2** is associated with a barrier of 38.0 kcal mol^{-1}. Moreover, we performed a two-dimensional relaxed scan along the O1-P and O2-P bonds in **2** using the RI–B3LYP/def2-TZVP method. A saddle point was found on the concerted path, indicating that the decomposition of **2** into **3**-PN is a concerted process (Figure S6 Supporting Information). The pyrolysis of starting material **1** at 700 °C also yielded infrared signals that were identified as **4**. The rearrangement of **2** to **4** is endothermic by +11.1 kcal mol^{-1} with an activation barrier of 47.2 kcal mol^{-1}. A second pathway describes a one-step process for the formation of **4** from **1a** through a barrier (**TS5**) of 47.5 kcal mol^{-1}. The intrinsic reaction paths associated with the rearrangement of **2** to **4** and **1a** to **4** are almost isoenergetic. The pyrolysis temperature at 850 °C promotes further decarbonylation of **3** and gave IR signals that were identified as **5**. The transition structure of this dissociation is associated with a substantial barrier of 61.9 kcal mol^{-1} (**TS7**).

According to our computations, **2** has a large singlet-triplet energy separation of $\Delta E_{ST} = -22.2$ kcal mol^{-1} at B3LYP/def2-TZVP, underlining its singlet ground-state nature. Nitrene **2** displays a C_{2v} point group with a $^1A_1$ electronic ground state, as a result of π-type stabilization of the electron-deficient nitrene center through the adjacent phosphorus *p*-lone pair. The PN bond length in **2** is 1.483 Å, which lies in the range of a P≡N triple bond. For example, the PN bond lengths in Mes-N≡P (**A**) (Mes = 2,4,6-tri-*tert*-butylphenyl) and bis(imidazolidin-2-iminato)phosphinonitrene (I) are 1.475 and 1.456 Å respectively.[14,24] A Wiberg bond index of 3.11 was computed for the PN bond in **2**, confirming the presence of a PN triple bond. Natural bond orbital (NBO) computations indicate that the nitrogen atom possesses a large negative charge (−1.02*e*), whereas phosphorus atom carries a large positive charge (+1.92*e*). The NBO charges at the oxygen atoms in **2** are −0.69, indicating zwitterionic character. This is in line with a natural resonance theory (NRT) analysis, which favors the zwitterionic resonance contributor (Figure S7). Our computational analysis for the **3**-PN complex gave a binding energy of −2.6 kcal mol^{-1} at B3LYP/def2-TZVP and of −6.0 kcal mol^{-1} at B3LYP–D3(BJ)/def2-TZVP. Complex **3**-PN is stabilized by electrostatic interactions between O···P with a shared potential electron density (ρ) of 0.0087 and a second Hessian eigenvalue (λ_2) of −0.0087 as derived from a topological non-covalent interaction (NCI) analysis (Figure 5 and Table S4),[37] which is consistent with the computed properties of the O···P interaction in the HO···PO complex (Figure S8).[38] The O···P distance in **3**-PN of 3.166 Å is smaller than the sum of the van der Waals radii of O (1.52 Å) and P (1.80 Å), respectively.[39]

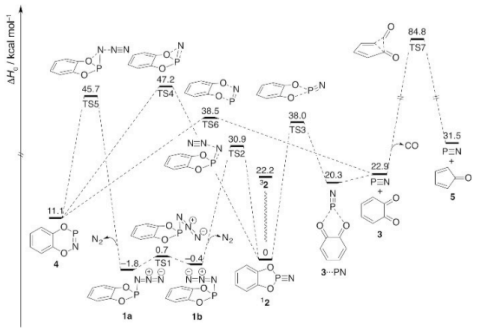

Figure 4. Potential energy hypersurface profile (ΔH_0, kcal mol^{-1}) of the reactions of **2** at B3LYP/def2-TZVP + ZPVE at 0 K.

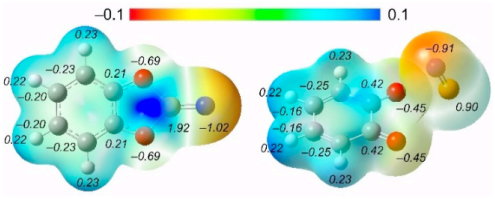

Figure 5. Calculated molecular electrostatic potential (ESP) maps (isovalue = 0.004) and natural population analysis (NPA) charges (numbers in *italics*) for **2** (left) and **3**-PN (right) at B3LYP/def2-TZVP.

Conclusion

Here, we report a *o*-benzoquinone-PN complex that was generated in cryogenic matrices utilizing UV light irradiation of the corresponding azide precursor. Besides IR and UV spectroscopic characterization, its recombination to covalently bonded (*o*-phenyldioxyl)-λ^5-phosphinonitrile was triggered by subsequent 523 nm irradiation through a concerted mechanism, which reveals the first observed reactivity of PN towards organic molecules. VFP and photolysis experiments suggest that (*o*-phenyldioxyl)phosphinoazide may be a viable precursor for PN in synthesis, and this will be the target of forthcoming work.

Acknowledgements

Financial support by the Deutsche Forschungsgemeinschaft (DFG) via the grant MA 8773/3-1 is gratefully acknowledged. Open Access funding enabled and organized by Projekt DEAL.

Conflict of Interest

The authors declare no conflict of interest.

Data Availability Statement

The data that support the findings of this study are available in the Supporting Information of this article.

Keywords: Matrix Isolation · Nitrenes · Phosphorus Mononitride · Photochemistry

[1] L. M. Ziurys, *Astrophys. J.* **1987**, *321*, L81–85.
[2] J. Chantzos, V. M. Rivilla, A. Vasyunin, E. Redaelli, L. Bizzocchi, F. Fontani, P. Caselli, *Astron. Astrophys.* **2020**, *633*, A54.
[3] T. Aota, Y. Aikawa, *Astron. Astrophys.* **2012**, *761*, 74.
[4] D. Haasler, V. M. Rivilla, S. Martín, J. Holdship, S. Viti, N. Harada, J. Mangum, K. Sakamoto, S. Muller, K. Tanaka, Y. Yoshimura, K. Nakanishi, L. Colzi, L. Hunt, K. L. Emig, R. Aladro, P. Humire, C. Henkel, P. van der Werf, *Astron. Astrophys.* **2022**, *659*, A158.
[5] C. Mininni, F. Fontani, V. M. Rivilla, M. T. Beltrán, P. Caselli, A. Vasyunin, *Mon. Not. R. Astron. Soc.: Lett.* **2018**, *476*, L39-L44.
[6] B. E. Turner, J. Bally, *Astrophys. J.* **1987**, *321*, L75.
[7] R. M. Atkins, P. L. Timms, *Spectrochim. Acta Part A* **1977**, *33*, 853.
[8] S. Liang, P. Hemberger, J. Levalois-Grützmacher, H. Grützmacher, S. Gaan, *Chem. Eur. J.* **2017**, *23*, 5595–5601.
[9] R. M. Atkins, P. L. Timms, *Inorg. Nucl. Chem. Lett.* **1978**, *14*, 113–115.
[10] J. L. Martinez, S. A. Lutz, D. M. Beagan, X. Gao, M. Pink, C.-H. Chen, V. Carta, P. Moënne-Loccoz, J. M. Smith, *ACS Cent. Sci.* **2020**, *6*, 1572–1577.
[11] M.-A. Courtemanche, W. J. Transue, C. C. Cummins, *J. Am. Chem. Soc.* **2016**, *138*, 16220–16223.
[12] L. Zhao, W. Yi, J. Botana, F. Gu, M. Miao, *J. Phys. Chem. C* **2017**, *121*, 28520–28526.
[13] X. Zheng, S. Lin, D. Kong, Y. Wei, K. Pang, R. Ku, N. T. Kaner, X. Xu, M. Sha, J. Liu, H. Huang, J. Yang, H. Shi, X. Li, W. Li, *Adv. Theory Simul.* **2022**, *5*, 2100305.
[14] E. Niecke, M. Nieger, F. Reichert, *Angew. Chem. Int. Ed. Engl.* **1988**, *27*, 1715–1716.
[15] R. Kinjo, B. Donnadieu, G. Bertrand, *Angew. Chem. Int. Ed.* **2010**, *49*, 5930–5933.
[16] A. Velian, C. C. Cummins, *J. Am. Chem. Soc.* **2012**, *134*, 13978–13981.
[17] C. Hering, A. Schulz, A. Villinger, *Chem. Sci.* **2014**, *5*, 1064–1073.
[18] A. K. Eckhardt, M.-L. Y. Riu, M. Ye, P. Müller, G. Bistoni, C. C. Cummins, *Nat. Chem.* **2022**, *14*, 928–934.
[19] H. A. Spinney, N. A. Piro, C. C. Cummins, *J. Am. Chem. Soc.* **2009**, *131*, 16233–16243.
[20] A. Mardyukov, F. Keul, P. R. Schreiner, *Angew. Chem. Int. Ed.* **2020**, *59*, 12445–12449.
[21] X. Chu, Y. Yang, B. Lu, Z. Wu, W. Qian, C. Song, X. Xu, M. Abe, X. Zeng, *J. Am. Chem. Soc.* **2018**, *140*, 13604–13608.
[22] X. Zhao, X. Chu, G. Rauhut, C. Chen, C. Song, B. Lu, X. Zeng, *Angew. Chem. Int. Ed.* **2019**, *58*, 12164–12169.
[23] R. Feng, Y. Lu, G. Deng, J. Xu, Z. Wu, H. Li, Q. Liu, N. Kadowaki, M. Abe, X. Zeng, *J. Am. Chem. Soc.* **2018**, *140*, 10–13.
[24] F. Dielmann, O. Back, M. Henry-Ellinger, P. Jerabek, G. Frenking, G. Bertrand, *Science* **2012**, *337*, 1526–1528.
[25] F. Dielmann, G. Bertrand, *Chem. Eur. J.* **2015**, *21*, 191–198.
[26] L. Liu, D. A. Ruiz, D. Munz, G. Bertrand, *Chem* **2016**, *1*, 147–153.
[27] Z. Wu, D. Li, H. Li, B. Zhu, H. Sun, J. S. Francisco, X. Zeng, *Angew. Chem. Int. Ed.* **2016**, *55*, 1507–1510.
[28] H. Li, Z. Wu, D. Li, X. Zeng, H. Beckers, J. S. Francisco, *J. Am. Chem. Soc.* **2015**, *137*, 10942–10945.
[29] H. F. Bettinger, H. Bornemann, *J. Am. Chem. Soc.* **2006**, *128*, 11128–11134.
[30] V. Bhagat, J. Schumann, H. F. Bettinger, *Angew. Chem. Int. Ed.* **2021**, *60*, 23112–23116.
[31] C. Wentrup, *Angew. Chem. Int. Ed.* **2018**, *57*, 11508–11521.
[32] A. L. Macdonald, J. Trotter, *J. Chem. Soc. Perkin Trans. 2* **1973**, 476–480.
[33] K. Piech, T. Bally, T. Ichino, J. Stanton, *Phys. Chem. Chem. Phys.* **2014**, *16*, 2011–2019.
[34] J. Mieres-Pérez, E. Mendez-Vega, K. Velappan, W. Sander, *J. Org. Chem.* **2015**, *80*, 11926–11931.
[35] D. C. De Jongh, R. Y. Van Fossen, *J. Org. Chem.* **1972**, *37*, 1129–1135.
[36] T. K. Ormond, A. M. Scheer, M. R. Nimlos, D. J. Robichaud, J. W. Daily, J. F. Stanton, G. B. Ellison, *J. Phys. Chem. A* **2014**, *118*, 708–718.
[37] T. Lu, F. Chen, *J. Comput. Chem.* **2012**, *33*, 580–592.
[38] X. Chu, W. Qian, B. Lu, L. Wang, J. Qin, J. Li, G. Rauhut, T. Trabelsi, J. S. Francisco, X. Zeng, *Angew. Chem. Int. Ed.* **2020**, *59*, 21949–21953.
[39] M. Mantina, A. C. Chamberlin, R. Valero, C. J. Cramer, D. G. Truhlar, *J. Phys. Chem. A* **2009**, *113*, 5806–5812.

Manuscript received: January 16, 2023
Accepted manuscript online: March 6, 2023
Version of record online: April 18, 2023

2.2 Triplet Phenylarsinidene and Its Oxidation to Dioxophenylarsine

Abstract: Carbenes and nitrenes are key intermediates involved in numerous chemical processes and they have attracted considerable attention in synthetic chemistry, biochemistry, and materials science. Even though parent arsinidene (H–As) has been characterized well, the high reactivity of subsituted arsinidenes has prohibited their isolation and characterization to date. Here, we report the preparation of triplet phenylarsinidene through the photolysis of phenylarsenic diazide, isolated in an argon matrix, and its subsequent characterization by infrared and UV/Vis spectroscopy. Doping the matrices containing phenylarsinidene with molecular oxygen leads to the formation of hitherto unknown *anti*-dioxyphenylarsine. The latter undergoes isomerization to novel dioxophenylarsine upon 465 nm irradiation. The assignments were validated by isotope-labeling experiments and agree very well with B3LYP/def2-TZVP computations.

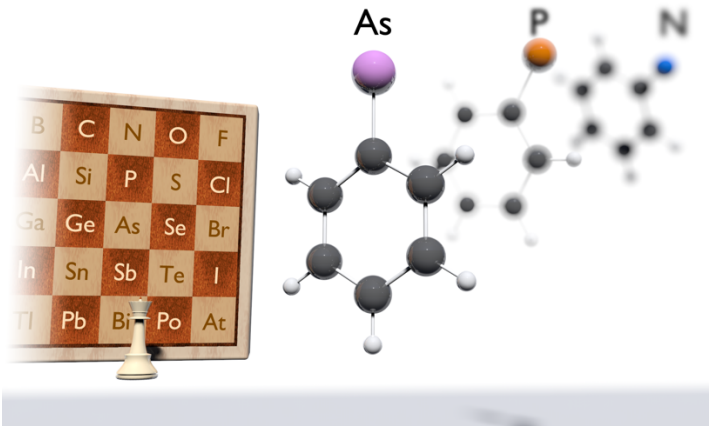

Original Source: Weiyu Qian, Peter R. Schreiner, Artur Mardyukov, *J. Am. Chem. Soc.* **2023**, *145*, 12755. (DOI: 10.1021/jacs.3c02935).

Highlight: a) Supplementary cover of this issue, b) Victoria Atkinson, Chemistry World, RSC **2023**, https://www.chemistryworld.com/news/first-synthesis-of-unusual-arsenic-reagent-reveals-that-it-breaks-periodic-trend/4017553.article, c) Malte Fischer, Dominikus Heift, Nachrichten aus der Chemie, **2024**, https://doi.org/10.1002/nadc.20244139259.

JACS
JOURNAL OF THE AMERICAN CHEMICAL SOCIETY
pubs.acs.org/JACS
Article

Triplet Phenylarsinidene and Its Oxidation to Dioxophenylarsine

Weiyu Qian, Peter R. Schreiner, and Artur Mardyukov*

Cite This: J. Am. Chem. Soc. 2023, 145, 12755−12759
Read Online
ACCESS | Metrics & More | Article Recommendations | Supporting Information

ABSTRACT: Carbenes and nitrenes are key intermediates involved in numerous chemical processes, and they have attracted considerable attention in synthetic chemistry, biochemistry, and materials science. Even though parent arsinidene (H-As) has been characterized well, the high reactivity of subsituted arsinidenes has prohibited their isolation and characterization to date. Here, we report the preparation of triplet phenylarsinidene through the photolysis of phenylarsenic diazide isolated in an argon matrix and its subsequent characterization by infrared and UV/vis spectroscopy. Doping matrices containing phenylarsinidene with molecular oxygen leads to the formation of hitherto unknown anti-dioxyphenylarsine. The latter undergoes isomerization to novel dioxophenylarsine upon 465 nm irradiation. The assignments were validated by isotope-labeling experiments and agree very well with B3LYP/def2-TZVP computations.

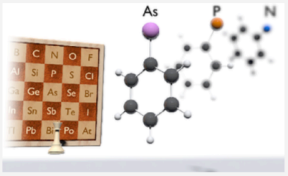

INTRODUCTION

Owing to their roles as versatile reagents and pivotal intermediates in numerous chemical processes, the properties and reactivity of carbenes (R−C̈−R)[1−3] and nitrenes (R−N̈:)[4−6] have been extensively studied despite their high reactivity and instability. However, there are still many families of reactive intermediates that have eluded isolation and spectroscopic identification. Among these are arsinidenes (R−Äs:), the neutral monovalent arsenic congeners of nitrenes, and phosphinidenes (R−P̈:) with six electrons in their valence shell. Depending on the nature of the R-substituent, they may adopt either a singlet or a triplet electronic ground state (Scheme 1A). Multiple attempts have been made to prepare free arsinidenes, but the detection and identification of these species has been hampered by their instability and fleeting existence.[7,8] To date, only electronic and vibrational transitions of parent arsinidene (H−Äs:) have been studied by flash photolysis of AsH_3.[9−12] All other evidence for the existence of arsinidenes has been derived from trapping and complexation experiments. For example, several terminal arsinidene complexes with transition metals were synthesized and structurally characterized by X-ray crystal structure analysis.[13−17] Furthermore, *N*-heterocyclic-carbenes (NHCs)[18,19] and *N*-heterocyclic silylenes (NHSis)[20] were also utilized for the stabilization of arsinidenes. In addition, HM=AsH (M = Ti, Zr, Hf) complexes were prepared by the reaction of group IV metal atoms with AsH_3 under matrix isolation conditions.[21] The arsaketene radical and anion were trapped in cryogenic matrices by the reaction of laser-ablated arsenic atoms with carbon monoxide.[22]

Phenylarsinidene (**1**), the heavier analogue of phenylphosphinidene (Ph−P̈:), is deemed to be a key intermediate in the synthesis of arsol-containing compounds in organic electronics[23] and as a ligand for the stabilization of isolable alumenenes.[24] Arsphenamine, also known under its trade name Salvarsan, the first modern antimicrobial agent, may be regarded as the trimer of an aryl arsinidene, which was synthesized from 3-nitro-4-hydroxyphenylarsonic acid.[25] Diarsenes (R−As=As−R), the arsinidene dimers, can be quantitatively obtained in situ from the thermolysis of arsa-Wittig reagents in solution.[26,27]

In contrast to the unknown arsinidenes, several "free" phosphinidenes have been isolated under matrix isolation conditions and characterized by IR, UV/vis, and EPR spectroscopy, which includes the parent phosphinidene (H−P̈:),[28] methoxyphosphinidene (CH_3O−P̈:),[29] phenylphosphinidene (Ph−P̈:),[30,31] mesitylphosphinidene (Mes−P̈:),[32,33]

Scheme 1. (A) Common Electronic Configurations of Pnictinidenes (OST, Open-Shell Triplet; OSS, Open-Shell Singlet; CSS, Closed-Shell Singlet); (B) Photochemical Generation of Phenylarsinidene 1 and Subsequent (Photo)Reactivity

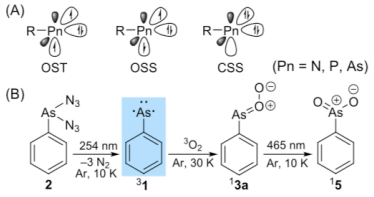

Received: March 21, 2023
Published: May 26, 2023

and ethynylphosphinidene (HCC–P̈:),[34] which have triplet electronic ground states. It has also been experimentally shown that strong π-donor substitution (e.g., R_2N–, R_2P–) stabilizes singlet phosphinidene over the triplet.[35,36] To date, however, there is no clear experimental evidence confirming the formation of uncomplexed alkyl- and aryl-arsinidenes; their reactivity is unknown. Herein, we report the first synthesis as well as IR and UV/vis spectroscopic characterization of phenylarsinidene **1** and its oxidation to *anti*-dioxyphenylarsine (**3a**) as well as dioxophenylarsine (**5**) through the reaction of **1** with molecular oxygen (O_2) and subsequent trapping in argon matrices at 10 K (Scheme 1B).

RESULTS AND DISCUSSION

It was shown recently that transient phosphorus species can be readily generated by thermal and photochemical N_2 extrusion from the corresponding azides.[29,37,38] Our strategy for the preparation of **1** was the photolysis of phenylarsenic diazide (**2**) in the reaction **2** → **1** + 3 N_2 (N_2 as the IR-invisible byproduct). Diazide **2** was synthesized from the corresponding dichloride precursor (for synthetic details, see the Supplementary Materials). The matrix-isolated IR spectrum of **2** shows two strong bands at 2109.9 and 2086.7 cm^{-1}, which were assigned as symmetric and asymmetric NNN stretching modes, respectively. In addition, two medium-intensity IR bands at 1240.5 and 1219.2 cm^{-1} could be tentatively assigned to the interior N═N symmetric and asymmetric stretching modes of **2**. Irradiation of matrices containing **2** with light λ = 254 nm results in the rapid disappearance of its IR bands, and simultaneously, a new set of IR bands appears at 1575, 1473, 1429, 1325, 1065, 1024, 994, 904, 731, 687, and 426 cm^{-1} (Figure 1b). The excellent agreement between the experimentally observed and computed IR spectra at B3LYP/def2-TZVP is taken as evidence for the formation of triplet **1** (^{3}**1**; Table S1). For example, the strong IR bands at 731 and 687 cm^{-1} are attributed to the C–H out-of-plane (o.o.p.) vibrational modes. At the B3LYP/def2-TZVP level of theory, the C–As stretch shows a frequency of 295 cm^{-1}, which is, unfortunately, at the lower limit of our IR spectrometer, and therefore cannot be detected.

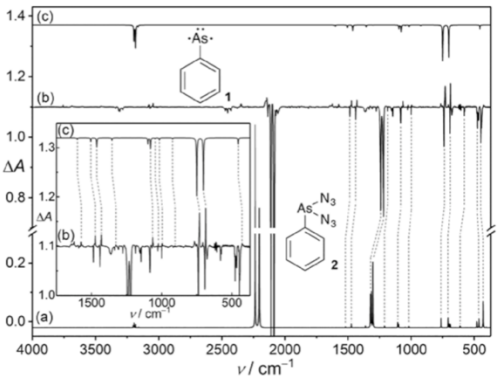

Figure 1. (a) Unscaled computed spectrum for ^{3}**1** at B3LYP/def2-TZVP. (b) IR difference spectrum shows the changes upon 5 min of 254 nm irradiation. (c) Unscaled computed spectrum for **2** at B3LYP/def2-TZVP. Inset: Expanded spectra for detail display in the range of 1750–400 cm^{-1}.

The UV/vis spectral analysis of **2** shows intensive absorptions in the UV region, which includes strong transition bands at 192, 218, and 272 nm (Figure 2). They completely vanish after 2 min of 254 nm irradiation, and simultaneously, the strong absorption band of ^{3}**1** at 262 nm together with weak bands at 280 and 342 nm appear. The UV/vis spectrum of ^{3}**1** qualitatively resembles the spectra of phenylphosphinidene in an argon matrix.[30] The experimental UV/vis spectrum of ^{3}**1** agrees well with the intense electronic absorptions at 277 and 296 nm (f = 0.128 and 0.086; f, oscillator strength), as well as medium absorptions at 343 and 375 nm (f = 0.007 and 0.009) computed at TD-B3LYP/def2-TZVP.

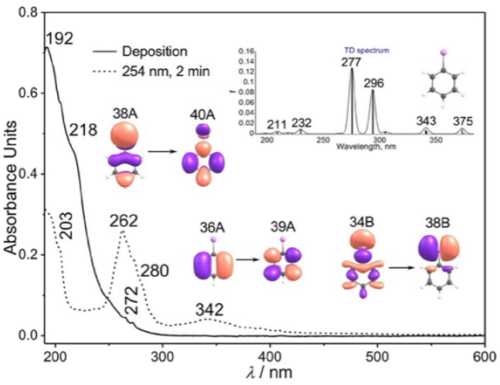

Figure 2. Solid line: UV/vis spectrum of **2** isolated in argon (10 K). Dashed line: UV/vis spectrum of ^{3}**1** at 10 K: the photochemistry of **2** after irradiation at λ = 254 nm in argon at 10 K. Inset: Computed [TD-B3LYP/def2-TZVP] electronic transitions for ^{3}**1**.

According to our B3LYP/def2-TVZP computations, **1** shows planar C_{2v} symmetry with an electronic $^3A_2$ ground state. Arsinidene **1** has a large singlet-triplet energy separation of ΔE_{ST} = 22.2 kcal mol^{-1} at B3LYP/def2-TZVP and 24.1 kcal mol^{-1} at CASPT2(8,8)/cc-pVDZ (Table S2), underscoring its triplet electronic ground state nature similarly to phenylphosphinidene (**6**) (ΔE_{ST} = 33.0 kcal mol^{-1} at B3LYP/def2-TZVP; ΔE_{ST} = 25.0 kcal mol^{-1} at CASPT2(8,8)/cc-pVDZ) and phenylnitrene (**7**) (ΔE_{ST} = 30.0 kcal mol^{-1} at B3LYP/def2-TZVP; ΔE_{ST} = 37.4 kcal mol^{-1} at CASPT2(8,8)/cc-pVDZ). We have also compared the key geometric parameters of **1** with those of **6** and **7**. The optimized structures are presented in Figure S1. As expected, the C–As bond length of **1** is considerably longer (1.932 Å) than C–P (1.791 Å) and C–N (1.318 Å) of **6** and **7**, respectively. Moreover, there are slight differences between the C═C bonds of the phenyl rings. In the case of **6** and **7**, the benzene rings show more bond alternation than in **1**. This implies that there is almost no delocalization of spin density from the arsenic atom into the phenyl ring, probably owing to a mismatch of the orbital sizes: the 2p (C) overlap with the 4p (As) is poor. This is in line with the computed spin densities: a higher positive spin density resides at the arsenic atom of 1.95 in **1** compared to nitrogen (1.57) in **6** and phosphorus (1.88) in **7** (Figure S1). The computed T_1 diagnostic values for **1** (0.036; Supplementary Materials), **6** (0.040), and **7** (0.039) exceed the historic

https://doi.org/10.1021/jacs.3c02935
J. Am. Chem. Soc. 2023, 145, 12755–12759

criterion $T_1 \leq 0.02$ for main group species,[39] which suggests that single-reference methods are likely not reliable for this system. Therefore, the geometry optimizations were also carried out at the CASSCF(8,8)/cc-pVDZ level of theory (Figure S1), which shows the same trend of the structural characteristics of **1**, **6**, and **7**. The thermodynamic stability of **1** over **6** and **7** is also evident by the sizable reaction enthalpy of the homodesmotic equation ΔH_r = 75.3 kcal mol^{-1} X = As, 63.9 kcal mol^{-1} X = P, and 39.1 kcal mol^{-1} X = N.

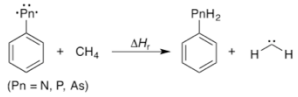

The preparation and matrix isolation of ^{3}**1** also enabled us to investigate its reaction with molecular oxygen ($^3O_2$) that may lead to the formation dioxophenylarsine ($PhAsO_2$, **5**), also a novel compound, which is a hitherto unknown arsenic analogue of nitrobenzene. Previously, Sander et al. demonstrated that the reaction of **7** with $^3O_2$ in xenon matrices yields the most stable *syn*-phenylnitroso oxide as an intermediate product, which isomerizes to nitrobenzene upon 460 nm irradiation.[40] We also reported the oxidation of **6**, where we detected only cyclic 3-phenyl-1,2,3-dioxaphosphirane.[30] Similar to the nitrogen analogue, the latter rearranges into phenyldioxophosphorane upon selective irradiation (Scheme 2).

Scheme 2. Summary of the Reactions of Phenylnitrene, Phenylphosphinidene, and Phenylarsinidene with Molecular Oxygen; Relative Energies (in kcal mol^{-1}) Computed at B3LYP/def2-TZVP

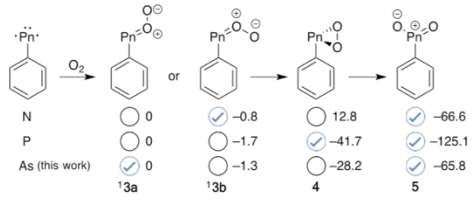

Doping argon matrices containing **2** with variable oxygen concentrations in the range of 0.1−1% and subsequent photolysis at 254 nm showed no changes in the IR spectrum; only **1** was observed. However, after annealing the matrix at 35 K for 5 min, a group of new peaks at 1478.3, 1436.2/1434.2, 1331.6, 1160.4, 1049.2, 1031.7, 993.5, 735.7, and 687.2 cm^{-1} appeared gradually (Figure S2). For example, a strong peak at 1031.7 cm^{-1} can be attributed to the O−O stretching vibration, and its position is quite close to that in *syn*-phenylnitroso oxide (1000 and 990 cm^{-1}, Xe-matrix).[40] By comparison with computed infrared vibrations for all potential candidates, this set of bands was assigned to *anti*-phenyldioxylarsinene (**3a**). The assignment of **3a** is further corroborated by ^{18}O-labeling experiments. For example, the O−O stretching vibration in **3a** is computed to have a 59.0 cm^{-1} redshift, which is in good accordance with the experimental shift of 59.6 cm^{-1}. However, because arsenic is less conjugated to the phenyl ring and much heavier than phosphorus and nitrogen, the other bands associated with the phenyl motif are barely disturbed upon isotope labeling (Table S3). We also found that **3a** is photolabile when exposed to 465 nm light. The IR bands of **3a** vanish rapidly, and a new group of peaks at 1490.4, 1447.4/1440.4, 1315.8, 1084.1, 1075.5, 1016.8, 923.2, 741.6, and 684.7 cm^{-1} appear contemporarily (Figure 3). The experimentally observed IR spectrum agrees

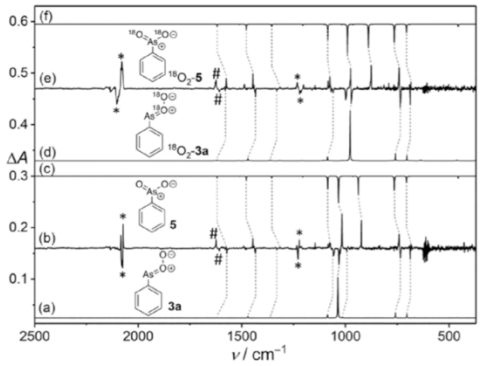

Figure 3. (a) Unscaled computed spectrum for **3a** at B3LYP/def2-TZVP. (b) IR difference spectrum shows the changes upon 1 min of 465 nm irradiation of 1% O_2 doped Ar matrix. (c) Unscaled computed spectrum for **5** at B3LYP/def2-TZVP. (d) Unscaled computed spectrum for $^{18}O_2$-**3a** at the B3LYP/def2-TZVP levels. (e) IR difference spectrum shows the changes upon 1 min of 465 nm irradiation of 1% $^{18}O_2$ doped Ar-matrix. (f) Unscaled computed spectrum for $^{18}O_2$-**5** at B3LYP/def2-TZVP. The matrix sites of unreacted **2** (*) and H_2O (#) are marked.

well with the computed spectrum of dioxophenylarsine **5**. The strong IR bands at 1016.8 and 923.2 cm^{-1} are due to the OAsO asymmetric and symmetric stretching modes, respectively. They show large shifts of 42.0 and 47.6 cm^{-1} in the ^{18}O-labeling experiment, which match nicely with the computed shifts of 43.1 and 48.5 cm^{-1}, respectively (Table S4).

The reaction of **1** with O_2 was also monitored by UV/vis spectroscopy. The transition bands of **1** disappear upon annealing at 35 K for several minutes, and simultaneously transitions at 192 and 218 nm (strong), 261 nm (moderate), and 478 nm (weak, broad) (Figure S3, solid line) appear. All new bands correlate well with the values of the electronic excitations of **3a** at 198 nm (f = 0.076), 260 nm (f = 0.163), and 456 nm (f = 0.158) computed at TD-B3LYP/def2-TZVP. Further irradiation at 465 nm results in the disappearance of the broad band at 478 nm and the formation of **5**.

We undertook a detailed computational analysis of the reaction of **1** with O_2 (Figure 4). The absence of characteristic bands of **3a** before annealing, even at a high O_2 concentration (>2%), implies that the reaction between **1** and O_2 has a sizable activation barrier. Note that the reaction mechanism of **1** with O_2 on the triplet surface from ^{3}**1** to ^{3}**3a** is slightly endothermic, followed by intersystem crossing (ISC) to ^{1}**3a**. Alternatively, the formation of ^{1}**3a** may happen through crossing of the triplet-to-singlet potential energy surface, which occurs at the minimum energy crossing point (MECP) at −9.2 kcal mol^{-1}. Additionally, the energy of MECP of **3b** (−5.9 kcal mol^{-1}) is higher than that of ^{1}**3a**, thus making the formation of **3b** unfavorable. Interestingly, Sander and co-workers reported that the reaction of phenylnitrene **6** with O_2 results in the formation of *syn*-phenylnitroso oxide, which is thermodynamically more stable than the *anti*-conformer (Scheme 2).[40] In our

https://doi.org/10.1021/jacs.3c02935
J. Am. Chem. Soc. 2023, 145, 12755−12759

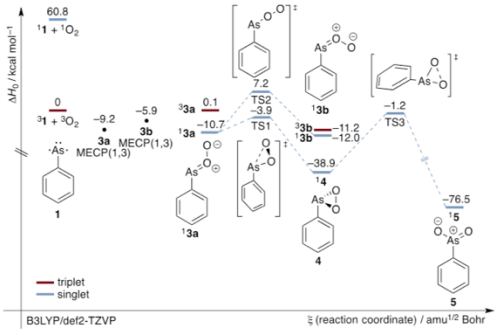

Figure 4. Potential energy profile (ΔH_0, kcal mol^{-1}) of the reactions of ^{3}**1** with molecular oxygen at B3LYP/def2-TZVP.

experiments, the *anti*-conformer **3a** formed exclusively, which is 1.3 kcal mol^{-1} (B3LYP/def2-TZVP) less stable than the *syn*-conformer **3b** with a rotamerization barrier of 17.9 kcal mol^{-1}. The tautomerization of **3a** to 3-phenyl-1,2,3-dioxaarsirane (**4**) proceeds with a barrier of 6.8 kcal mol^{-1}. The subsequent rearrangement of **4** to **5** is associated with a barrier of 37.7 kcal mol^{-1}. Although we did not observe **4** spectroscopically, this was to be expected since the conversion of **3a** to **5** through **4** can only be accomplished via photoexcitation. According to TD-B3LYP/def2-TZVP computations, **4** has an electronic transition at 383 nm (f = 0.011) (Figure S4), which suggests the intermediacy of this highly labile species upon irradiation.

■ CONCLUSIONS

In summary, we generated triplet phenylarsinidene in cryogenic matrices and characterized it spectroscopically by means of IR and UV/vis spectroscopy. Doping matrices of phenylarsinidene with molecular oxygen led to oxidation to *anti*-phenyldioxylarsinene, with reactivity different from that of the reactions of phenylphosphinidene and phenylnitrene with oxygen. Dioxophenylarsine, the arsenic analogue of nitrobenzene, was obtained through subsequent irradiation. Our disclosure of a straightforward preparation of phenylarsinidine contributes to our knowledge of fundamental chemistry of a higher pnictogen sextet species and provides new entry points for the use of arsinidenes in synthetic and materials chemistry.

■ ASSOCIATED CONTENT

Supporting Information

The Supporting Information is available free of charge at https://pubs.acs.org/doi/10.1021/jacs.3c02935.

IR and UV/vis spectra, NMR spectra, IR table, Cartesian coordinates, absolute energies of all optimized geometries, and experimental procedures and simulations (PDF)

■ AUTHOR INFORMATION

Corresponding Author

Artur Mardyukov – *Institute of Organic Chemistry, Justus Liebig University, Giessen 35392, Germany*; orcid.org/0000-0003-3908-6967; Email: artur.mardyukov@org.chemie.uni-giessen.de

Authors

Weiyu Qian – *Institute of Organic Chemistry, Justus Liebig University, Giessen 35392, Germany*

Peter R. Schreiner – *Institute of Organic Chemistry, Justus Liebig University, Giessen 35392, Germany*; orcid.org/0000-0002-3608-5515

Complete contact information is available at: https://pubs.acs.org/10.1021/jacs.3c02935

Author Contributions

The manuscript was written through contributions of all authors. All authors have given approval to the final version of the manuscript.

Funding

No competing financial interests have been declared.

Notes

The authors declare no competing financial interest.

■ ACKNOWLEDGMENTS

Financial support by the Deutsche Forschungsgemeinschaft (DFG) via the grant MA 8773/3-1 is gratefully acknowledged.

■ REFERENCES

(1) Bourissou, D.; Guerret, O.; Gabbaï, F. P.; Bertrand, G. Stable Carbenes. *Chem. Rev.* **2000**, *100*, 39−92.

(2) Sander, W.; Bucher, G.; Wierlacher, S. Carbenes in matrixes: spectroscopy, structure, and reactivity. *Chem. Rev.* **1993**, *93*, 1583−1621.

(3) Hirai, K.; Itoh, T.; Tomioka, H. Persistent Triplet Carbenes. *Chem. Rev.* **2009**, *109*, 3275−3332.

(4) Dielmann, F.; Back, O.; Henry-Ellinger, M.; Jerabek, P.; Frenking, G.; Bertrand, G. A Crystalline Singlet Phosphinonitrene: A Nitrogen Atom-Transfer Agent. *Science* **2012**, *337*, 1526−1528.

(5) Wentrup, C. Carbenes and Nitrenes: Recent Developments in Fundamental Chemistry. *Angew. Chem., Int. Ed.* **2018**, *57*, 11508−11521.

(6) Sun, J.; Abbenseth, J.; Verplancke, H.; Diefenbach, M.; de Bruin, B.; Hunger, D.; Würtele, C.; van Slageren, J.; Holthausen, M. C.; Schneider, S. A platinum(ii) metallonitrene with a triplet ground state. *Nat. Chem.* **2020**, *12*, 1054−1059.

(7) Hinz, A.; Hansmann, M. M.; Bertrand, G.; Goicoechea, J. M. Intercepting a Transient Phosphino-Arsinidene. *Chem. − Eur. J.* **2018**, *24*, 9514−9519.

(8) Yao, S.; Grossheim, Y.; Kostenko, A.; Ballestero-Martínez, E.; Schutte, S.; Bispinghoff, M.; Grützmacher, H.; Driess, M. Facile Access to NaOC≡As and Its Use as an Arsenic Source To Form Germylidenylarsinidene Complexes. *Angew. Chem., Int. Ed.* **2017**, *56*, 7465−7469.

(9) Dixon, R. N.; Lamberton, H. M. The A, $^3\Pi_i$−X, $^{3-}$ band systems of AsH and AsD. *J. Mol. Spectrosc.* **1968**, *25*, 12−33.

(10) Arens, M.; Richter, W. Spectroscopic observation of the $b^1\Sigma^+ \rightarrow \tilde{X}^3\Sigma^-$ transition of AsH. *J. Chem. Phys.* **1990**, *93*, 7094−7096.

(11) Berkowitz, J. Photoionization mass spectrometric studies of AsH_n (n=1−3). *J. Chem. Phys.* **1988**, *89*, 7065−7076.

(12) Hensel, K. D.; Hughes, R. A.; Brown, J. M. IR spectrum of the AsH radical in its X $^3\Sigma^-$ state, recorded by laser magnetic resonance. *J. Chem. Soc., Faraday Trans.* **1995**, *91*, 2999−3004.

(13) Sharma, M. K.; Neumann, B.; Stammler, H.-G.; Andrada, D. M.; Ghadwal, R. S. Electrophilic terminal arsinidene-iron(0) complexes with a two-coordinated arsenic atom. *Chem. Commun.* **2019**, *55*, 14669−14672.

(14) Fischer, M.; Reiß, F.; Hering-Junghans, C. Titanocene pnictinidene complexes. *Chem. Commun.* **2021**, *57*, 5626−5629.

(15) Bonanno, J. B.; Wolczanski, P. T.; Lobkovsky, E. B. Arsinidene, Phosphinidene, and Imide Formation via 1,2-H2-Elimination from

(silox)3HTaEHPh (E = N, P, As): Structures of (silox)3Ta:EPh (E = P, As). *J. Am. Chem. Soc.* **1994**, *116*, 11159−11160.
(16) Wildman, E. P.; Balázs, G.; Wooles, A. J.; Scheer, M.; Liddle, S. T. Triamidoamine thorium-arsenic complexes with parent arsenide, arsinidiide and arsenido structural motifs. *Nat. Commun.* **2017**, *8*, 14769.
(17) Pugh, T.; Kerridge, A.; Layfield, R. A. Yttrium Complexes of Arsine, Arsenide, and Arsinidene Ligands. *Angew. Chem., Int. Ed.* **2015**, *54*, 4255−4258.
(18) Arduengo, A. J.; Calabrese, J. C.; Cowley, A. H.; Dias, H. V. R.; Goerlich, J. R.; Marshall, W. J.; Riegel, B. Carbene−Pnictinidene Adducts. *Inorg. Chem.* **1997**, *36*, 2151−2158.
(19) Doddi, A.; Weinhart, M.; Hinz, A.; Bockfeld, D.; Goicoechea, J. M.; Scheer, M.; Tamm, M. N-Heterocyclic carbene-stabilised arsinidene (AsH). *Chem. Commun.* **2017**, *53*, 6069−6072.
(20) Präsang, C.; Stoelzel, M.; Inoue, S.; Meltzer, A.; Driess, M. Metal-Free Activation of EH3 (E=P, As) by an Ylide-like Silylene and Formation of a Donor-Stabilized Arsasilene with a HSi=AsH Subunit. *Angew. Chem., Int. Ed.* **2010**, *49*, 10002−10005.
(21) Andrews, L.; Cho, H.-G. Matrix Infrared Spectra and Quantum Chemical Calculations of Ti, Zr, and Hf Dihydride Phosphinidene and Arsinidene Molecules. *Inorg. Chem.* **2016**, *55*, 8786−8793.
(22) Zhang, L.; Dong, J.; Zhou, M. Formation and characterization of the AsCO and AsCO− molecules. A matrix isolation FTIR and theoretical study. *Chem. Phys. Lett.* **2001**, *335*, 334−338.
(23) Green, J. P.; Han, Y.; Kilmurray, R.; McLachlan, M. A.; Anthopoulos, T. D.; Heeney, M. An Air-Stable Semiconducting Polymer Containing Dithieno[3,2-b:2′,3′-d]arsole. *Angew. Chem., Int. Ed.* **2016**, *55*, 7148−7151.
(24) Fischer, M.; Nees, S.; Kupfer, T.; Goettel, J. T.; Braunschweig, H.; Hering-Junghans, C. Isolable Phospha- and Arsaalumenes. *J. Am. Chem. Soc.* **2021**, *143*, 4106−4111.
(25) Lloyd, N. C.; Morgan, H. W.; Nicholson, B. K.; Ronimus, R. S. The Composition of Ehrlich's Salvarsan: Resolution of a Century-Old Debate. *Angew. Chem., Int. Ed.* **2005**, *44*, 941−944.
(26) Smith, R. C.; Gantzel, P.; Rheingold, A. L.; Protasiewicz, J. D. Arsa-Wittig Complexes (ArAsPMe3) as Intermediates to Diarsenes. *Organometallics* **2004**, *23*, 5124−5126.
(27) Weber, L. The chemistry of diphosphenes and their heavy congeners: synthesis, structure, and reactivity. *Chem. Rev.* **1992**, *92*, 1839−1906.
(28) Qian, W.; Lu, B.; Tan, G.; Rauhut, G.; Grützmacher, H.; Zeng, X. Vibrational spectrum and photochemistry of phosphaketene HPCO. *Phys. Chem. Chem. Phys.* **2021**, *23*, 19237−19243.
(29) Chu, X.; Yang, Y.; Lu, B.; Wu, Z.; Qian, W.; Song, C.; Xu, X.; Abe, M.; Zeng, X. Methoxyphosphinidene and Isomeric Methylphosphinidene Oxide. *J. Am. Chem. Soc.* **2018**, *140*, 13604−13608.
(30) Mardyukov, A.; Niedek, D.; Schreiner, P. R. Preparation and Characterization of Parent Phenylphosphinidene and Its Oxidation to Phenyldioxophosphorane: The Elusive Phosphorus Analogue of Nitrobenzene. *J. Am. Chem. Soc.* **2017**, *139*, 5019−5022.
(31) Mardyukov, A.; Niedek, D. Photochemical reactions of triplet phenylphosphinidene with carbon monoxide and nitric oxide. *Chem. Commun.* **2018**, *54*, 13694−13697.
(32) Bucher, G.; Borst, M. L. G.; Ehlers, A. W.; Lammertsma, K.; Ceola, S.; Huber, M.; Grote, D.; Sander, W. Infrared, UV/Vis, and W-band EPR spectroscopic characterization and photochemistry of triplet mesitylphosphinidene. *Angew. Chem., Int. Ed.* **2005**, *44*, 3289−3293.
(33) Akimov, A. V.; Ganushevich, Y. S.; Korchagin, D. V.; Miluykov, V. A.; Misochko, E. Y. The EPR Spectrum of Triplet Mesitylphosphinidene: Reassignment and New Assignment. *Angew. Chem., Int. Ed.* **2017**, *56*, 7944−7947.
(34) Lawzer, A.-L.; Custer, T.; Guillemin, J.-C.; Kolos, R. An Efficient Photochemical Route Towards Triplet Ethynylphosphinidene, HCCP. *Angew. Chem., Int. Ed.* **2021**, *60*, 6400−6402.
(35) Liu, L.; Ruiz, D. A.; Munz, D.; Bertrand, G. A Singlet Phosphinidene Stable at Room Temperature. *Chem* **2016**, *1*, 147−153.
(36) Transue, W. J.; Velian, A.; Nava, M.; García-Iriepa, C.; Temprado, M.; Cummins, C. C. Mechanism and Scope of Phosphinidene Transfer from Dibenzo-7-phosphanorbornadiene Compounds. *J. Am. Chem. Soc.* **2017**, *139*, 10822−10831.
(37) Mardyukov, A.; Keul, F.; Schreiner, P. R. Isolation and Characterization of the Free Phenylphosphinidene Chalcogenides $C_6H_5P{=}O$ and $C_6H_5P{=}S$, the Phosphorous Analogues of Nitrosobenzene and Thionitrosobenzene. *Angew. Chem., Int. Ed.* **2020**, *59*, 12445−12449.
(38) Zhao, X.; Chu, X.; Rauhut, G.; Chen, C.; Song, C.; Lu, B.; Zeng, X. Phosphorus Analogues of Methyl Nitrite and Nitromethane: CH_3OPO and CH_3PO_2. *Angew. Chem., Int. Ed.* **2019**, *58*, 12164−12169.
(39) Lee, T. J.; Taylor, P. R. A diagnostic for determining the quality of single-reference electron correlation methods. *Int. J. Quantum Chem.* **1989**, *36*, 199−207.
(40) Mieres-Pérez, J.; Mendez-Vega, E.; Velappan, K.; Sander, W. Reaction of Triplet Phenylnitrene with Molecular Oxygen. *J. Org. Chem.* **2015**, *80*, 11926−11931.

https://doi.org/10.1021/jacs.3c02935
J. Am. Chem. Soc. 2023, 145, 12755−12759

2.3 Preparation and Photochemistry of Parent Triplet Vinylarsinidene

Abstract: Vinyl pnictinidenes are an elusive family of molecules that have been suggested as key intermediates in multiple chemical reactions and commonly display a predisposition towards the open-shell electronic ground states (as evident from quantum chemical computations). However, owing to their expected extremely high reactivity, no vinyl pnictinidene has ever been isolated and characterized spectroscopically. Here we report the synthesis and spectroscopic characterization of vinylarsinidene, a higher congener of vinylnitrene. As we demonstrate, triplet vinylarsinidene can be prepared through low-temperature photolysis of diazidovinylarsine at 10 K in an argon matrix. The title compound can also be generated through high-vacuum flash pyrolysis of the diazide at 700 °C and trapped analogously. Triplet vinylarsinidene was characterized by IR and UV/Vis spectroscopy and displays remarkably rich unimolecular photochemistry. Upon selective photoirradiation, it rearranges to vinylidenearsine, 2*H*-arsirene, or an arsinidene (H–As) acetylene complex. The formation mechanisms of these products were rationalized with DFT and CASPT2 computations.

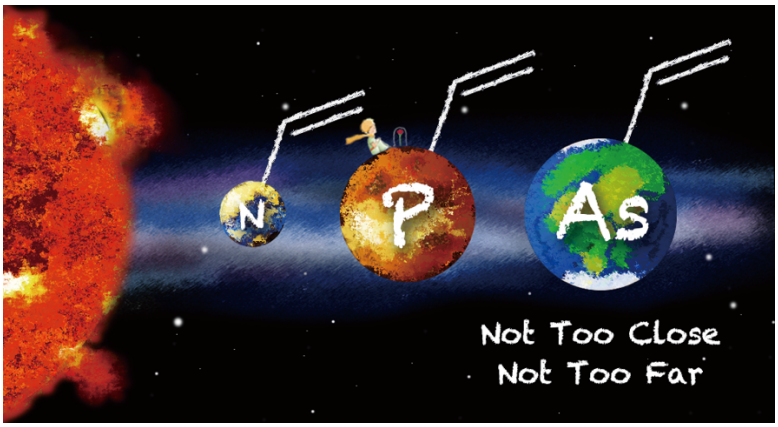

Original Source: Weiyu Qian, Peter R. Schreiner, Artur Mardyukov, *J. Am. Chem. Soc.* **2024**, *146*, 930. (DOI: 10.1021/jacs.3c11432).

Highlight: ChemistryViews, Chemistry Europe **2023**, https://www.chemistryviews.org/triplet-vinylarsinidene-synthesized/.

JACS
JOURNAL OF THE AMERICAN CHEMICAL SOCIETY
pubs.acs.org/JACS
Article

Preparation and Photochemistry of Parent Triplet Vinylarsinidene

Weiyu Qian, Peter R. Schreiner, and Artur Mardyukov*

Cite This: J. Am. Chem. Soc. 2024, 146, 930−935
Read Online
ACCESS | Metrics & More | Article Recommendations | Supporting Information

ABSTRACT: Vinyl pnictinidenes are an elusive family of molecules that have been suggested as key intermediates in multiple chemical reactions and commonly display a predisposition toward open-shell electronic ground states (as is evident from quantum chemical computations). However, owing to their expected extremely high reactivity, no vinyl pnictinidene has ever been isolated and characterized spectroscopically. Here, we report the synthesis and spectroscopic characterization of vinylarsinidene, a higher congener of vinylnitrene. As we demonstrate, triplet vinylarsinidene can be prepared through the low-temperature photolysis of diazidovinylarsine at 10 K in an argon matrix. The title compound can also be generated through high-vacuum flash pyrolysis of the diazide at 700 °C and trapped analogously. Triplet vinylarsinidene was characterized by IR and UV/vis spectroscopy and displayed remarkably rich unimolecular photochemistry. Upon selective photoirradiation, it rearranges to vinylidenearsine, 2*H*-arsirene, triplet ethynylarsinidene or an arsinidene (H−As) acetylene complex. The formation mechanisms of these products were rationalized with DFT and CASPT2 computations.

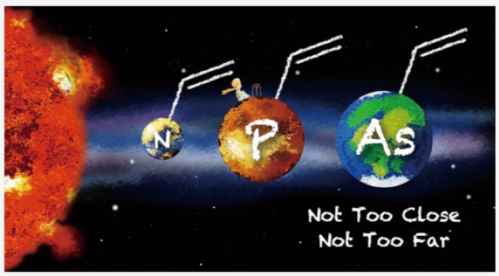

INTRODUCTION

The pursuit of sustainable chemistry has stimulated interest in light as an environmentally friendly catalyst for synthesis.[1] An example is the use of vinylazides as versatile reagents in the synthesis of heterocyclic compounds under the action of light.[2−5] However, the widespread use of photoreactive vinyl azides depends on a deeper understanding of complex reaction mechanisms. These mechanisms depend on various factors: the structure of the vinyl azides, the exposure wavelength, and whether light is absorbed directly or passes through sensitizers.[6−9] The potential energy surface surrounding parent vinylnitrene (**1**) reveals intriguing isomers that push the boundaries of our understanding of structure and bonding.[10−12] Nitrene **1** has thus far escaped direct spectroscopic identification because of its significant 1,3-diradical character, which renders it susceptible to structural rearrangement or fragmentation.[13−15] The attempted photochemical or thermal preparation of **1** from vinyl azide gives the singlet state that undergoes rapid isomerization (Scheme 1A), although the triplet is the electronic ground state (ΔE_{ST} = ∼14 kcal mol^{-1}).[14,16−19] As the rate for intersystem crossing is considered to be lower than the rate for intramolecular isomerization, it is highly unlikely to access the triplet state through conventional nitrene preparation methods.[20−22] However, the structural rigidity of vinylnitrenes attached to cyclic structural moieties (e.g., naphthalene-1,4-dione and 1*H*-inden-1-one) can make them accessible at cryogenic temperatures, favoring the formation of their triplet states.[23−25]

Vinylphosphinidene (**2**) and vinylarsinidene (**3**) are equally unreported higher congeners of **1** (Scheme 1B). It has been proposed that **2** is produced as a fleeting intermediate in the pyrolysis of vinylphosphirane, which is subsequently converted to phosphapropyne.[26−29] Phosphirane-[30−33] and diazide-based compounds[34−36] and phosphines[37] are viable photochemical/thermal sources for the synthesis of highly reactive (organic) phosphorus species. Recently, we exemplified that phenylarsenic diazide can be used to prepare triplet phenylarsinidene under matrix isolation conditions.[38] Analogously, here, we demonstrate that photolysis of diazidovinylarsine (**4**, Scheme 2) gives **3** through the elimination of three nitrogen molecules. In contrast to the recently reported phenylarsinidene,[38] **3** displays unexpectedly rich unimolecular photochemistry: irradiation of **3** with an appropriate wavelength provides access to the hitherto unreported vinylidenearsane (**5**), triplet ethynylarsinidene (HCCA) as well as 2*H*-arsirene (**6**), or a caged complex of arsinidene (H−As) and acetylene. We used matrix-isolated infrared (IR) and UV/vis spectroscopy, complemented by density functional theory (DFT) and complete active space (CAS) computational analyses, to elucidate the reaction mechanism of the formation of **3**

Received: October 15, 2023
Revised: December 12, 2023
Accepted: December 13, 2023
Published: December 25, 2023

https://doi.org/10.1021/jacs.3c11432
J. Am. Chem. Soc. 2024, 146, 930−935

Journal of the American Chemical Society pubs.acs.org/JACS Article

Scheme 1. (A) Reactivity of Vinylnitrene (1); (B) Vinyl Pnictinidenes: Vinylnitrene (^{3}1), Vinylphosphinidene (^{3}2), and Vinylarsinidene (^{3}3)

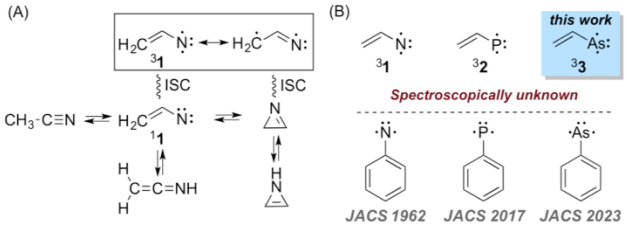

Scheme 2. Photochemical Generation of Triplet Vinylarsinidene (^{3}3) and Subsequent (Photo)reactivity[a]

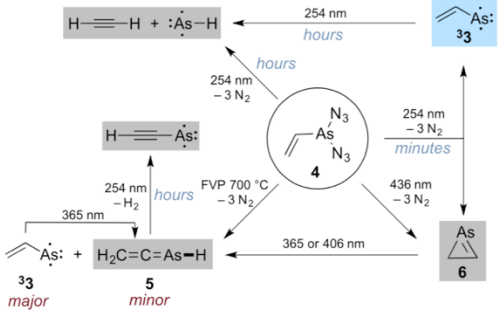

[a]Apart from the FVP reaction, all reactions were observed at 10 K in an Ar matrix.

together with its unexplored photochemistry and unique electronic structures.

■ RESULTS AND DISCUSSION

Novel diazide **4** was prepared from the corresponding dichloride precursor (for synthetic details, see Supporting Information) and evaporated from the storage flask at −20 °C, followed by trapping and isolation in an inert argon matrix at 10 K. When **4** was irradiated for 1−5 min with 254 nm light, aside from the few matrix sites of **4** (2099.5, 1210.1, and 974.6 cm^{-1}), a species having intense bands at 969.9 and 915.5 cm^{-1} accumulated as the main product (Figure 1). The IR peaks of the product were readily assigned to triplet vinylarsinidene **3** by comparison with an IR spectrum computed at B3LYP/def2-TZVP. For example, the two most intense IR bands at 969.9 and 915.5 cm^{-1} are assigned to the C−H out-of-plane and bending modes of **3**. The successful preparation of **3** is underscored by the strong correlation between experimentally observed and computed (B3LYP/def2-TZVP) IR frequencies (Figure 1 and Table S1). Arsinidene **3** can also be prepared by flash vacuum pyrolysis (FVP) of **4** at 700 °C, followed by trapping with an excess of argon at 10 K. The pyrolysis of **4** results in the formation of **3** as the major product, and a small amount of vinylidenearsine (**5**) was also present via the secondary rearrangement of **3** in the gas phase (Figure S1).

The UV/vis spectrum of **4** exhibits strong absorptions in the UV region, which includes strong transition bands at 205 and 243 nm (Figure 2). After 2 min of 254 nm irradiation, the bands of **4** completely vanish, while concomitantly strong

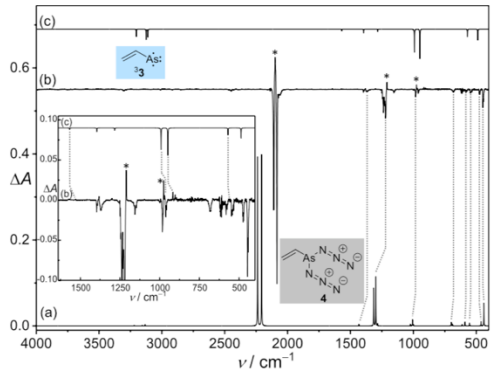

Figure 1. (a) Unscaled computed IR spectrum for **4** at B3LYP/def2-TZVP. (b) Difference IR spectrum showing the changes after 5 min of 254 nm irradiation. For comparison, see Figure S12. (c) Unscaled computed IR spectrum for ^{3}3 at B3LYP/def2-TZVP. Expanded spectra were in the range of 1750−400 cm^{-1}. Matrix sites for **4** are marked (*).

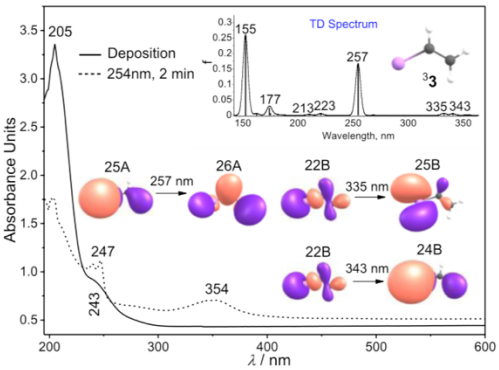

Figure 2. Solid line: UV/vis spectrum of **4** isolated in argon (10 K). Dashed line: UV/vis spectrum of ^{3}3 at 10 K: photochemistry of **4** after irradiation at λ = 254 nm in argon at 10 K. Inset: computed [TD-B3LYP/def2-TZVP] electronic transitions were performed for ^{3}3.

absorption bands at 204, 247, and 354 nm emerge. The new UV/vis spectrum resembles the computed TDDFT spectrum for **3** very well. TD-B3LYP/def2-TZVP computations exhibit two moderate transitions at 335 (f = 0.007; 22B → 25B, n →

https://doi.org/10.1021/jacs.3c11432
J. Am. Chem. Soc. 2024, 146, 930−935

π^*) and 343 nm (f = 0.005; 22B → 24B, $n \rightarrow \pi^*$) as well as a strong transition at 257 nm (f = 0.168; 25A → 26A, $\pi \rightarrow \pi^*$) (Figure 2).

Matrices containing **3** show intense absorption, with a maximum of 354 nm. Subsequent irradiation of the matrix with light λ = 365 nm for about 5 min resulted in a decrease of the intensities of the bands of **3** and the appearance of a characteristically intense peak at 1696.9 cm^{-1}, indicating the formation of a product having a cumulenic double bond, which was identified as vinylidenearsine (**5**) (Figure 3), the arsenic

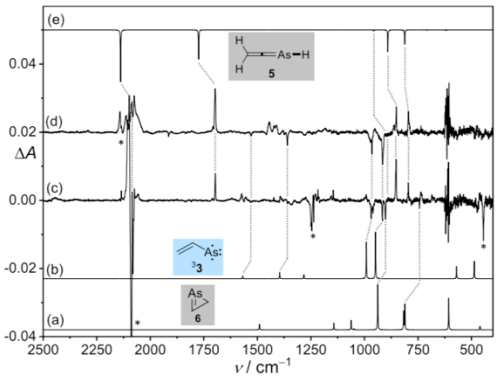

Figure 3. (a) Unscaled computed IR spectrum for 6 at B3LYP/def2-TZVP. (b) Unscaled computed IR spectrum for ^{3}3 at B3LYP/def2-TZVP. (c) Difference IR spectrum showing the changes after subsequent 5 min 365 nm irradiation. (d) Difference IR spectrum showing the changes after 5 min 365 nm irradiation of FVP (700 °C) products. (e) Unscaled computed IR spectrum for 5 at B3LYP/def2-TZVP. Peaks for 4 are marked (*).

analogue of allene. With the help of the computations, other strong and moderate-intensity IR bands at 2087.4, 904.5, 850.6, and 795.0 cm^{-1} were also assigned to **5**. For example, the IR bands at 2087.4 and 795.2 cm^{-1} can be attributed to the As−H stretching and deformation modes, respectively (Table S2). Upon photolysis using 365 nm light, the UV/vis absorptions of **3** vanish (Figure S2). It is also noteworthy that arsinidene ^{3}**3** is a photolabile species, whereas the previously described phenylarsinidene does not undergo photoisomerization upon photoexcitation.[38] Differences in the (photo)reactivity of phenylarsinidene and **3** could be ascertained by comparing the electronic structures of their lowest singlet states and the different thermochemistries of their isomerization products.

Irradiation of a matrix containing **4** for about 5 min at 436 nm yielded a different product exhibiting a weak but characteristic peak at 902.3 cm^{-1} (Figure S3). This and additional weak IR bands at 1038.5, 745.3, and 743.5 cm^{-1} correlate well with computed values of 1062.2, 816.8, and 810.6 cm^{-1} for 2*H*-arsirene (**6**) as a candidate with a C═As double bond (Table S3). Formation of **6** presumably occurs on the singlet potential energy surface from singlet vinylarsinidene (^{1}A′-^{1}**3**) by a barrierless process (vide infra). Upon 365 or 406 nm photoexcitation, **6** rearranges to form **5** (Figure 3).

The formation of compounds **5** and **6** was also monitored by UV/vis spectroscopy. The computed TD-DFT spectra for **5** and **6** are very similar in the 200−300 nm region. When **4** was exposed to light at 436 nm, a weak transition band appeared at 336 nm (as a shoulder close to the band of **3** at 354 nm). The weak transition band at 336 nm correlates well with the computed value of the electronic excitation of **6** at 298 nm (f = 0.044) (Figure S4). Irradiation at 365 nm results in the disappearance of the bands of **3** and **6**, and the formation of new bands at 193 and 320 nm: the band at 247 nm is superimposed with the band of **3** at 247 nm. The new bands are assigned to **5**, which match well with the computed TD-DFT transitions of **5**: 186 (f = 0.677), 245 (f = 0.161), and 289 nm (f = 0.003) (Figure S2).

Prolonged irradiation of a matrix containing **4** at λ = 254 nm produced a large amount of acetylene,[39,40] evident by the strong IR bands at 3285.8 and 737.7 cm^{-1} due to the C−H stretching and C−H deformation modes, which are shifted by −3.0 and +0.9 cm^{-1} from the uncomplexed HCCH (Figure S5). Obviously, the residual fragment must be H−As, which

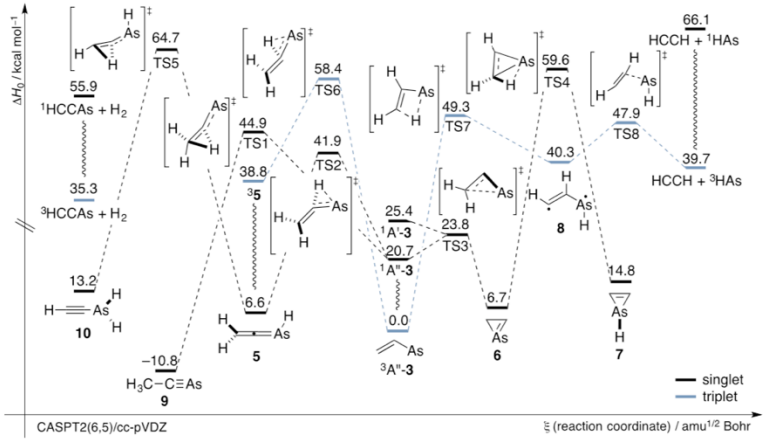

Figure 4. Potential energy profile (ΔH_0, kcal mol^{-1}) for the isomerization of ^{3}3 at CASPT2(6,5)/cc-pVDZ//CASSCF(6,5)/cc-pVDZ.

https://doi.org/10.1021/jacs.3c11432
J. Am. Chem. Soc. 2024, 146, 930−935

could be a complex involving acetylene and H−As. However, due to its low intensity and overlap with the strong IR band of **4**, it could not be detected.[41,42] The mechanism for the formation of acetylene and H−As from **3** requires a cascade of reaction steps (Figure 4), probably as a result of the two-step conversion via 1,3-diradical **8**. In the low-temperature experiments, no evidence of any intermediate was found for this reaction, even when the matrix was exposed to light for only seconds or minutes. When we exposed the matrix containing **5** to λ = 254 nm for 3 h, **5** vanished and new bands at 1892.7 and 1201.0 cm^{-1} appeared. By comparing these with those reported in the literature,[43] we assigned them to triplet ethynylarsinidene (HCCAs) (Figure S6). However, no other intermediates or isomers (e.g., ethylidynearsine **9** and ethynylarsine **10**) were detected.

To better estimate the energy gap between the singlet and triplet configurations of **3**, we performed CASSCF and CASPT2 computations using the cc-pVDZ basis set and an active space with 6-electron and 5-orbital. The geometries of the different spin states were optimized at the CASSCF(6,5)/cc-pVDZ level, and single-point energies were computed at the CASPT2(6,5)/cc-pVDZ level. For comparison, we performed similar computations on the singlet and triplet states of **1** and **2** (Table S4). According to CASPT2(6,5)/cc-pVDZ//CASSCF-(6,5)/cc-pVDZ computations, **3** displays a C_s point group with a $^3A''$ electronic ground state. Analogous to **1** and **2**, **3** has a large singlet−triplet energy separation ($^1A'-^3A''$) of ΔE_{ST} = 25.2 kcal mol^{-1} (for **1**, ΔE_{ST} = 42.4 kcal mol^{-1}; for **2**, ΔE_{ST} = 27.7 kcal mol^{-1}). The energy difference between $^1A''$-**3** and $^3A''$-**3** (21.2 kcal mol^{-1}) is larger than that for **1** (16.2 kcal mol^{-1}) and **2** (19.4 kcal mol^{-1}). The C−As bond length in **3** is 1.932 Å, which is identical to the C−As bond length in phenylarsinidene.[38] As expected, the computed C−P and C−N bond lengths in **1** and **2** are considerably shorter, 1.791 Å and 1.318 Å, respectively. Notably, there are remarkable differences between the C═C bond lengths of **1** (1.401 Å), **2** (1.355 Å), and **3** (1.350 Å), with **3** exhibiting the shortest double bond, which is in the typical range of carbon−carbon double bonds (Figure S7).[44] As a result, there is minimal sharing of spin density between the arsenic atom and the vinyl moiety, likely due to a mismatch of orbital sizes, specifically the poor overlap between the 2p orbitals of carbon and the 4p orbitals of arsenic. This is in accordance with the computed spin densities: the arsenic atom in **3** possesses the highest spin population (1.91), similar to that in phenylarsinidene (1.91), whereas nitrogen in **1** has a spin population of 1.37 and phosphorus in **2** has a spin population of 1.85 (Figure S7).

Next, we examined which formal resonance structure corresponds to **1**−**3**: 1,1-diradical (**1a**−**3a**) or 1,3-diradical (**1b**−**3b**) (Scheme 3A). Natural resonance theory (NRT) analysis at the B3LYP/def2-TZVP level reveals predominant (69%) 1,1-diradical resonance structure **3a** and 19% 1,3-diradical structure **3b**. A similar pattern is observed for **2**, where resonance structure **2a** exhibits a significant 1,1-diradical character (62%), while structure **2b** has a 1,3-diradical character of approximately 27%. For **1**, the computations predict the ratio of both structures to be approximately 1:1. The characteristic 1,3-diradical nature of triplet **1** allows for its flexibility, enabling facile double bond isomerization.[13,45] A Mayer bond index[46,47] of approximately 1.5 is computed for the CC bond in **1**, supporting facile resonance, whereas the CC bond indices in **2** and **3** are 1.87 and 1.91, respectively, underscoring the largely present double bond nature of the

Scheme 3. (A) NRT Analysis for 1, 2, and 3 at the B3LYP/def2-TZVP Level; (B) Isodesmic Equation

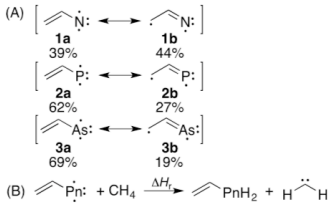

vinyl group (Figure S7). All of these data suggest that **3** must be thermodynamically the most stable species in this series, which is also validated by the sizable reaction enthalpy of the isodesmic equation (ΔH_r = 75.3 kcal mol^{-1} X = As, 63.9 kcal mol^{-1} X = P, and 39.1 kcal mol^{-1} X = N (Scheme 3B).

We analyzed possible mechanisms for the formation of compound **3** and its subsequent rearrangements. All computations were carried out with CASPT2(6,5)/cc-pVDZ//CASSCF(6,5)/cc-pVDZ (Figure 4) and B3LYP/def2-TZVP (Figure S8). Irradiation of **4** results in photo-denitrogenation to give singlet **3**, which then undergoes intersystem crossing to give triplet ^{3}**3**. According to CASPT2 computations, the two lowest open-shell ($^1A''$) and closed-shell singlets ($^1A'$) states lie 21.2 and 25.2 kcal mol^{-1} (electronic energy, denoted as ΔE) higher in energy than ^{3}**3** (Table S4). The reduced separation between the closed-shell singlet states ($^1A'$) and triplet states ($^3A''$) in **3** compared to **1** and **2** is a consequence of the decrease in the conjugation between the double bond and the arsenic atom in **3**.[45,48] The first reaction path implies intramolecular [1,2]H atom transfer from the CH group to the CH_2 group to give ethylidynearsine ($CH_3C{\equiv}As$; **9**) via **TS1** (Figure 4), the heavier analogue of acetonitrile. The barrier is 24.2 kcal mol^{-1} (including the zero-point vibrational energy (ZPVE) correction and enthalpy correction computed at the CASSCF(6,5)/cc-pVDZ, denoted as ΔH_0), which is 3.0 kcal mol^{-1} higher than that for the intramolecular [1,2]H atom transfer from the vinyl group to an arsenic atom (As) in $^1A''$-**3** to give **5** via **TS2** and thus is unfavorable. The [1,2]H atom transfer in $^3A''$-**3** is associated with a barrier of 58.4 kcal mol^{-1} (**TS6**), thus implying that arsine **5** most probably formed photochemically from singlet $^1A''$-**3**. Ethynylarsine **10** may be generated from [1,3]H atom transfer from the CH_2 group to the AsH group in **5** by overcoming a high barrier of 58.1 kcal mol^{-1} (**TS5**). The subsequent dehydrogenation to singlet ethynylarsinidene (HCCAs) is endothermic by 42.7 kcal mol^{-1}. The formation of arsirene (**6**) from $^1A''$-**3** is accompanied by a barrier of 3.1 kcal mol^{-1} (**TS3**). $^1A'$-**3** is 1.6 kcal mol^{-1} higher in energy than **TS3**. At the B3LYP/def2-TZVP level of theory, no transition structure was located for the process from $^1A'$-**3** to **6**, and the IRC of **TS2** shows a smooth conversion from **6** to **5** with ^{1}**3** as a stationary point (Figures S8 and S9). Subsequent intramolecular hydrogen atom transfer from the CH_2 group to the As atom in **6** yields 1*H*-arsirene (**7**) with an activation barrier (**TS4**) of 52.9 kcal mol^{-1}. The formation mechanism of acetylene and H−As from $^3A''$-**3** involves two successive reaction steps. The intramolecular [1,3]H shift from the terminal methylene group to the As atom in $^3A''$-**3** to give 1,3-diradical **8** proceeds with an activation barrier of 49.3 kcal mol^{-1} (**TS7**), followed by C−As bond fission to acetylene and triplet H−As with a barrier of 7.6

https://doi.org/10.1021/jacs.3c11432
J. Am. Chem. Soc. 2024, 146, 930−935

kcal mol^{-1} (**TS8**). The formation of acetylene and triplet H–As is endothermic by 39.7 kcal mol^{-1}.

CONCLUSIONS

The main question remains why arsinidene ^{3}**3** can be trapped while the closely related nitrene ^{3}**1** has evaded spectroscopic identification. This can be explained by the different thermodynamic stabilities between ^{3}**3** and ^{3}**1** (Scheme 3B). Furthermore, due to the higher 1,1-diradical character of **3**, the decay via ISC from the first singlet state to the triplet state is expected to be faster than the rearrangement into other isomers from the first singlet electronic state. Nitrene **1** exhibits a more 1,3-diradical character, as is evident by the longer C–C double bond length and NRT analysis (Scheme 3), which also makes double bond isomerization more feasible. Similarly, the spin density of **1** also indicates its propensity to undergo isomerization, leading to the formation of the corresponding azirene.

It is quite remarkable that ^{3}**3** is much closer in energy to **9** (Figure 4) in contrast to ^{3}**1** and ^{3}**2** (Figures S10 and S11), which are much higher-lying on their respective potential energy surfaces. For instance, ethenimine (**11**) and phosphaallene (**14**) are 32.5 and 3.5 kcal mol^{-1} more stable than ^{3}**1** and ^{3}**2**, respectively. The formation of 2*H*-azirine (**12**) and 2*H*-phosphirene (**15**) is also an exothermic process according to CASPT2(6,5)/cc-pVDZ//CASSCF(6,5)/cc-pVDZ computations. The cyclization of ^{1}A″-**1** is barrierless, while in the case of ^{1}A″-**2** it requires an activation energy of merely 2.0 kcal mol^{-1}. Furthermore, the barriers of the [1,2]H atom transfer from the CH to the CH_2 group in ^{1}A″-**2** (**TS14**) and ^{1}A″-**3** (**TS1**) are 3.6 and 3.0 kcal mol^{-1} higher than those of the [1,2] H atom transfer from the CH group to P (**TS15**) or As (**TS2**), respectively, while the trend is reversed in the case of ^{1}A″-**1** (−5.5 kcal mol^{-1}). Based on this analysis, we also can project that vinylphosphinidene ^{3}**2** is expected to behave similarly to ^{3}**3**. Therefore, it is plausible to hypothesize that ^{3}**2** could be experimentally observable under low-temperature conditions. Our discovery of the intriguing photochemistry of ^{3}**3** significantly extends our fundamental understanding of pnictinidenes and their reactivity and provides new entry points for explicating their roles in sustainable synthesis.

ASSOCIATED CONTENT

Supporting Information

The Supporting Information is available free of charge at https://pubs.acs.org/doi/10.1021/jacs.3c11432.

Experimental, spectroscopic, and computational data (PDF)

AUTHOR INFORMATION

Corresponding Author

Artur Mardyukov – *Institute of Organic Chemistry, Justus Liebig University, 35392 Giessen, Germany*; orcid.org/0000-0003-3908-6967; Email: artur.mardyukov@org.chemie.uni-giessen.de

Authors

Weiyu Qian – *Institute of Organic Chemistry, Justus Liebig University, 35392 Giessen, Germany*; orcid.org/0000-0003-3275-1063

Peter R. Schreiner – *Institute of Organic Chemistry, Justus Liebig University, 35392 Giessen, Germany*; orcid.org/0000-0002-3608-5515

Complete contact information is available at: https://pubs.acs.org/10.1021/jacs.3c11432

Notes

The authors declare no competing financial interest.

ACKNOWLEDGMENTS

Financial support by the Deutsche Forschungsgemeinschaft via the grant MA 8773/3-1 is gratefully acknowledged.

REFERENCES

(1) Schultz, D. M.; Yoon, T. P. Solar Synthesis: Prospects in Visible Light Photocatalysis. *Science* **2014**, *343* (6174), 1239176.

(2) Fu, J.; Zanoni, G.; Anderson, E. A.; Bi, X. α-Substituted vinyl azides: an emerging functionalized alkene. *Chem. Soc. Rev.* **2017**, *46* (23), 7208–7228.

(3) Kanchupalli, V.; Katukojvala, S. [1 + 1 + 3] Annulation of Diazoenals and Vinyl Azides: Direct Synthesis of Functionalized 1-Pyrrolines through Olefination. *Angew. Chem., Int. Ed.* **2018**, *57* (19), 5433–5437.

(4) Lei, W.-L.; Wang, T.; Feng, K.-W.; Wu, L.-Z.; Liu, Q. Visible-Light-Driven Synthesis of 4-Alkyl/Aryl-2-Aminothiazoles Promoted by In Situ Generated Copper Photocatalyst. *ACS Catal.* **2017**, *7* (11), 7941–7945.

(5) Liu, L.; Zhang, Q.; Wang, C. Redox-Neutral Generation of Iminyl Radicals by N-Heterocyclic Carbene Catalysis: Rapid Access to Phenanthridines from Vinyl Azides. *Org. Lett.* **2022**, *24* (32), 5913–5917.

(6) Yang, J.-C.; Zhang, J.-Y.; Zhang, J.-J.; Duan, X.-H.; Guo, L.-N. Metal-Free, Visible-Light-Promoted Decarboxylative Radical Cyclization of Vinyl Azides with N-Acyloxyphthalimides. *J. Org. Chem.* **2018**, *83* (3), 1598–1605.

(7) Osisioma, O.; Chakraborty, M.; Ault, B. S.; Gudmundsdottir, A. D. Wavelength-dependent photochemistry of 2-azidovinylbenzene and 2-phenyl-2H-azirine. *J. Mol. Struct.* **2018**, *1172*, 94–101.

(8) Rajam, S.; Jadhav, A. V.; Li, Q.; Sarkar, S. K.; Singh, P. N. D.; Rohr, A.; Pace, T. C. S.; Li, R.; Krause, J. A.; Bohne, C.; Ault, B. S.; Gudmundsdottir, A. D. Triplet Sensitized Photolysis of a Vinyl Azide: Direct Detection of a Triplet Vinyl Azide and Nitrene. *J. Org. Chem.* **2014**, *79* (19), 9325–9334.

(9) Rajam, S.; Murthy, R. S.; Jadhav, A. V.; Li, Q.; Keller, C.; Carra, C.; Pace, T. C. S.; Bohne, C.; Ault, B. S.; Gudmundsdottir, A. D. Photolysis of (3-Methyl-2H-azirin-2-yl)-phenylmethanone: Direct Detection of a Triplet Vinylnitrene Intermediate. *J. Org. Chem.* **2011**, *76* (24), 9934–9945.

(10) Bégué, D.; Dargelos, A.; Berstermann, H. M.; Netsch, K. P.; Bednarek, P.; Wentrup, C. Nitrile Imines and Nitrile Ylides: Rearrangements of Benzonitrile N-Methylimine and Benzonitrile Dimethylmethylide to Azabutadienes, Carbodiimides, and Ketenimines. Chemical Activation in Thermolysis of Azirenes, Tetrazoles, Oxazolones, Isoxazolones, and Oxadiazolones. *J. Org. Chem.* **2014**, *79* (3), 1247–1253.

(11) Isomura, K.; Ayabe, G.-I.; Hatano, S.; Taniguchi, H. Evidence for vinyl nitrene intermediates in the thermal rearrangement of 2H-azirines into indoles. *J. Chem. Soc., Chem. Commun.* **1980**, No. 24, 1252–1253.

(12) Smolinsky, G. Section Of Chemical Sciences: Nitrenes And Vinyl Azide Chemistry*. *Trans. N. Y. Acad. Sci.* **1968**, *30* (4 Series II), 511–516.

(13) Bornemann, C.; Klessinger, M. Conical intersections and photoreactions of 2H-azirines. *Chem. Phys.* **2000**, *259* (2–3), 263–271.

https://doi.org/10.1021/jacs.3c11432
J. Am. Chem. Soc. 2024, 146, 930–935

(14) Wentrup, C.; Nunes, C. M.; Reva, I. Comment on "Computational Study on the Vinyl Azide Decomposition. *J. Phys. Chem. A* **2014**, *118* (27), 5122−5123.
(15) Bock, H.; Dammel, R.; Aygen, S. Gas-phase reactions. 36. Pyrolysis of vinyl azide. *J. Am. Chem. Soc.* **1983**, *105* (26), 7681−7685.
(16) L'Abbe, G.; Mathys, G. Mechanism of the thermal decomposition of vinyl azides. *J. Org. Chem.* **1974**, *39* (12), 1778−1780.
(17) Timén, Å. S.; Risberg, E.; Somfai, P. Improved procedure for cyclization of vinyl azides into 3-substituted-2H-azirines. *Tetrahedron Lett.* **2003**, *44* (28), 5339−5341.
(18) Duarte, D. J. R.; Miranda, M. S.; Esteves da Silva, J. C. G. Computational Study on the Vinyl Azide Decomposition. *J. Phys. Chem. A* **2014**, *118* (27), 5038−5045.
(19) Maier, G.; Schmidt, C.; Reisenauer, H. P.; Endlein, E.; Becker, D.; Eckwert, J.; Andes, B. H., Jr; Schaad, L. J. Blausäure-N-methylid: Darstellung, spektroskopische Eigenschaften und seine Beziehung zu anderen C_2H_3N-Isomeren. *Chem. Ber.* **1993**, *126* (10), 2337−2352.
(20) Mieres-Perez, J.; Costa, P.; Mendez-Vega, E.; Crespo-Otero, R.; Sander, W. Switching the Spin State of Pentafluorophenylnitrene: Isolation of a Singlet Arylnitrene Complex. *J. Am. Chem. Soc.* **2018**, *140* (49), 17271−17277.
(21) Mieres-Perez, J.; Mendez-Vega, E.; Velappan, K.; Sander, W. Reaction of Triplet Phenylnitrene with Molecular Oxygen. *J. Org. Chem.* **2015**, *80* (24), 11926−11931.
(22) Smolinsky, G.; Wasserman, E.; Yager, W. A. The E.P.R. of Ground State Triplet Nitrenes. *J. Am. Chem. Soc.* **1962**, *84* (16), 3220−3221.
(23) Sarkar, S. K.; Sawai, A.; Kanahara, K.; Wentrup, C.; Abe, M.; Gudmundsdottir, A. D. Direct Detection of a Triplet Vinylnitrene, 1,4-Naphthoquinone-2-ylnitrene, in Solution and Cryogenic Matrices. *J. Am. Chem. Soc.* **2015**, *137* (12), 4207−4214.
(24) Sarkar, S. K.; Osisioma, O.; Karney, W. L.; Abe, M.; Gudmundsdottir, A. D. Using Molecular Architecture to Control the Reactivity of a Triplet Vinylnitrene. *J. Am. Chem. Soc.* **2016**, *138* (45), 14905−14914.
(25) Shields, D. J.; Sarkar, S. K.; Sriyarathne, H. D. M.; Brown, J. R.; Wentrup, C.; Abe, M.; Gudmundsdottir, A. D. Transforming Triplet Vinylnitrene into Triplet Alkylnitrene at Cryogenic Temperatures. *Org. Lett.* **2019**, *21* (18), 7194−7198.
(26) Haber, S.; Le Floch, P.; Mathey, F. Synthesis of phosphapropyne by flash thermolysis of 1-vinylphosphirane or divinylphosphine. *J. Chem. Soc., Chem. Commun.* **1992**, No. 24, 1799−1800.
(27) Berger, D. J.; Gaspar, P. P.; Grev, R. S.; Mathey, F. Molecular orbital study of the vinylphosphinidene to phosphapropyne rearrangement. *Organometallics* **1994**, *13* (2), 640−646.
(28) Berger, D. J.; Gaspar, P. P.; LeFloch, P.; Mathey, F.; Grev, R. S. Computational View of the Mechanism of Vinylphosphirane Pyrolysis and A New Route to Phosphaalkynes. *Organometallics* **1996**, *15* (23), 4904−4915.
(29) Liu, L. L.; Zhou, J.; Cao, L. L.; Andrews, R.; Falconer, R. L.; Russell, C. A.; Stephan, D. W. A Transient Vinylphosphinidene via a Phosphirene-Phosphinidene Rearrangement. *J. Am. Chem. Soc.* **2018**, *140* (1), 147−150.
(30) Mardyukov, A.; Niedek, D.; Schreiner, P. R. Preparation and Characterization of Parent Phenylphosphinidene and Its Oxidation to Phenyldioxophosphorane: The Elusive Phosphorus Analogue of Nitrobenzene. *J. Am. Chem. Soc.* **2017**, *139* (14), 5019−5022.
(31) Akimov, A. V.; Ganushevich, Y. S.; Korchagin, D. V.; Miluykov, V. A.; Misochko, E. Y. The EPR Spectrum of Triplet Mesitylphosphinidene: Reassignment and New Assignment. *Angew. Chem., Int. Ed.* **2017**, *56* (27), 7944−7947.
(32) Misochko, E. Y.; Akimov, A. V.; Korchagin, D. V.; Ganushevich, Y. S.; Melnikov, E. A.; Miluykov, V. A. Generation and direct EPR spectroscopic observation of triplet arylphosphinidenes: stabilisation versus internal rearrangements. *Phys. Chem. Chem. Phys.* **2020**, *22* (47), 27626−27631.
(33) Bucher, G.; Borst, M. L. G.; Ehlers, A. W.; Lammertsma, K.; Ceola, S.; Huber, M.; Grote, D.; Sander, W. Infrared, UV/Vis, and W-band EPR spectroscopic characterization and photochemistry of triplet mesitylphosphinidene. *Angew. Chem., Int. Ed.* **2005**, *44* (21), 3289−3293.
(34) Mardyukov, A.; Keul, F.; Schreiner, P. R. Isolation and Characterization of the Free Phenylphosphinidene Chalcogenides C_6H_5P = O and C_6H_5P = S, the Phosphorous Analogues of Nitrosobenzene and Thionitrosobenzene. *Angew. Chem., Int. Ed.* **2020**, *59* (30), 12445−12449.
(35) Qian, W.; Wende, R. C.; Schreiner, P. R.; Mardyukov, A. Selective Preparation of Phosphorus Mononitride (P≃N) from Phosphinoazide and Reversible Oxidation to Phosphinonitrene. *Angew. Chem., Int. Ed.* **2023**, *62* (23), No. e202300761.
(36) Chu, X.; Yang, Y.; Lu, B.; Wu, Z.; Qian, W.; Song, C.; Xu, X.; Abe, M.; Zeng, X. Methoxyphosphinidene and Isomeric Methylphosphinidene Oxide. *J. Am. Chem. Soc.* **2018**, *140* (42), 13604−13608.
(37) Lawzer, A.-L.; Custer, T.; Guillemin, J.-C.; Kołos, R. An Efficient Photochemical Route Towards Triplet Ethynylphosphinidene, HCCP. *Angew. Chem., Int. Ed.* **2021**, *60* (12), 6400−6402.
(38) Qian, W.; Schreiner, P. R.; Mardyukov, A. Triplet Phenylarsinidene and Its Oxidation to Dioxophenylarsine. *J. Am. Chem. Soc.* **2023**, *145* (23), 12755−12759.
(39) Mardyukov, A.; Sanchez-Garcia, E.; Sander, W. Matrix Isolation and Ab Initio Study of the Noncovalent Complexes between Formamide and Acetylene. *J. Phys. Chem. A* **2009**, *113* (6), 1086−1095.
(40) Sanchez-Garcia, E.; Mardyukov, A.; Tekin, A.; Crespo-Otero, R.; Montero, L. A.; Sander, W.; Jansen, G. Ab initio and matrix isolation study of the acetylene-furan dimer. *Chem. Phys.* **2008**, *343* (2−3), 168−185.
(41) Arens, M.; Richter, W. Spectroscopic observation of the b $1\Sigma^+ \rightarrow \tilde{X}\ 3\Sigma^-$ transition of $AsH\ ^1\Sigma^+ \rightarrow \tilde{X}\ ^3\Sigma^-$ transition of AsH. *J. Chem. Phys.* **1990**, *93* (10), 7094−7096.
(42) Hensel, K. D.; Hughes, R. A.; Brown, J. M. IR spectrum of the AsH radical in its $X^3\Sigma^-$state, recorded by laser magnetic resonance$^3\Sigma^-$ state, recorded by laser magnetic resonance. *J. Chem. Soc., Faraday Trans.* **1995**, *91* (18), 2999−3004.
(43) Lawzer, A.-L.; Ganesan, E.; Gronowski, M.; Custer, T.; Guillemin, J.-C.; Kołos, R. Free Ethynylarsinidene and Ethynylstibinidene: Heavier Analogues of Nitrenes and Phosphinidenes. *Chem.—Eur. J.* **2023**, *29* (46), No. e202300887.
(44) Sanderson, R. Carbon—carbon bond lengths. *Science* **1952**, *116* (3002), 41−42.
(45) Parasuk, V.; Cramer, C. J. Multireference configuration interaction and second-order perturbation theory calculations for the 1 3A″, 1 1A″, and 1 1A′ electronic states of vinylnitrene and vinylphosphinidene^{3}A″, 1 ^{1}A″, and 1 ^{1}A′ electronic states of vinylnitrene and vinylphosphinidene. *Chem. Phys. Lett.* **1996**, *260* (1−2), 7−14.
(46) Mayer, I. Charge, bond order and valence in the AB initio SCF theory. *Chem. Phys. Lett.* **1983**, *97* (3), 270−274.
(47) Lu, T.; Chen, F. Multiwfn: A multifunctional wavefunction analyzer. *J. Comput. Chem.* **2012**, *33* (5), 580−592.
(48) Galbraith, J. M.; Gaspar, P. P.; Borden, W. T. What Accounts for the Difference between Singlet Phenylphosphinidene and Singlet Phenylnitrene in Reactivity toward Ring Expansion? *J. Am. Chem. Soc.* **2002**, *124* (39), 11669−11674.

https://doi.org/10.1021/jacs.3c11432
J. Am. Chem. Soc. 2024, 146, 930−935

2.4 N_6: A Synthetic Leap Towards Neutral Nitrogen Allotropes

Abstract: Compounds consisting only of the element nitrogen (polynitrogens or nitrogen allotropes), are deemed the cleanest and ideal energy storage materials due to their immense energy content and because they release only harmless nitrogen (N_2) upon decomposition. However, their extreme instability poses a significant synthetic challenge and no neutral molecular nitrogen allotrope beyond N_2 has been isolated. Here, we present the room temperature preparation of C_{2h}-N_6 through the gas-phase reaction of chlorine or bromine with silver azide, followed by trapping in argon matrices at 10 K. We also prepared neat C_{2h}-N_6 as a film at liquid nitrogen temperature (77 K), indicating its unexpectedly high stability and the scalability of the synthesis. Infrared and ultraviolet spectroscopy, ^{15}N-isotope labelling experiments, and *ab initio* computations firmly support our findings. The preparation of a metastable nitrogen allotrope beyond N_2 opens new vistas for the development of highly sought-after high-energy materials.

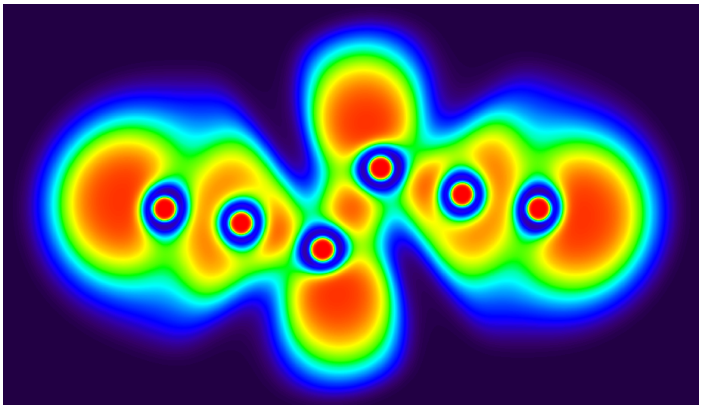

Original Source: Weiyu Qian, Artur Mardyukov, Peter R. Schreiner, *Nature* **2025**, *642*, 356. (DOI: 10.1038/s41586-025-09032-9).

Hexanitrogen (N_6): A Synthetic Leap Towards Molecular Neutral Nitrogen Allotropes

Weiyu Qian (钱伟煜)[1], Artur Mardyukov[1]* & Peter R. Schreiner[1]*
[1]Institute of Organic Chemistry, Justus Liebig University, Heinrich-Buff-Ring 17, 35392 Giessen, Germany
* Correspondence to: artur.mardyukov@org.chemie.uni-giessen.de and prs@uni-giessen.de.

Summary
As the availability of renewable energy varies drastically over space and time, energy storage is a prime challenge. Current strategies include battery systems or high-energy molecules including hydrogen or ammonia for chemical energy storage. Compounds consisting only of the element nitrogen (polynitrogens or nitrogen allotropes), are deemed promising clean energy storage materials due to their immense energy content (about five times higher than hydrogen) and because they release only harmless nitrogen upon decomposition[1]. However, their extreme instability poses a significant synthetic challenge and no neutral molecular nitrogen allotrope beyond N_2 has been isolated[2,3]. Here, we present the room temperature preparation of molecular N_6 (hexanitrogen) through the gas-phase reaction of chlorine or bromine with silver azide, followed by trapping in argon matrices at 10 K. We also prepared neat N_6 as a film at liquid nitrogen temperature (77 K), indicating its stability. Infrared and UV/Vis spectroscopy, ^{15}N-isotope labelling, and *ab initio* computations firmly support our findings. The preparation of a metastable molecular nitrogen allotrope beyond N_2 opens new vistas for the development of new high-energy density materials.

Introduction
Molecular nitrogen allotropes beyond N_2 are promising for the development of high-energy-density materials[4] because they release enormous energy upon dissociation into gaseous N_2. As the major component of air, N_2 is inert, non-toxic, and not a greenhouse contributor[5-7]. Unlike carbon, N_2 is the only nitrogen allotrope found in nature, and strategies for synthesizing higher neutral molecular nitrogen allotropes are highly sought after[8-14]. However, they are deemed extremely unstable, especially when uncharged and with an even electron count[15]. Consequently, only two examples have been reported. The azide radical (•N_3) (Fig. 1a), was identified in the gas phase through rotational spectroscopy in 1956[16,17]. In 2002, N_4 was detected by gas-phase neutralization-reionization mass spectrometry (NRMS); its structure has not been revealed[18]. The intermediacy of an N_6 species was tentatively suggested in 1970 in the decay of azide radicals in aqueous solution but no definitive spectroscopic evidence was provided[19].

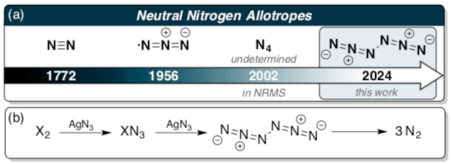

Fig. 1| All known neutral molecular nitrogen allotropes and preparation of N_6. a) Discovery timeline (year given), composition, and structure (the structure of N_4 has not been determined); b) Reaction sequence utilized in the present study.

There are many computations proposing molecular allotropes spanning from N_4 to N_{120}, including chains, rings, and cages[7,20], most of which have low dissociation barriers into N_2. For example, hexazine (*cyc*-N_6, the nitrogen analogue of benzene) exhibits a computed barrier of only 4.2 kcal mol^{-1} for decomposition into three N_2[21]. Quantum mechanical tunnelling (QMT) effects could further reduce the lifetime of higher nitrogen allotropes, adding to their difficulty of preparation.
While the pursuit of higher neutral molecular nitrogen allotropes is extremely challenging, several homonuclear polynitrogen ions have been isolated. The synthesis and characterization of $[N_5]^+[PnF_6]^-$ (Pn = As, Sb) salts with a bent pentanitrogen cation represents a milestone[22,23]. Christe *et al.* initially identified the *cyclo*-N_5^- anion using mass spectrometry in 2002 and 2003[24,25]; Zhang *et al.* reported in 2017 the synthesis of a salt featuring the *cyclo*-N_5^- anion[26]. The synthesis of various metal pentazolates was achieved through the reaction of $[Na(H_2O)(N_5)]•2H_2O$ with metal salts[27,28].
In the realm of solid-state (non-molecular) structures, a breakthrough was the high-temperature (2,000 K), high-pressure (110 GPa) diamond-like solid-state cubic gauche nitrogen phase in which all atoms are connected by single bonds[29,30]. An aromatic cyclic hexazine N_6^{4-} was identified through solid-state X-ray diffraction of K_9N_{56}[31] under pressures above 40 GPa and temperatures above 2,000 K[31]. Greschner *et al.* predicted a novel nitrogen molecular crystal comprising N_6 units with an open-chain structure stabilized by electrostatic interactions[32], in line with assessments for the molecular species[9].
In our analysis of the proposed molecular nitrogen allotropes, acyclic neutral N_6 (hexaaza-1,2,4,5-tetraene, hexanitrogen, diazide) stands out because N_2 moieties are not discernible (Fig. 1). The central N–N-bond would lead to unproductive *endothermic* dissociation (ΔG_{298K} theor. +26.1 kcal mol^{-1}, *vide infra*) into two •N_3. Additionally, the computed dissociation barrier into three N_2 molecules of $\Delta G^{\ddagger}_{298K}$ = 14.8 kcal mol^{-1} makes N_6 a promising candidate for synthesis. Here we show that N_6 indeed can be made from through the reaction of Cl_2 or Br_2 with AgN_3 under reduced pressure, followed by cryogenic trapping[33]. The characterization was accomplished by infrared (including ^{15}N-isotope labelling) as well as UV/Vis spectroscopy and *ab initio* computations. We also demonstrate the preparation and stability of C_{2h}-symmetric N_6 (hereinafter referred to as N_6) in neat form as a film at the temperature of liquid nitrogen (77 K).

Results
Synthesis of N_6

As AgN_3 is an excellent reagent for the synthesis of polyazides[34] and halogen azides both in the gas-phase[35] and in solution[36,37], we hypothesized that the reaction of AgN_3 with XN_3 (X = halogen) is a viable route to N_6 (Fig. 1b). The reactions were conducted either in a quartz tube or in a U-trap by flowing gaseous Cl_2 through solid AgN_3 under reduced pressure at room temperature (see Synthesis Details and Fig. S1). Apart from the known bands of ClN_3[38] and HN_3[39], a distinct group of bands at 2076.6, 2049.0, 1177.6, and 642.1 cm^{-1} was recorded (Fig. S2). After irradiating the matrices with 436 nm light (Fig. 2a (middle trace) and S3), all bands vanish. However, the rates of decomposition of the newly observed IR bands differ from those attributed to ClN_3 (Fig. S4 and S5). There were no discernible products other than chloronitrene (ClN) detected in the difference spectrum after irradiation. Furthermore, identical bands were detected when Br_2 was used instead of Cl_2, indicating that the unidentified species does not contain halogens (Fig. 2a (upper trace) and S6). In addition, BrN_3 does not decompose upon 436 nm irradiation, thus providing clean decomposition spectra of the yet unidentified species.

The intensive vibrational band at 2076.6 cm^{-1} compares favourably with the asymmetric stretching band of the azide moiety in isoelectronic N_3–NCO (2099.1 cm^{-1}, Ar-matrix)[40]. Compared with the computed harmonic vibrations at CCSD(T)/cc-pVTZ, the four bands noted above could be attributed to N_6, except the band at 2049.0 cm^{-1} of moderate intensity, though it disappeared together with the other bands upon photolysis (Fig. S4 and S7). To determine the origin of the band at 2049.0 cm^{-1}, anharmonic vibrational frequencies were computed at B3LYP/def2-TZVP (Table S1). This analysis indicates that this band derives from a combination of fundamentals ν_8 (a_g symmetric N^3N^4 stretching mode) and ν_9 (b_u asymmetric $N^3N^2N^1$ stretching mode). The substantial anharmonic contribution of intensity (219 km mol^{-1}, Table S2) of the fundamental ν_{11} at 2143.5 cm^{-1} and the $\nu_8 + \nu_9$ combination is notably stronger than its fundamentals suggest that the combination $\nu_8 + \nu_9$ gains energy through Fermi resonance from the adjacent strong fundamental ν_{11}[40].

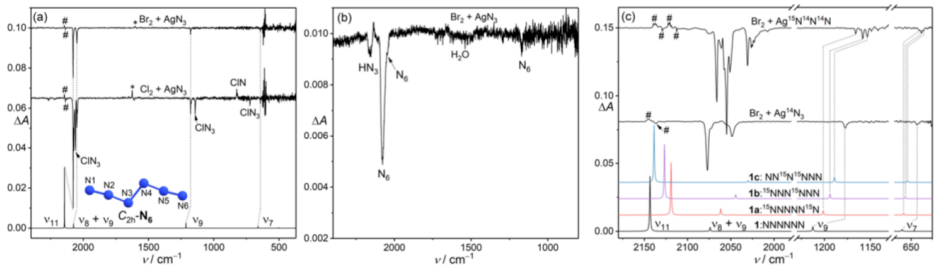

Fig. 2. **Infrared spectra of N_6 isotopomers and side products.** (a) Lower trace: computed anharmonic infrared spectrum of N_6 at B3LYP/def2-TZVP, including the $\nu_8 + \nu_9$ combination. Middle trace: difference spectrum showing the changes after 8 min of 436 nm irradiation of the products of the reaction of Cl_2 with AgN_3. Upper trace: difference spectrum showing the changes after 6 min of 436 nm irradiation of the reaction products of Br_2 with AgN_3. (b) Difference spectrum of a neat N_6 film at 77 K showing the changes after 8 min 436 nm irradiation. (c) Bottom to top traces: computed anharmonic infrared spectrum of N_6, $^{15}NNNNN^{15}N$ (**1a**), $^{15}NNN^{15}NNN$ (**1b**), and $NN^{15}N^{15}NNN$ (**1c**) at B3LYP/def2-TZVP, including the $\nu_8 + \nu_9$ combination; difference spectrum showing the changes after 8 min of 436 nm irradiation of the reaction products of Br_2 with AgN_3; difference spectrum showing changes after 8 min of 436 nm irradiation of the reaction products of Br_2 with $Ag^{15}N^{14}N^{14}N$. Matrix sites from natural abundance and isotope-labelled HN_3 (#) and H_2O (*) are marked.

To confirm our assignments, isotope-labelling experiments were conducted using $Ag^{15}N^{14}N^{14}N$. Three groups of distinct peaks can be discerned in the infrared spectra (Fig. 2c and S8), indicating the presence of two N_3 moieties in the molecule, which can be attributed to three types of isotopomers (**1a**: $^{15}NNNNN^{15}N$, **1b**: $^{15}NNN^{15}NNN$, **1c**: $NN^{15}N^{15}NNN$), respectively. In particular, the unsymmetric isotopic substitutions in **1b** lower its point group from C_{2h} to C_s. Computations delineate that the terminal (N^1 or N^6) and internal (N^3 or N^4) ^{15}N-substitutions primarily influence the terminal (ν_{11}) and internal asymmetric stretching vibration (ν_9) of the N_3 moieties, respectively. This leads to a red-shift of the $\nu_8 + \nu_9$ combination and a blue-shift of the ν_{11} fundamental in going from **1a** to **1c**, resulting in their gradual separation. The intensity ratio of the $\nu_8 + \nu_9$ combination and the ν_{11} fundamental in **1a** is nearly 1:1, which is significantly higher than that in **1c** (ca. 1:17). These findings align well with the DFT computed anharmonic infrared intensities (Table S3), which are attributed to the closer proximity of the $\nu_8 + \nu_9$ combination to the strong ν_{11} fundamental in **1a**, resulting in an increase of the Fermi resonance and *vice versa* in **1c**. Statistically, the anticipated ratio of the three isotopomers should be **1a**:**1b**:**1c** = 1:2:1, which is reflected in the observed fundamental ν_7 in the experimental spectrum (Fig. 3). Furthermore, the computed intensity of ν_9 in **1c** (107 km mol^{-1}, Table S3) is higher than that in **1a** (92 km mol^{-1}) and **1b** (98 km mol^{-1}), which matches the intensity ratios of ν_9 observed in **1a** and **1b** (approx. 1:2). The experimentally observed intensities agree with these findings and display a slightly higher intensity of ν_9 in **1c** than in **1a**.

To explore the intrinsic stability of N_6, we also prepared *neat* N_6 at room temperature and condensed it at liquid nitrogen temperature (77 K) as a film on the surface of the matrix window without using argon as a host gas. Irradiation of such N_6 films resulted in very similar spectral changes as those observed in argon matrices at 10 K (Fig. 2b and Fig. S9). That is, neat N_6 is sufficiently stable at the temperature of liquid nitrogen to allow its direct identification.

Additional evidence is provided by the UV/Vis spectrum of N_6. After 6 min of 436 nm irradiation of the reaction products of Br_2 with AgN_3, we observed the disappearance of the transitions at 190 and 249 nm and, consistent with the IR experiments, no new transitions appeared (Fig. 3). All transitions correlate well with the values for the electronic excitations of N_6 at 186 (f = 0.8512)

and 248 nm (f = 0.0078) computed at TD-B3LYP/def2-TZVP. Additionally, the computations reveal a weak electronic excitation at 422 nm (f = 0.0004), corresponding to a $\pi \rightarrow \pi^*$ transition, which aligns well with the observed photochemistry.

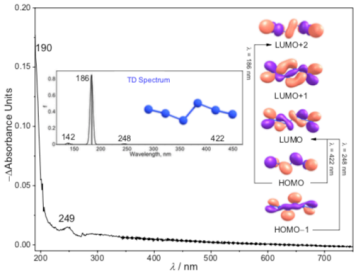

Fig. 3. Measured and computed UV/Vis spectrum of N_6 and molecular orbitals involved in the electronic transitions. Experimental difference UV/Vis spectrum reflecting changes upon 4 min 436 nm irradiation of the reaction products of Br_2 with AgN_3 in argon at 10 K. Inset: Computed [TD-B3LYP/def2-TZVP] electronic transitions for N_6 and molecular orbitals involved.

Computations

To better understand the structure and the potential energy landscape of N_6, we computed its energy profile at CCSD(T)/cc-pVTZ (Fig. 4a (ΔG_{298K}) and Fig. S10 (ΔH_0), see Computational Details in the SI). Only the C_{2h}-N_6 *trans*-conformer is a local minimum; the C_{2v}-N_6 *cis*-conformer is a higher-order stationary point and chemically not relevant[41,42]. The formal double bond lengths in the N_3 moieties are much longer than the triple bond in N_2 (theor. 1.104 Å; expt. 1.098 Å)[43], indicating double bond character. Indeed, the computed $N^2{=}N^3/N^4{=}N^5$ bond length (1.251 Å) is close to that of *trans*-diazene (HN=NH, theor. 1.253 Å; expt. 1.252 Å)[44]. The structure of N_6 is quite different from the azide radical (•N=N=N, theor. 1.183 Å; expt. 1.181 Å)[45], but comparable with the N_3 moiety in hydrazoic acid (HN_3, theor. 1.247 and 1.136 Å; expt. 1.237 and 1.133 Å for the $N^1{=}N^2$ and $N^2{=}N^3$ bonds, respectively). The N^3–N^4 bond in N_6 (1.460 Å) compares favourably with that in hydrazine (H_2N–NH_2, theor. 1.445 Å; expt.1.446 Å). This geometric analysis is well captured by the Lewis-structure of N_6 (Fig. 1). These conclusions are supported by natural bond orbital computations, which indicate that the terminal nitrogen atoms are electronically neutral, while small positive and negative charges are located at N^2 and N^5 (+0.2e) as well as on N^3 and N^4 (–0.2e), respectively (Fig. 4a). Equally, N^1–N^2/N^5-N^6 possess the highest bond order (2.1), followed by N^2–N^3/N^4–N^5 (1.4) and N^3–N^4 (1.1).

We visualized the Laplacian of the electron density to gauge where the bonds in N_6 are likely to break (Fig. 4b) and why the computed barrier for decomposition into three moles of N_2 is, compared to other systems, rather high ($\Delta G_{298K}^{\ddagger}$ = 14.8 kcal mol^{-1}). This barrier implies appreciable kinetic stability that is mirrored by our observations. For comparison, the computed barrier of hypothetical D_{2h}-N_4 dissociating into two N_2 is 6.5 kcal mol^{-1} at MR-AQCC/VTZ[46]. With the electron density analysis, the "Achilles' heel" was discerned at the N^2–N^3/N^4–N^5 bonds as evident from the vertex of positive Laplacian of the in-plane electron density. This is confirmed by the electron localization function (ELF) analysis (Fig. 4c)[47]. Both the Laplacian of the electron density and the ELF analysis indicate the electron density minimum around the N^2–N^3/N^4–N^5 bonds. Hence, even though the Lewis structure would indicate N_6 breaking into two •N_3 radicals, i.e., breaking of the central N^3–N^4 single bond, the computed barrier for this process amounts to sizeable ΔG_{298K} = 26.1 kcal mol^{-1} and is unproductive.

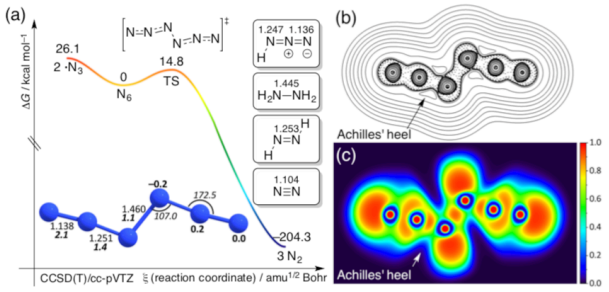

Fig. 4. Computational analyses for N_6. (a) Potential energy profile (ΔG_{298K}, kcal mol^{-1}) for N_6 at CCSD(T)/cc-pVTZ. The optimized parameters of N_6 are given in Ångstrom (regular), degrees (italic), natural charges in bold, and natural bond orders in bold italics. Insets: computed NN bond lengths for N_2, *trans*-HNNH, hydrazine, and HN_3 at CCSD(T)/cc-pVTZ. (b) Contour line map of the Laplacian of the electron density of N_6; solid and dashed lines represent positive and negative regions, respectively. (c) ELF map.

On the other hand, $\Delta G^{\ddagger}_{298K}$ for the elementary decomposition into three N_2 is 14.8 kcal mol^{-1}, implying a finite lifetime of N_6 at room temperature. CVT/SCT computations at B3LYP/def2-TZVP reveal that N_6, unlike hexazine (*cyc*-N_6)[21], is unlikely to decompose through QMT[21,48,49], with an estimated half-life of N_6 of over 132 years at 77 K (Table S4). At 298 K, the computed

half-life still amounts to 35.7 ms. This supports our finding that N_6 exists long enough in the gas phase at ambient temperature to be trapped subsequently in cryogenic matrices.
According to CCSD(T)/cc-pVTZ (ΔH_0) computations, the decomposition of N_6 into three N_2 is exothermic by 185.2 kcal mol^{-1}, which is 2.2 and 1.9 times higher than TNT (2,4,6-trinitrotoluene) and HMX (1,3,5,7-tetranitro-1,3,5,7-tetrazocane, octogen) by weight (details in the SI)[50].
We report here the facile synthesis and spectroscopic identification of experimentally unreported hexanitrogen N_6. This represents the first experimentally realized neutral molecular nitrogen allotrope beyond N_2 that exhibits unexpected stability at least up to the temperature of liquid nitrogen. This discovery challenges the long-held belief of the elusiveness of neutral molecular nitrogen allotropes.

Methods

Matrix Apparatus Design. For the matrix isolation studies, we used an APD Cryogenics HC-2 cryostat with a closed-cycle refrigerator system, equipped with an inner CsI window for IR measurements. Spectra were recorded at the temperature of the matrix (10 K) with a Bruker Vertex 70 FT-IR spectrometer with a spectral range of 4000−400 cm^{-1} and a resolution of 0.7 cm^{-1} and UV/Vis spectra were recorded with a JASCO V-670 spectrophotometer equipped with an inner sapphire window. A high-pressure mercury lamp (HBO 200, Osram) with a monochromator (Bausch & Lomb) was used for irradiation. Cl_2 or Br_2 was evaporated (Cl_2-CCl_4: –140 °C, Br_2: –85 °C) from a storage bulb into the quartz tube or U-trap. While not directly measured, all reaction products were co-condensed with a large excess of argon (typically 60−120 mbar from a 2000 mL storage bulb) onto the surface of the matrix window at 10 K in about a few milliseconds.

Synthesis Details. ***Caution!*** *Silver azide and halogen azides are extremely hazardous and explosive. Such compounds should be handled with utmost care and only in very small quantities (< 5 mmol). Appropriate safety precautions (blast screens, face shields, Kevlar gloves, soundproof earmuffs, and protective leather clothing) are necessary. Make sure to eliminate static electricity before handling. It is also crucial to avoid friction and light exposure and prevent any contact with metals during sample handling to ensure safety.*

Silver azide was synthesized by adding a stoichiometric amount of a silver nitrate-water solution to a sodium azide-water solution in the dark. The precipitate was washed three times with anhydrous ethanol. The resulting slurry was loosely dispersed on one side of the inner surface of a straight quartz tube (ø 10 × 1) or the inner surface of a U-trap (inside diameter 10 mm), then brought to reduced pressure to remove the solvent. Typically, 0.6 mmol and 2.5 mmol of AgN_3 are required for the straight quartz tube and U-trap, respectively. $Na^{15}N^{14}N^{14}N$ (> 99% ^{15}N, Sigma-Aldridge) was used for isotope labelling experiments. Chlorine gas was bubbled into CCl_4 at 0 °C and degassed before using. Bromine was purified by vacuum distillation before use. Typically, 3 mmol of halogen were stored in the storage bulb for the reaction.

Author contributions

W.Q., A.M., and P.R.S. conceived the project. W.Q. and A.M. designed and conducted the experiments, performed computations, and collected all data. W.Q. conceptualized, wrote the original manuscript. W.Q., A.M. and P.R.S. revised the manuscript. A.M. and P.R.S. supervised the project.

Acknowledgments

Financial support by the Deutsche Forschungsgemeinschaft (DFG) via the grant MA 8773/3-1 (AM) is gratefully acknowledged. The authors sincerely thank Xihe Bi (NENU), Thomas M. Klapötke (LMU Munich), and Yongquan Ning (NENU) for their valuable suggestions for the synthesis of silver azide, and Tian Lu (Keinsci) for advice regarding the detonation performance computations. We also thank Xiaoqing Zeng (Fudan U) for carefully reading and commenting on the manuscript.

References

1 Christe, K. O. Polynitrogen chemistry enters the ring. *Science* **355**, 351-351 (2017). https://doi.org/doi:10.1126/science.aal5057
2 Wang, Y. *et al.* Stabilization of hexazine rings in potassium polynitride at high pressure. *Nat. Chem.* **14**, 794-800 (2022). https://doi.org/10.1038/s41557-022-00925-0
3 Ninet, S. Benzene-like N_6 hexazine rings. *Nat. Chem.* **15**, 595-596 (2023). https://doi.org/10.1038/s41557-023-01189-y
4 Yao, Y. & Adeniyi, A. O. Solid Nitrogen and Nitrogen-Rich Compounds as High-Energy-Density Materials. *Phys. Status Solidi B* **258**, 2000588 (2021). https://doi.org/10.1002/pssb.202000588
5 Klapötke, T. M. & Witkowski, T. G. Nitrogen-Rich Energetic 1,2,5-Oxadiazole-Tetrazole – Based Energetic Materials. *Prop., Explos., Pyrotech.* **40**, 366-373 (2015). https://doi.org/https://doi.org/10.1002/prep.201400294
6 Nguyen, M. T. Polynitrogen compounds: 1. Structure and stability of N_4 and N_5 systems. *Coordin. Chem. Rev.* **244**, 93-113 (2003). https://doi.org/https://doi.org/10.1016/S0010-8545(03)00101-2
7 Zarko, V. E. Searching for ways to create energetic materials based on polynitrogen compounds (review). *Combust. Explos. Shock Waves* **46**, 121-131 (2010). https://doi.org/10.1007/s10573-010-0020-x
8 Larson, Å., Larsson, M. & Östmark, H. Theoretical study of rectangular (D_{2h}) N_4. *J. Chem. Soc. Faraday Trans.* **93**, 2963-2966 (1997). https://doi.org/10.1039/a702835k
9 Glukhovtsev, M. N. & von Ragué Schleyer, P. Structures, bonding and energies of N_6 isomers. *Chem. Phys. Lett.* **198**, 547-554 (1992). https://doi.org/https://doi.org/10.1016/0009-2614(92)85029-A
10 Glukhovtsev, M. N., Jiao, H. & Schleyer, P. v. R. Besides N_2, What Is the Most Stable Molecule Composed Only of Nitrogen Atoms? *Inorg. Chem.* **35**, 7124-7133 (1996). https://doi.org/10.1021/ic9606237
11 Strout, D. L. Acyclic N_{10} Fails as a High Energy Density Material. *J. Phys. Chem. A* **106**, 816-818 (2002). https://doi.org/10.1021/jp0132073

12 Hirshberg, B., Gerber, R. B. & Krylov, A. I. Calculations predict a stable molecular crystal of N_8. *Nat. Chem.* **6**, 52-56 (2014). https://doi.org/10.1038/nchem.1818

13 Strout, D. L. Cage Isomers of N_{14} and N_{16}: Nitrogen Molecules That Are Not a Multiple of Six. *J. Phys. Chem. A* **108**, 10911-10916 (2004). https://doi.org/10.1021/jp046496e

14 Samartzis, P. C. & Wodtke, A. M. All-nitrogen chemistry: how far are we from N_{60}? *Int. Rev. Phys. Chem.* **25**, 527-552 (2010). https://doi.org/10.1080/01442350600879319

15 Mikhailov, O. V. Molecular and Electronic Structures of Neutral Polynitrogens: Review on the Theory and Experiment in 21st Century. *Int. J. Mol. Sci.* **23**, 2841 (2022). https://doi.org/10.3390/ijms23052841

16 Thrush, B. A. & Norrish, R. G. W. The detection of free radicals in the high intensity photolysis of hydrogen azide. *Proc. R. Soc. London Ser. A* **235**, 143-147 (1956). https://doi.org/doi:10.1098/rspa.1956.0071

17 Beaman, R. A., Nelson, T., Richards, D. S. & Setser, D. W. Observation of azido radical by laser-induced fluorescence. *J. Phys. Chem.* **91**, 6090-6092 (1987). https://doi.org/10.1021/j100308a006

18 Cacace, F., de Petris, G. & Troiani, A. Experimental Detection of Tetranitrogen. *Science* **295**, 480-481 (2002). https://doi.org/10.1126/science.1067681

19 Hayon, E. & Simic, M. Absorption spectra and kinetics of the intermediate produced from the decay of azide radicals. *J. Am. Chem. Soc.* **92**, 7486-7487 (1970). https://doi.org/10.1021/ja00728a049

20 Zhou, H., Wong, N.-B., Zhou, G. & Tian, A. Theoretical Study on "Multilayer" Nitrogen Cages. *J. Phys. Chem. A* **110**, 3845-3852 (2006). https://doi.org/10.1021/jp056435w

21 Sedgi, I. & Kozuch, S. Quantum tunneling instability of the mythical hexazine and pentazine. *Chem. Commun.* **60**, 2038-2041 (2024). https://doi.org/10.1039/d3cc05840a

22 Christe, K. O., Wilson, W. W., Sheehy, J. A. & Boatz, J. A. N_5^+: A Novel Homoleptic Polynitrogen Ion as a High Energy Density Material. *Angew. Chem. Int. Ed.* **38**, 2004-2009 (1999). https://doi.org/10.1002/(sici)1521-3773(19990712)38:13/14<2004::Aid-anie2004>3.0.Co;2-7

23 Vij, A. *et al.* Polynitrogen Chemistry. Synthesis, Characterization, and Crystal Structure of Surprisingly Stable Fluoroantimonate Salts of N_5^+. *J. Am. Chem. Soc.* **123**, 6308-6313 (2001). https://doi.org/10.1021/ja010141g

24 Vij, A., Pavlovich, J. G., Wilson, W. W., Vij, V. & Christe, K. O. Experimental detection of the pentaazacyclopentadienide (pentazolate) anion, *cyclo*-N_5^-. *Angew. Chem. Int. Ed.* **41**, 3051-3054 (2002). https://doi.org/10.1002/1521-3773(20020816)41:16<3051::AID-ANIE3051>3.0.CO;2-T

25 Östmark, H. *et al.* Detection of pentazolate anion (*cyclo*-N_5^-) from laser ionization and decomposition of solid *p*-dimethylaminophenylpentazole. *Chem. Phys. Lett.* **379**, 539-546 (2003). https://doi.org/10.1016/j.cplett.2003.08.081

26 Zheng, J. *et al.* Gaussrate, version 2017-B. *University of Minnesota: Minneapolis* (2017).

27 Xu, Y. *et al.* A series of energetic metal pentazolate hydrates. *Nature* **549**, 78-81 (2017). https://doi.org/10.1038/nature23662

28 Xu, Y., Tian, L., Li, D., Wang, P. & Lu, M. A series of energetic cyclo-pentazolate salts: rapid synthesis, characterization, and promising performance. *J. Mater. Chem. A* **7**, 12468-12479 (2019). https://doi.org/10.1039/C9TA01077G

29 Eremets, M. I., Gavriliuk, A. G., Trojan, I. A., Dzivenko, D. A. & Boehler, R. Single-bonded cubic form of nitrogen. *Nat. Mater.* **3**, 558-563 (2004). https://doi.org/10.1038/nmat1146

30 Benchafia, E. M. *et al.* Cubic gauche polymeric nitrogen under ambient conditions. *Nat. Commun.* **8**, 930 (2017). https://doi.org/10.1038/s41467-017-01083-5

31 Laniel, D. *et al.* Aromatic hexazine $[N_6]^{4-}$ anion featured in the complex structure of the high-pressure potassium nitrogen compound K_9N_{56}. *Nat. Chem.* **15**, 641-646 (2023). https://doi.org/10.1038/s41557-023-01148-7

32 Greschner, M. J. *et al.* A New Allotrope of Nitrogen as High-Energy Density Material. *J. Phys. Chem. A* **120**, 2920-2925 (2016). https://doi.org/10.1021/acs.jpca.6b01655

33 W. Y. Qian, A. Mardyukov & Schreiner, P. R. Hexanitrogen (N_6): A Synthetic Leap Towards Neutral Nitrogen Allotropes. Preprint at http://doi.org/10.26434/chemrxiv-2024-90vvx. (2024).

34 Zeng, X. *et al.* Reaction of AgN_3 with $SOCl_2$: Evidence for the Formation of Thionyl Azide, $SO(N_3)_2$. *Inorg. Chem.* **43**, 4799-4801 (2004). https://doi.org/10.1021/ic049442s

35 Raschig, F. Über Chlorazid N_3Cl. *Ber. Dtsch. Chem. Ges.* **41**, 4194-4195 (1908). https://doi.org/10.1002/cber.190804103130

36 Lyhs, B., Bläser, D., Wölper, C., Schulz, S. & Jansen, G. A Comparison of the Solid-State Structures of Halogen Azides XN_3 (X=Cl, Br, I). *Angew. Chem. Int. Ed.* **51**, 12859-12863 (2012). https://doi.org/10.1002/anie.201206028

37 Buzek, P., Klapötke, T. M., von Ragué Schleyer, P., Tornieporth-Oetting, I. C. & White, P. S. Iodine Azide. *Angew. Chem. Int. Ed.* **32**, 275-277 (1993). https://doi.org/10.1002/anie.199302751

38 Shurvell, H. F. & Hyslop, D. W. Infrared Spectrum of Cyanogen Azide. *J. Chem. Phys.* **52**, 881-887 (1970). https://doi.org/10.1063/1.1673068

39 Pimental, G. C. & Charles, S. W. Infrared spectral perturbations in matrix experiments. *Pure Appl. Chem.* **7**, 111-124 (1963). https://doi.org/10.1351/pac196307010111

40 Zeng, X., Beckers, H. & Willner, H. Matrix isolation of two isomers of N_4CO. *Angew. Chem. Int. Ed. Engl.* **50**, 482-485 (2011). https://doi.org/10.1002/anie.201005177

41 Tobita, M. & Bartlett, R. J. Structure and Stability of N_6 Isomers and Their Spectroscopic Characteristics. *J. Phys. Chem. A* **105**, 4107-4113 (2001). https://doi.org/10.1021/jp003971+

42 Gagliardi, L., Evangelisti, S., Barone, V. & Roos, B. O. On the dissociation of N_6 into 3 N_2 molecules. *Chem. Phys. Lett.* **320**, 518-522 (2000). https://doi.org/10.1016/S0009-2614(00)00281-5

43 Huber, K. P. & Herzberg, G. in *Molecular Spectra and Molecular Structure* (eds K. P. Huber & G. Herzberg) Ch. Chapter 2, 8-689 (Springer US, 1979).

44 Carlotti, M., Johns, J. W. C. & Trombetti, A. The ν_5 Fundamental Bands of N_2H_2 and N_2D_2. *Can. J. Phys.* **52**, 340-344 (1974). https://doi.org/10.1139/p74-048

45 Brazier, C. R., Bernath, P. F., Burkholder, J. B. & Howard, C. J. Fourier transform spectroscopy of the ν_3 band of the N_3 radical. *J. Chem. Phys.* **89**, 1762-1767 (1988). https://doi.org/10.1063/1.455122

46 Bittererová, M., Östmark, H. & Brinck, T. Ab initio study of the ground state and the first excited state of the rectangular $(D_{2h})N_4$ molecule. *Chem. Phys. Lett.* **347**, 220-228 (2001). https://doi.org/10.1016/S0009-2614(01)01002-8

47 Lu, T. & Chen, F. Multiwfn: a multifunctional wavefunction analyzer. *J. Comput. Chem.* **33**, 580-592 (2012). https://doi.org/10.1002/jcc.22885

48 Garrett, B. C. & Truhlar, D. G. Generalized transition state theory. Bond energy-bond order method for canonical variational calculations with application to hydrogen atom transfer reactions. *J. Am. Chem. Soc.* **101**, 4534-4548 (1979). https://doi.org/10.1021/ja00510a019

49 Truhlar, D. G., Issacson, A., Skodje, R. & Garrett, B. C. Additions and Corrections - Incorporation of Quantum Effects in Generalized-Transition-State Theory. *J. Phys. Chem.* **87**, 4554-4554 (1983). https://doi.org/10.1021/j100245a604

50 Weggel, D. C. in *Blast Protection of Civil Infrastructures and Vehicles Using Composites* (ed Nasim Uddin) 3-43 (Woodhead Publishing, 2010).

Acknowledgement

I would like to extend my sincere thanks to those who offered valuable assistance and support during the course of my doctoral research.

Prof. Peter R. Schreiner. Thank him for the opportunity to work in the group and for his support. I am thankful for the complete freedom in all my projects and developing all my ideas.

Dr. Artur Mardyukov. Thank him for providing me with the opportunity to work here and for his priceless support throughout my stay, both in research and in life. I am deeply grateful for the freedom he gave me in pursuing my research and a period of time in my life that do not have to care about anything else than the research I like.

Dr. Dennis Gerbig. Thank him for the kind help in reaching computational resources.

Dr. Boryslav Tkachenko. Thank him for chemicals. N_6 project would not exist without him.

Dr. Raffael C. Wende. Thank him for the kind help in translation and nice working atmosphere.

Akkad Danho. Thank him for the kind help in translation and in gym.

Anja Beneckenstein. Thank her for her brilliant glass works to make all the projects come true.

Prof. Xiaoqing Zeng. Thank him for his continuous support and valuable suggestions as well as discussion. He provided me with many important fundamental qualities for scientific research.

Prof. Thomas M. Klapötke. Thank him for greatly valuable suggestions on the synthesis of explosive compounds and for his “good luck”. His research has inspired me to dedicate myself fully to the pursuit of science.

Prof. Xihe Bi and **Prof. Yongquan Ning**. Thank them for the greatly valuable information for the synthesis of explosive compounds.

Dr. Tian Lu. Thank him for his valuable assistance with quantum chemical calculations. I greatly appreciate his selfless support in helping countless researchers.

The world is absurd and steeped in tragedy. Having experienced his life, Faust realized that life is a sigh of smoke, humanity is insatiable greed, and satisfaction dissolves the moment it is attained. We are all Sisyphus, condemned to ceaseless toil. But rather than resigning to the "foolishness" Zheng Xie proposes to pretend unawareness or succumbing to physical or philosophical suicide, I prefer defiance. I decide to defy fate and authority, whose existence is as futile as mine. In that rebellion, I reclaim my life—each step forward belongs to me because I negate that which seeks to negate me. I refuse to be Apollonian, to anaesthetize myself with fantasies woven of illusions. Instead, I embrace the Dionysian spirit, revelry self and directly confront tragedy of the world with direct, unbending will. Like Don Quixote, I will remain resolute in my own one-man quest, however futile, and undergo the process of transformation as Zarathustra said: from the obedient camel to the rebellious lion, and finally, to the child—one who reinvents himself, unencumbered by the burden of what was. That is the Romaticism I conceive.

"Great spirits have always encountered violent opposition from mediocre minds. The mediocre mind is incapable of understanding the man who refuses to bow blindly to conventional prejudices and chooses instead to express his opinions courageously and honestly."

—— Albert Einstein (1879–1955)